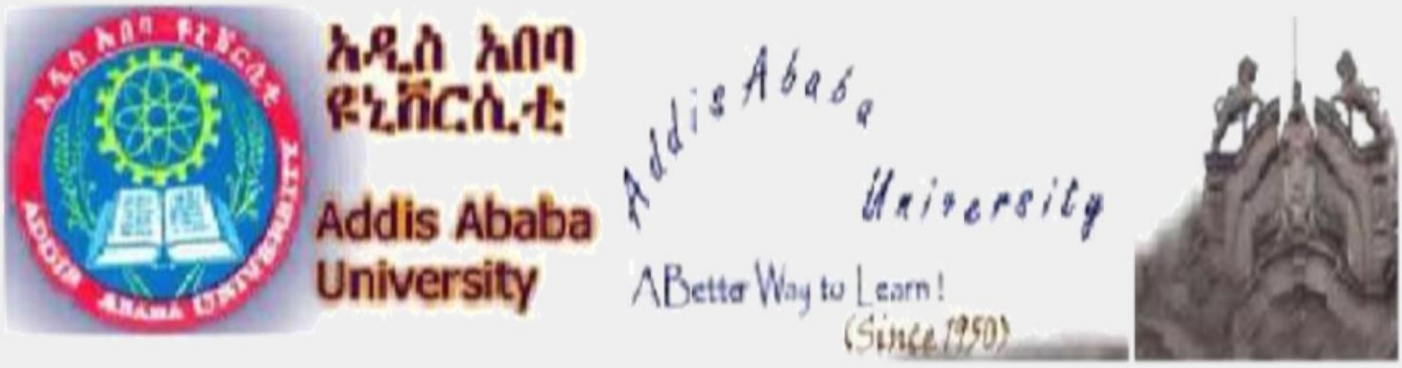

ADDIS ABABA UNIVERSITY
COLLEGE OF NATURAL AND COMPUTATIONAL SCIENCES SCHOOL OF EARTH SCIENCES

EVALUATION OF RECHARGE AND GROUNDWATER FLOW DYNAMICS IN BELES BASIN, UPPER BLUE NILE BASIN, NORTHWESTERN ETHIOPIA.

By
Zerihun Muleta
GSR/7125/14

A THESIS SUBMITTED TO
SCHOOL OF EARTH SCIENCIES OFADDIS ABABA UNIVERSITY
IN PARTIAL FULFILLMENT OF THE REQUIREMENTS FOR THE DEGREE OF MASTERS OF SCIENCE IN HYDROGEOLOGY

Addis Ababa, Ethiopia
October 2023

Certificate

I hereby confirm that the thesis titled "Evaluation of recharge and groundwater flow dynamics in Beles basin, Upper Blue Nile, Northwestern Ethiopia," authored by Zerihun Muleta, submitted for the partial fulfillment of the requirements for the degree of Master of Science in Hydrogeology, adheres to the regulations of the university and upholds the recognized standards in terms of originality and quality.

Approved by Examining Board

	Name	Signature	Date
Chairman, School of Earth science:	_____	_____	_____
	Name	Signature	Date
Examiner: Dr. Dessie Nedaw		_____	_____
	Name	Signature	Date
Examiner: Dr. Tilahun Azagegn		_____	_____
	Name	Signature	Date

Declaration

I declare that the work contained in this thesis, which I completed in 2022/23 while working under Prof. Tenalem Ayenew's supervision at Addis Ababa University's School of Earth Sciences, is entirely original. I further declare that this work has not previously been presented to or submitted to any other college, institution, or university to receive a diploma or degree. The thesis work includes properly credited and acknowledged references to all secondary data, sources, and materials.

Zerihun Muleta Daba (MSc. Candidate)

Signature _____ Date _____

This is to certify that, to the best of my knowledge, the candidate's above declaration is true.

Prof. Tenalem Ayenaw (Advisor)

Signature _____ Date _____

Acknowledgments

Glory and praise be to God first and foremost for providing me with perfect health, inner peace, knowledge, and wisdom to complete this thesis work and for being by my side throughout my entire life.

My deepest appreciation is extended to my advisor, professor Tenalem Ayenew, for his helpful guidance, courteous consultation, and providing of crucial reference resources that were helpful for this study effort and enabled me to complete it. I will never forget his heroic perseverance and persistent commitment to assisting me during this investigation. His advice was helpful to me throughout the entire research and thesis-writing process. For my Master's degree, I couldn't have asked for a greater advisor and mentor.

A special thanks go out to Prof. Gezahegn Yirgu, Dr. Behailu Birahanu, Dr. Dessie Nedaw, Dr. Tilahun Azagegn, Dr. Ameha Atnafu, Prof. Tigistu Haile, Prof. Bekele Abebe, and all of the instructors at Addis Ababa University's School of Earth Sciences who helped me learn vital information about the subject and related fields.

I gratefully recognize the Ethiopian National Meteorological Service Agency (ENMSA), the Ministry of Water and Energy, and the Water, Mines, and Energy offices of the Amhara Region as the sources of the data.

My firm, Waki Engineering PLC, deserves a special note of thanks for providing me with financial aid and enabling me to pursue my postgraduate studies.

Finally, I would like to extend my sincere appreciation to the experts and friends who wholeheartedly contributed to the successful completion of this research endeavor. I express special gratitude to Mr. Tofik Yasin and Mr. Zakarias Ashine for their valuable cooperation in discussing the proposed methods and the obtained results throughout this thesis.

Abstract

The demand for groundwater is growing, leading to the identification of this valuable resource as the focal point for investigation, administration, and preservation. The Beles basin's groundwater resources and groundwater dynamics have been both quantitatively and qualitatively analyzed in this work. Therefore, evaluating groundwater recharge and groundwater flow dynamics utilizing Wetspass,baseflow separation and chloride mass balance approaches was the primary goal of the current research project.

The annual recharge of the basin is predicted to be 223.40 mm/year based on the results of the Wetspass model, which corresponds to around 13.86% of the annual rainfall that infiltrates into the aquifer. The model also shows that around 36.35% of the total annual precipitation is accounted for by direct runoff.

Furthermore, the Main Beles River at Beles Bridge and the Gilgel Beles river catchments near Mandura town were selected as the primary rivers for assessing the recharge process within the Beles basin. Through baseflow separation, it was determined that the basin experiences an annual recharge of 203.52 mm/year, accounting for 12.63% of the total annual rainfall that replenishes the aquifer. Interestingly, the basin exhibits higher baseflow during the summer months due to increased precipitation and higher evapotranspiration rates. The baseflow index, which indicates the contribution of groundwater to rivers, is highest during the rainy season and lowest during the dry season.

Lastly, the chloride mass balance method was employed to estimate groundwater recharge in the area. The findings revealed chloride concentrations of 0.74 mg/L in rainfall and 4.93 mg/L in groundwater. As a result, the CMB method determined that the groundwater recharge in the Beles catchment is approximately 241.9 mm/year, which corresponds to 15% of the annual precipitation that infiltrates into the groundwater reservoir.

By examining groundwater level readings from 3 boreholes, 12 shallow wells, 16 hand-dug wells, and information from 89 springs, the groundwater flow dynamics is controlled by surface morphology and structures and flows from the northeast towards the west, aligning with the flow of the Beles River.

Keywords: Baseflow separation, chloride mass balance, groundwater flow dynamics, Recharge evaluation, Wetspass.

TABLE OF CONTENTS

List of Figures

List of Tables

List of Annex

ACRONYMS

AET	Actual evapotranspiration
ASCII	American Standard Code for Information Exchange
BFI	Base Flow Index
CMB	Chloride Mass Balance
DBF	Data Base Files
DEM	Digital Elevation model
EIGS	Ethiopian Institute of Geological Survey
FAO	Food and Agriculture Organization
GIS	Geographical Information System
HDW	Hand Dug Well
ITCZ	Inter- Topical Convergence Zone
LAI	Leaf Area Index
LULC	Land Use Land Cover
masl	Meter Above Sea Level
mm/yr	millimeter per year
NMA	National Metrological Agency
PET	Potential Evapotranspiration
SRTM	Shuttle Radar Topography Mission
SW	Shallow Well
TBL	Table of Values
UTM	Universal Transvers Mercator
USDA	United States Department of Agriculture
USGS	United States Geological Survey
WetSpass	Water and Energy Transfer between Soil, Plant, and Atmosphere at quesi-steady State

CHAPTER ONE

1. Introduction

1.1. Background

One of the significant tributaries of the Nile River, the Blue Nile, originates in a substantial portion of the Ethiopian highlands. Despite the availability of evidence on the historical origins of the White Nile, the hydrology of the Blue Nile has received comparatively less attention in scientific literature, as noted in Livingstone's 1980 paper. Conway's 2000 research reveals that the Upper Blue Basin, spanning a surface area of 176,000 km2, is one of Ethiopia's largest basins in terms of water discharge.

Ethiopia is blessed with several significant tributaries, including the Besheilo, Welaka, Jemma, Muger, Guder, Finchaa, Anger, Didessa, and Dabus on the left bank, as well as the North Gojam, South Gojam, Wombera, and Beles on the right bank, as documented by McCartney and Girma in 2012. The region's topography varies greatly, ranging from an elevation of 485 meters to over 4257 meters. Among the major tributaries on the right bank is the Beles basin, located southwest of Lake Tana. Within this basin, two perennial rivers named Main Beles and Gilgel Beles converge at Pawe woreda to form the Beles River. Originating from a place called Alefa in North Achefor, the Beles River holds the distinction of being one of the largest tributaries of the Abay River. The Beles basin encompasses the West Gojam, North Gojam, and Awi zones within the Amhara regional state, as well as the Metekel zone in the Benshangul Gumuz regional state. The river follows a southwest trajectory and eventually merges with the Abbay River. In addition to the Beles River, the basin contains various smaller perennial and intermittent rivers. Both surface water and groundwater play crucial roles in providing water resources for the communities residing in the basin. However, there is relatively limited expertise in managing both surface and groundwater within the basin. Both natural

and man-made sources affect groundwater recharge in the basin. Agricultural activity, deforestation, and their adverse impacts on runoff and groundwater recharge are among the anthropogenic factors that tend to deplete groundwater in the basin. Today, as a result of global climate change, the pattern of rainfall has slowed the expansion of agriculture, water supplies, and hydroelectric power, all of which are crucial to the nation's economic development. Natural springs, wetlands, and surface waterways are all currently drying off. The alarming rise in population density, inadequate widespread farming, and unrestrained settlement in the basin are detrimental to the health of the natural ecosystems. Any farm with land use methods involving deforestation has reductions in infiltration capacity, groundwater recharge, surface runoff and erosion, soil evaporation, and surface storage.

Large sums of money are being invested in the Lake Tana sub-basin for the proper land use management and development of both surface and groundwater resources for drinking, irrigation, and hydroelectric power in Tana-Beles, among other activities carried out in the basin to address these issues and promote sustainable development, as cited (Engida et al., 2007).

For all actions involving economic growth in the basin, knowledge of and understanding of hydrology and hydrogeologic processes are essential. One of the most crucial elements affecting the sustainable yield of groundwater and surface water utilization is groundwater recharge.

Understanding and regulating aspects of the amount that enters and departs the basin depend on knowledge of the water utilization and management system of the available water. The volume and rate of recharge determine how much water may be drawn from an aquifer and surface water without creating depletion. Effective management of groundwater and surface water resources requires quantification of the rate of natural recharge. It is especially crucial in the basin, where there is a high demand for both surface and groundwater supplies and where these resources

are essential for economic growth.

The identification of the Beles basin aquifers, groundwater dynamics, groundwater environmental assurance, and methodical planning and execution of research on these topics is crucial.

As a result, groundwater dynamics is the reality that nature is influenced by many types of influencing circumstances in certain environments, as cited in Chen et al. (1988). The evaluation of groundwater recharge and the dynamics of groundwater in the Beles basin must therefore be closely monitored and researched. Therefore real groundwater management plan advancement is based on detailed aquifer characterization and ambient spatiotemporal groundwater monitoring.

This study aims to begin dealing with groundwater recharge and groundwater dynamics by evaluating groundwater recharge based on obtained meteorological, hydrological, and hydrogeological data and by using base flow separation and WetSpass methods for effective use of the groundwater resource of the Beles basins.

Since the basin is relevant for Ethiopia and northeastern countries, it is highly beneficial to carry out recharge estimation and evaluate groundwater dynamics in the Beles basin.

1.2. Statement of the problem

For the goal of sustainable groundwater management, it is crucial to accurately and consistently assess groundwater recharge and the dynamics of groundwater flow given the rising demand for and pressures on groundwater resources.

The Upper Blue Nile basin contains the largest portion of the Nile River's water. The availability of water in this basin is vital for millions of people living both upstream and downstream along the river. Therefore, it is of utmost importance to conduct a comprehensive hydrological analysis of the basin, examining hydrological processes and runoff components. This analysis will provide valuable insights for water managers and decision-makers, enabling them to develop

sustainable water resource strategies in the region.

The basin exhibits significant variations in rainfall and runoff throughout the year and between years. Additionally, there is geographical diversity in terms of soil, geology, vegetation, and topographic characteristics within the basin. The hydrological processes within the basin are complex and subject to frequent spatial and temporal variations due to these heterogeneities. Through interactions with the natural system, human activities also have an impact on hydrological processes. The main interferences in the basin that change the hydrological processes in the basin include intensive grazing, deforestation, and incorrect and intense farming techniques on unsuitable soil. The highlands of Ethiopia have been devastated by these issues, which result in crop yield decline, erosion of agricultural land, and significant siltation of irrigation canals and reservoirs downstream.

In comparison to the lower portion of the basin, research on the hydrology of the upper Blue Nile basin, particularly the Beles region, has received less attention. Conducting comprehensive investigations and in-depth analyses of the hydrology of the basin has been difficult due to the lack of sufficient hydrological and meteorological data. Due to its uneven distribution and concentration solely in towns along major routes, the current observational network collecting hydro-climate data is insufficiently large. It does not take into account the mountains' spatial variability, where there is a high perception of precipitation. Most of the time, the stream gauges don't accurately represent the rain gauge upstream of the catchment outflows. As a result, estimating water resources using hydrological models or additional hydrological research is frequently challenging and not sufficiently supported by data.

Consequently, this study plays a crucial role in conducting a comprehensive examination and analysis of groundwater recharge and flow dynamics in the upper Blue Nile's Beles basin.

1.3. Objectives of the research

1.3.1. General objective

The main objective of the study is to estimate the groundwater recharge and understand the groundwater flow system (dynamics).

1.3.2 Specific objectives

The specific objectives include;

- The total quantity of groundwater recharge will be assessed by employing different approaches.
- The assessment aimed to identify the various sources of groundwater recharge.

1.4. Research questions

Generally based on the objectives of the study area the following question is addressed to be answered in this study area.

- What is the annual recharge rate of groundwater in the Beles basin?
- Is the Groundwater recharged from local rainfall or rainfall from the highlands of Wombera, Balaya, or Kar Mountain?
- What is the characteristics of groundwater flow dynamics in the basin?

1.5. Scope of the study

The objective of the study was to gain insights into the origin, mechanisms, and accessibility of the primary water balance elements within the Beles basin. This investigation encompasses the assessment of groundwater recharge, runoff, interception, and actual water loss through evapotranspiration, as well as the influence of land use and land cover. The study aimed to identify the spatial and temporal factors that govern the various components mentioned. It attempted to study the hydrometeorological and physical characteristics of the watershed, as these factors play a vital role in hydrological processes. Apart from estimating groundwater recharge and other relevant hydrological elements, the study also aimed to determine the sustainable yield of the watershed and provide insights for

effective groundwater management. By considering these aspects, a comprehensive understanding of the hydrological dynamics of the watershed can be achieved.

1.6. Significance of the study

This research holds great importance in the realm of sustainable groundwater management. It aims to propose an optimal utilization of the aquifers within the area, ensuring their maximum benefits while safeguarding their long-term sustainability. The findings of this research will serve as a fundamental reference and basis for future groundwater exploration and investigations. Additionally, the data generated during this study will serve as a crucial input for related studies in the future, thereby contributing to the overall understanding and advancement of groundwater research and management practices. Furthermore, the study introduces a technique for assessing the extent of changes in land use and land cover and their influence on hydrological patterns. This has been accomplished by integrating the hydrological model WetSpass, which enables the simulation of hydrological processes, with the analysis of land use and land cover modifications.

CHAPTER TWO

2. LITERATURE REVIEW

There has typically been less hydrogeological, geological, and geophysical study done on the Abay basin and its sub-basin. One of the Abay River's lesser-explored subbasins is the Beles Basin. The investigation into the Beles Basin started at a regional level or in a specific location for water borehole placement and urban water distribution, taking into consideration the hydrogeological state of the catchment. The Beles basin and its surroundings are thoroughly reviewed and summarized in this research, despite the incomplete evaluation of the geological and hydrogeological properties of the basin, which is directly relevant to the current study detailed below.

The Abay River Basin Integrated Development Master Plan Project was carried out by BCEOM in 1998 with the goal of providing crucial data on the climatology, hydrology, and hydrogeology sections of the whole Abay Basin. The hydrogeology component of the study was conducted with the following goals in mind: The hydric balance, which considers factors including precipitation, evapotranspiration, direct runoff, and a predicted distribution of soil retention capacity, is used to evaluate recharge. This hypothesis has been further supported by observations of variations in the water table. It was found that the predicted recharge values for Gilgel Abay, Koga, Ribb, Gummera, and Megach were 305mm, 203mm, 35mm, and 90.55mm, respectively.

Kebede et al. (2005) conducted the other assessment of the geochemical evolution, circulation, and groundwater recharge in the Ethiopian area that serves as the source of the Blue Nile River. In order to get a thorough knowledge of groundwater recharge, circulation, and hydrochemical changes within the Upper Blue Nile basin in Ethiopia, this study uses geochemical analysis and environmental isotopes. According to the data, there are two prominent zones with structural deformations that each have their own unique groundwater circulation patterns and evolutionary

trajectories. In general, this study helps to create a regional perspective on the hydrogeological dynamics of the Upper Blue Nile basin and illustrates the distinctive features of the groundwater in this particular area.

Getachew Hadush (2008), on the other hand, had done research on calculating recharge and the groundwater's contribution to the upper Blue Nile flows. In this study, various techniques were used to evaluate the groundwater recharge of the basin. To assess the chemical composition, baseflow, rainfall-runoff simulations using the BASF model, and a chemical balancing approach utilizing chloride as a tracer were used. According to the BASF model and baseflow separation utilizing Eckhardt's (2005) model, which depicts the natural groundwater recharge of the basin, the groundwater recharge fluctuated between 70mm and 120mm per year.

A research on the hydrological equilibrium of the Lake Tana Upper Blue Nile Basin was done by Wale (2008). Since measurement gauges were absent in around 48% of the catchment area, the investigation revealed a substantial knowledge gap about the key elements of the lake water balance. The study used a combination of a rainfall-runoff model and a spreadsheet water balance model to predict daily lake levels in order to close this gap. The incorporation of runoff from the ungauged catchments received special attention. A semi-distributed conceptual model called HBV was used to simulate the daily flows from the ungauged catchments, using model parameters taken from the gauged catchments. The study's conclusions showed that model parameters from gauged catchments with relative volume errors under 5% and Nash-Sutcliffe coefficients larger than 0.6 may be effectively applied to ungauged catchments. This parameter transfer was based on variables including the regional model, closeness to other areas, and catchment area.

Ayenew Tenalem and Addisu Girma (2010) have researched the topic of the characterization of the Beles River in northwest Ethiopia's hydrological and hydrochemical conditions. The hydrogeological investigation of the area revealed the existence of various aquifer types, which include porous aquifers such as

alluvium and colluvium, fissured and karst aquifers composed of marble, fissured aquifers consisting of sandstone and volcanic rock, fissured aquifers with limited potential associated with certain non-carbonate metamorphic and intrusive rocks, as well as aquitards found in certain non-carbonate metamorphic and intrusive rocks. The aquifer in the basin was divided into formations that ranged in productivity from very low to high.

Surface-groundwater resource evolution and water balance were investigated by ENTRO (2013) for joint usage in the Tana-Beles sub-basin. The study's primary goals are to estimate the sub-basin's groundwater hydrology and evaluate any potential joint surface-groundwater use. The watershed was found to have two broad aquifer systems. The investigation shows that the area has two different aquifer systems. The first system consists of a highly fractured rock aquifer made up of Tertiary and Quaternary volcanic deposits and operates as a regional flow system. The second system is mostly made up of loose sediments generated by alluvial processes in the valleys. Unconsolidated aquifer groundwater levels change with the seasons and in reaction to river levels, peaking in the winter's heavy precipitation and declining in the summer.

Tefere et al. (2016) used arc hydro techniques in Arc Gis to characterize the Bele River Basin of the Blue Nile River Sub-basin in northwestern Ethiopia. The results of this study show that higher elevations have higher drainage densities, particularly when there is a thick weathered layer or a significant network of geological structures crossing the rocks. The topography determines which way the rivers flow. The streams originate in highlands that rise to a maximum of 2729 meters above sea level. These highlands are typically humid and mountainous, while the lowlands that surround them rise to a minimum of 458 meters above sea level. On the highlands, these geographic variations cause soil erosion, limited retention in soil layers, and rapid runoff.

Ashebir H. (2017) used the HEC-HMS Model to carry out water resource assessment

and management options in the Beles River catchement. The HEC-HMS 3.5 calibration of the Beles River sub-basin utilized daily precipitation and flow data from 2003 and 2004. These data were employed to create GIS layers using Arc GIS 9.3. Subsequently, validation of the GIS layers was carried out in 2005, employing statistical tests such as relative error and the residual method. After validation, the water balance evaluation was performed using the validated surface runoff.The delineation of the entire basin and sub-basin revealed the drainage areas for the sub-watersheds: Lower Beles with 9078.20 km2, Upper Beles with 3461.80 km2, and Gilgel Beles with 747.11 km2. The average monthly simulated runoff results indicate that Gilgel Beles receives 76mm, Upper Beles receives 55.7mm, and Lower Beles receives 42.4mm. Upon assessing the water balance, it was observed that the years 2004 (-463 mm/yr) and 2003 (-180 mm/yr) exhibited the highest water deficits for the Lower Beles sub-watershed. However, 2004 was identified as a water surplus year for both the Gilgel Beles and Upper Beles sub-watersheds. Conversely, 2003 indicated a deficit year for the entire basin.

Imran Ahmad et al. (2019), "Investigating the Delineation of Favorable Groundwater Potential Areas Applying a Geographic Information System in the Beles River Basin, Ethiopia," 2019. The different groundwater potential influencing variables (slope, drainage density, stream power index, fault density, hydrological soil groups, soil texture, saturated hydraulic conductivity, available water capacity, soil bulk density, soil organic carbon, soil depth, soil erodibility, and soil type) have been examined and reclassified based on their potential for infiltration and groundwater potential. The "weighted index overlay analysis" approach was used for each deciding element in the geographic information system domain. The very low, low, moderate, and high groundwater potential areas are depicted on the final groundwater prospectus map. High groundwater potential was discovered in 19.34% of the entire area. While areas with moderate, low, and extremely low groundwater potential make up 41.82%, 32.06%, and 6.79% of the whole area, respectively.

CHAPTER THREE

3. MATERIALS AND METHODS

3.1. Description of the Study Area

3.1.1 Location of Study Area

The Beles basin, which was the focus of the study, is situated in the northwestern region of Ethiopia, specifically southwest of Lake Tana. The study area encompasses portions of the Amhara regional state, particularly the Gojam, South Gondar, and Awi zones, as well as the Benishangul Gumuz regional state, specifically the Metekel zone.

The Beles basin is geographically bounded between latitudes 10°56'00''N to 12°00'00''N and longitudes 35°15'00''E to 37°00'00''E. It covers a total area of approximately 14,200 km2. The basin is characterized by two major rivers, namely the Gilgel Beles and Main Beles. These rivers converge in the middle to form the Beles River, which flows southwestward and eventually joins the Abay River before crossing the border between Ethiopia and Sudan. The topography of the area is predominantly flat to undulating, with elevations ranging from approximately 458 meters to 2,720 meters above sea level. The sub-basin of the Beles River exhibits variations in altitude throughout its different regions. The northern, southwestern, and eastern parts of the sub-basin are characterized by highlands that are situated at higher elevations. On the other hand, the western parts of the sub-basin, particularly on the periphery of the Beles and Abay Rivers, consist of lowlands with altitudes below 800 meters above sea level (msl).

In terms of hydrometeorological conditions, the study area experiences a range of mean annual rainfall between 700mm and 1800mm. The average daily minimum and maximum temperatures exhibit seasonal variations, with annual averages falling within the range of 16°C to 33°C.

.

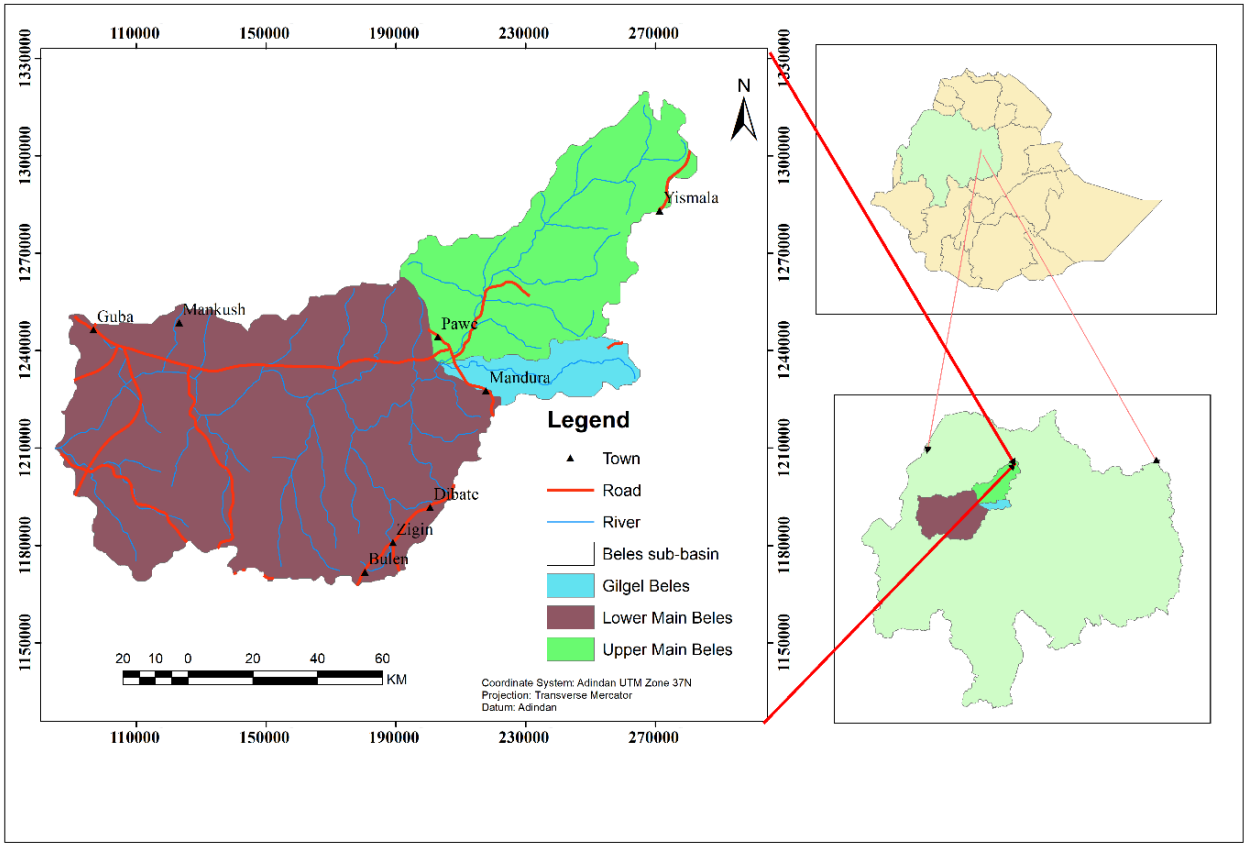

Figure 3. 1. Location map of Beles basin

3.1.2. Physiography and drainage

The area is situated in the northwestern region of Ethiopia. It is characterized by distinct topographical features. In the northern part, there are undulating mountains that span across areas such as Dangur, Balaya, north Achefor, Kunzila, and Dangila. These highland areas contribute to the rugged and hilly terrain of the region. On the other hand, in the southwestern part of the study area, there is the prominent presence of the east Kar mountain, which is surrounded by the Wombera highland. In contrast, the western and central parts of the basin consist of relatively lower-lying areas, known as lowlands. The basin is primarily characterized by a gently undulating to flat topography. Figure 3.2 presents the digital elevation model derived from SRTM data, providing a visualization of the basin's topography. The

geomorphology of the area has been influenced by a combination of volcanic and tectonic activities, as well as erosional and denudational processes. Notably, the formation and configuration of the major rivers within the basin are primarily controlled by tectonic forces. These rivers tend to follow the alignment of regional and sub-regional lineaments, indicating the strong influence of geological structures on their courses and patterns of flow. The rivers found in the basin flow parallel to the lineaments.

Except for the Wombera Plateaus, the general trend in elevation within the study area is a gradual decrease towards the south and west. The central regions, which encompass the major perennial rivers such as Abay and Beles, as well as the western lowlands, have altitudes below 600 meters above sea level. These areas are characterized by relatively flat to gently rolling terrain, extending as a continuation of the sudan plain.

Beles River merges from the highland of Alefa in north Achefer and flows toward the southwest and joins Abay before crossing Ethio-Sudan boundaries. The major river in the basin is controlled by topography and regional and sub-regional lineaments. The rivers flow parallel to the lineaments. The drainage patterns of both perennial and seasonal streams in the study area predominantly exhibit a dendritic pattern, with some slight parallel features observed in lowland regions. The formation and arrangement of these drainage patterns are influenced by various factors, including tectonic activity and geological variations across the area. The density and pattern of drainage networks are, to some extent, controlled by these geological and tectonic factors, which shape the flow and distribution of water throughout the landscape.

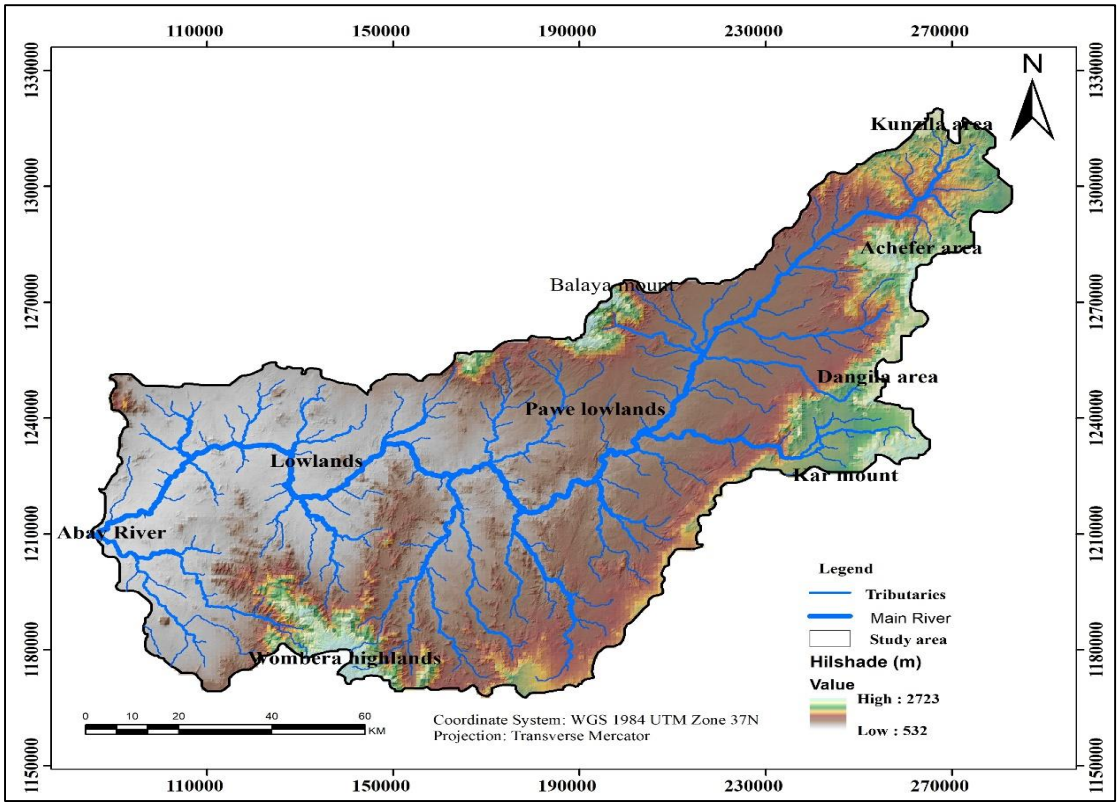

Figure 3. 2. Physiographic and Drianage map of the study area

3.1.3. Climate

The Ethiopian climate is categorized into five distinct climatic zones based on altitude and temperature. These zones are Dega, Woina-Dega, Wurch, Kola, and Berha. The Berha zone is a hyper-arid region situated at an elevation below 500 meters above sea level (m.a.s.l.) and characterized by very hot conditions. The Kola zone is also a hot and arid region, ranging from 500 to 1500 m.a.s.l. The Woina-Dega zone, with an optimal temperature range, spans from 1500 to 2500 m.a.s.l. The Dega and Wurch zones are located in highland areas, with altitudes ranging from 2500–3000 m.a.s.l. and exceeding 3000 m.a.s.l., respectively. These climatic zones provide a framework for understanding the diverse climatic conditions across different elevations in Ethiopia (NMA, 2001).

The climate in the area is described as warm and subtropical. There is a noticeable difference in climate based on elevation, with areas above 1500 meters above sea level (masl) being cooler and receiving more rainfall compared to areas below 1500 meters, which are characterized by hot and dry conditions. The topography of the region exhibits a significant contrast, with elevations ranging from slightly above 2720 masl at Balaya Mountain to less than 500 masl at the Abay River. The majority of the lowland areas in the region can be classified as arid or semi-arid. Daniel Gamachu (1977) classified the climate of Ethiopia based on the Thorthwait system, as shown in Table 3.1and the study area encompasses all climatic zones except for Kur. Specific locations such as Balaya, Wombera, certain parts of Dangila, and mountainous areas of Mandura (Kar Mountain), North Achefer, and Dangur can be categorized as Dega, while the transitional escarpments of all Woredas fall under the Woinadega climatic zone.

The lowlands in the study area are divided into two categories: Kolla and Berha. Berha specifically refers to the extreme western lowlands near the Abay River. The upper Beles region experiences a relatively moderate amount of precipitation, with an average of approximately 1000 mm per year. Interestingly, even in drought years

that greatly impact neighboring areas, the upper Beles still receives a considerable amount of rainfall. The annual potential evapotranspiration, a measure of water loss through evaporation and plant transpiration, is estimated to be around 1500 mm in the study area.

Table 3. 1. Climatic Classification (Daniel Gamachu, 1977)

Mean annual Temperature	Climatic classification		Region altitude (m.a.s.l)
Less than 10°C	Kur	Alpine	Above 3300
10- 15 °C	Dega	Temperate	2300 - 3300
15-20°C	Weina Dega	Subtropical	1500 - 2300
Greater than 30°C	Kolla	Tropical	800 - 1500
Above 40°C	Bereha	Desert	less than 800

3.1.4. Settlements

Numerous factors have an impact on how the population is distributed in the research region.There are several key determinants that contribute to the spatial patterns of human settlement. These factors include the compatibility of the climate with human habitation, the presence or absence of perennial water bodies, the suitability of the land for agriculture and livestock rearing, and the accessibility of communities to roads and marketplaces, among others.

In areas with favorable climatic conditions and the availability of perennial water sources, a significant population is found. This is particularly true in the lowland regions where water sources are present, or in close proximity to highland areas. Specific locations that have relatively larger populations include the highlands of the Wombera plateau, the Dangur and Balaya Mountains, the Dangila areas, as well as the lowlands of the Pawe and Dangur Manbuk areas. Additionally, populations

tend to cluster around water sources in other lowland regions.

3.1.5. Regional Geology

Western Ethiopia has a fairly complicated geology in general. The complex basement Precambrian rocks that make up this enormous lowland area, which borders the western and northwestern highlands, are covered with a surprisingly large number of Quaternary sediments. Tertiary volcanic are present in the elevated surrounding highlands and transitional regions.

According to the geological survey of Ethiopia Abu Ramla sheet, based on lithological associations, deformation types, and levels of metamorphism, it is possible to classify the geology of the basement rocks in western Ethiopia into three litho-structural zones. Across all of the domains, intrusive bodies and rocks of varying metamorphic grades can be seen. The lithological units can be divided into five major groups as follows:

- Gneiss and associated high-grade metamorphic rocks,
- Low-grade supra-crustal metamorphic rocks; which are mainly metavolcanic, metasediments, and associated ultramafic rocks,
- Syn- and post-tectonic intrusive of acidic to intermediate composition,
- Cenozoic volcanic rocks, and
- Quaternary sediments

Based on the stratigraphical sequence, four lithostratigraphic units can be identified. These are:

- Precambrian stratified and intrusive rocks (dominant in the area);
- Tertiary volcanic; and
- Quaternary sediments cover a wide area in the lowlands and along major river courses.

Three main domains are used to categorize the basement complex rocks in the area, each of which exhibits variations in lithology, structure, and metamorphic intensity. Between the western and eastern domains lies a high-grade center domain. Most of it is made up of premium gneiss. It is thought that the gneisses in the middle to upper amphibolite facies are Archaean or early Proterozoic in age and display migmatitic characteristics. A significant exposure of felsic to mafic metavolcanic rocks, interbedded metasediments, and instances of modified ultramafic bodies within the upper green-schist to lower amphibolite facies are all present next to this gneissic unit. Tectonic action produced the border between the gneissic unit discussed above and the metavolcanic unit. A number of foliated mafic to felsic plutons that originated as a result of significant tectonic processes have invaded both divisions. Additionally, the region has low-grade schist. Precambrian rocks are covered by Tertiary volcanic deposits in elevated areas. Alluvial, eluvial, and colluvial sediments cover large regions in the lower parts of the Abay River and its major tributaries, as well as at their confluence. unit.

3.1.6. Structural and Tectonic Setting of the study area

The predominant structural and tectonic orientations in the region are east-west (E-W), north-south (N-S), northeast-southwest (NE-SW), and northwest-southeast (NW-SE). Among these, the two most significant sets of linear features are the N-S and NE-SW lineaments. These lineaments exert a strong influence on the alignment of streams and rivers, as many of them flow parallel to these linear features. Sheared zones, which often run in a north-south direction, are typically 40 to 800 meters wide and consist of intensely deformed and fractured rocks. Additionally, there are numerous E-W trending lineaments that intersect the N-S lineaments. Springs are commonly found along these major regional structures, adding to the hydrological significance of these lineaments. A limited number of folds have been observed in the region, with the most prominent ones occurring in the western and south-central areas. The meta-sedimentary schists exhibit a parallel

alignment of bedding with the foliation, suggesting isoclinal folding. These folds are particularly noticeable on the escarpments that mark the boundaries of the Wonbera Plateau.

3.1.7. Local Geology

Different geological units are observed in the field and from geological maps prepared by different researchers, Ethiopian geological survey explanatory notes of Abu Ramla, Bure, Bahir Dar, and Asosa Sheet, and geophysical investigations of unpublished reports. The Beles basin is characterized by a geological composition that consists primarily of widespread Tertiary trap basalts and heavily folded and faulted Precambrian rocks. Thin layers of Mesozoic sedimentary rocks are interspersed between these two main formations. The geological unit exposed within the basin is described based on the information provided in the geological map of Ethiopia, which was compiled at a scale of 1:250,000.

Basement Complex Rocks - These rocks are highly variable in kind and distribution. Several distinct units can be identified in the area as described below. The Precambrian rocks can be grouped into two major groups: Stratified basement rocks and Intrusive.

A. Stratified basement rock can be identified in the study area.

1. **Gneiss** - These include biotite and hornblende-biotite gneiss. High-grade gneisses of amphibolite facies underlay the lowlands of Bullen, Dibate, and Wonbera woredas and along the Sudanese border. The biotite and biotite-hornblende gneiss are medium-grained, well-foliated, gray to dark gray colors with well-developed compositional layering.
2. **Meta-ultramafic rocks** - twelve meta-ultramafic bodies up to 0.5 km in width and 2 to 12 km in length have been identified in southern Bullen and Dibate woredas.
3. **Amphibolite**-mafic schists of predominantly volcanic origin are common in

patches in Mandura Woreda. This unit also includes amphibolite and quartzo-feldspathic schists which has primary features such as amygdala, indicating a volcanic origin.

4. **Metasediments** - The dominant rock types are of psammitic origin, with mafic schists of volcanic origin. Metasediments and metavolcanic include pelitic schists and rocks of felsic to mafic volcanic origin. In this unit quartzofeldspathic and graphitic schist are common. Metasedimentary schists, which are of low metamorphic grade, consist of intercalated green-schist, quartzofeldspathic schist, graphite schist, phyllite, quartzite with lesser biotite schist, meta-conglomerate, and marble.

5. **Marble (pgmb)** – Extended marble belt is evident in Guba, Bullen, Dibate, and Wonbera woredas. In this study area in Bullen, Dibate, and Wombera areas are not mappable. This unit is aligned along the N-S and NW-SE tectonic lines. The unit occurs as resistant ridges that can easily be delineated from aerial photographs and satellite images. These rocks are fine-grained and dark green, brown, or yellow. In a few places, they can easily be identified as white patches. Generally, they are massive and dense and cut by numerous quartz veins. Along some fractures, big cavities are observed which are likely produced due to the dissolution of calcite by percolating water.

B. Precambrian intrusive rocks have been identified in the study area.

1. **Metagabbro (mgb)** – patches of gabbroic plutons have been identified on the escarpments of Dibate woreda and as patches in Mandura woreda.

2. **Metaquartz diorite (dt) and meta tonalite (tn)** - rocks of plutonic origin occupy limited areas in patches. They range in composition from granite to diorite. They form a large, composite mass of batholithic dimensions in few places. Meta-tonalite is intimately associated with meta-quartz diorite and meta-granodiorite. They are massive or weakly foliated

3. **Metagranodiorite(pgdr):** - a large part of Central Dibate and Bullen woredas are underlain by meta-granodioritic rocks. This unit is associated with meta granite that shows strong foliation. They also form small stocks to large batholiths.
4. **Granite (gt1):** - outcrops in sixteen discrete, generally massive granite plutons ranging from 1 to 8 km in diameter are reported in the region. Plutons were probably emplaced during the last stages of regional deformation.

C. **Cenozoic (Tertiary and quaternary) Volcanics: -** Substantial portion of the study area is covered with Tertiary and quaternary volcanic. The most important ones are volcanic of the Dangur highlands and the Pawe plains along the course of the Beles River and adjoining mountainous areas. A few patches of basalt overlying the basement rocks have been identified in the northern part of Dibate Woreda.

Generally, in the study areas Tertiary and quaternary volcanic units can be identified below.

Ashangi Basalts:-Ashangi Basalts, which were formed approximately 55 to 24 million years ago during the Eocene-Oligocene period, exhibit distinct characteristics within the area. These basalts contribute to the formation of flat topography across most of the region, while in other parts, they give rise to elongated ridges and gorges. The basalt flows within this group are poorly defined and deeply weathered, with limited occurrences of tuffs. In some instances, these basalt flows may be tilted in relation to younger volcanic formations. The outcrops of Ashangi Basalts can be found in various locations, including the periphery of Balaya and Dangur plateau, as well as in the woredas of Jawi, North Achefer, and Dangila.

Figure 3. 3 . Ashangi basalt exposed at the lowland of Pawe

Tarmaber-Gussa Formation (E3tm): -is found in the northern Dangur region and the southeastern part of the study area. The basalt within this formation is extensively weathered and exhibits fractures on the outcrops. In certain areas, it has decomposed into soil, forming regolith. The hydrogeological characteristics of this formation vary depending on the local topography. It primarily consists of medium-to-coarse-grained rock containing plagioclase, pyroxene, and opaque minerals.

Aiba Basalts (E2ab):- are found in the southern, eastern, and northern regions of the study area, forming a rugged and undulating topography. They are highly weathered and fractured, with interconnected fractures allowing water percolation. The cliff-like structure and steep slopes reduce the storage capacity of the Aiba formation. However, groundwater can be obtained in the foothills through dug wells, serving local communities. The basalt appears dark grey when fresh and

reddish to yellowish brown when weathered. It is mostly porphyritic, exhibiting vesicular cavities filled with secondary minerals like zeolite and/or calcite. This group is exposed in the highlands of the northern Achefor and Kunzila areas.

Ignimbrite (Nig):- Ignimbrite (Nig) is a type of rock that is coarse-grained and densely welded. It consists of vitrophyric fiamme and lithic fragments, accompanied by rhyolitic lava flows that are interspersed with ash and unwelded tuffs.

Rhyolite with Minor Tuffs (Nrt):- it displays a color range from light grey to pink. It primarily consists of alkali feldspar, quartz, and mica. This rock type gives rise to small domes and circular to elliptical hills with gentle slopes that are unevenly distributed. In certain areas, the rock exhibits weak to strong joints oriented both vertically and horizontally. Additionally, intercalations of fine ash and unwelded tuffs can be observed in certain locations.

Quaternary Basalt (Qpb):- represents the youngest and largest unit of volcanic rock on the plateau located to the east of the study area. This unit is known for forming flat plateaus that extend horizontally. Within this unit, there is a variation in texture observed in the exposed outcrops. The Quaternary volcanic succession primarily comprises basaltic breccia and tuffs, as well as blocky, fractured, and vesicular basalt. These basalts have a porphyritic and glassy structure. The thickness of the Quaternary volcanic rocks is estimated to exceed 100 meters, potentially reaching 200 to 300 meters.

Figure 3. 4. Quaternary basalt exposed at Kar Mountain

Quaternary Deposits The Geological Survey of Ethiopia's geological map of the area ignores areas of Quaternary cover, either because soil types may be inferred from bedrock types or because the area of thick alluvial cover is too tiny to be visible at the size of the map.

The Quaternary deposits in the region are dominantly alluvial and in wide flat areas of residual soils and they mainly deposit along the river course and lowland of the study area. The alluvial deposit was exposed in the west of Wombera at the periphery of the Abay and Beles Rivers. The thickest deposit is found along the course of the major rivers. Groundwater in the alluvial deposit may not be deep. The colluvial deposit was also observed in the Guba woredas in a small part of the study area. In most cases, the thickness of the Quaternary deposits is less than ten meters. This does not allow storing substantial groundwater.

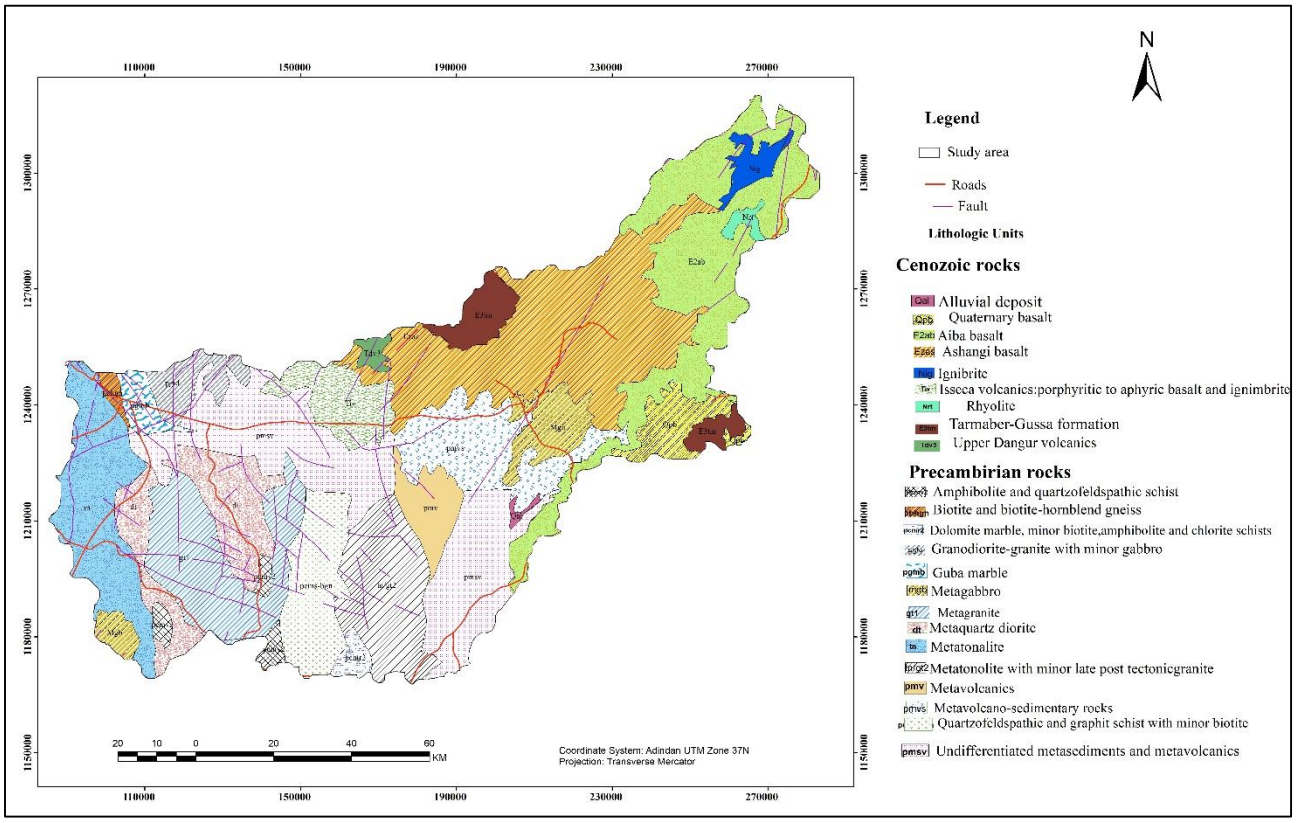

Figure 3. 5. Geological map of Beles (Modified from GSE, 1997, 2002, 2007, 2010)

3.1.8. Hydrogeology

The hydrogeology of the study area is primarily influenced by various factors, including the geological background, terrain formation, rainfall patterns, and groundwater movement through interconnected primary and secondary porosity within the aquifer system. To assess the productivity of the aquifer, field observations and geological/lithological descriptions play a crucial role. These observations provide indirect evidence regarding the potential of a rock unit to serve as an aquifer with low, moderate, or high water quality. Key hydrogeological field observations include the distribution and volume of spring discharges, the degree of rock unit fracturing, the thickness of formations, grain size, rounding, and sorting, clay proportions, the type and degree of cementation, as well as the extent of weathering. The aquifer classification in the study area relies solely on

indirect hydrogeological field observations since pumping test data is not available. Geological formations naturally contain groundwater, and its presence is influenced by the water-bearing properties of the rocks, which are primarily determined by their origin and geological processes. Based on a qualitative assessment of water-carrying qualities, various hydrogeological units were identified, including fissured and fractured basalt aquifers, fractured and karst openings in marble formations, weathered and fractured portions of crystalline basement rocks, as well as slightly weathered and locally fractured crystalline basement rocks. The GSE explanatory notes highlight that groundwater in metamorphic rocks is predominantly stored in tectonically affected regions, fractured zones, and the weathered mantle known as the overburden or regolith. Tertiary and Quaternary volcanic rocks are widespread in the northern and eastern highland plateaus, as well as the north-central lowland plateaus, covering approximately 39.66% of the total area..

The study area's groundwater distribution is greatly influenced by the local climate. The highland plateaus in northern Balaya, northeastern Dangilla, eastern Kar Mountain, and southwestern Wombera, covered mostly with volcanic rocks, experience abundant rainfall annually. In contrast, the central and western regions, dominated by a basement complex, receive relatively low rainfall, resulting in low drainage density and limited groundwater recharge. The highland plateaus, intersected by perennial rivers, serve as the primary source of groundwater recharge.

As one moves from the northern and eastern highland plateaus to the low-lying Beles basin, rainfall gradually decreases due to decreasing elevation and forest cover. Tectonic events also play a significant role in shaping the flow and distribution of groundwater in the study area. Regional structures, deformational processes, and metamorphic events impact the Precambrian rocks present. Lineaments, causing isolated volcanic ridges and depressions, create a small hydrogeological basin with shallow groundwater. These lineaments also give rise

to localized alluvial fans and deposits from intermittent streams.

Aquifer classification considers the representative rock forms within isolated areas to evaluate the usable groundwater supply. During the field investigation, over 2500 water points were surveyed, with 120 of them inventoried and sampled. These points, including boreholes (BH), springs (CSP), and hand-dug wells (HDW), were used to create groundwater flow direction and contour maps.

The aquifer/aquitard system in the area has been determined through various sources, including the GSE hydrogeology explanatory notes by Getahun Seyid (2002) at a scale of 1:250,000, unpublished reports on geophysical investigations, and data from field inventory hydrogeological characterizations.

Porous aquifers – such as alluvium and colluvium, store groundwater within the pores of unconsolidated materials. Alluvial fans, mainly composed of sand and gravel, exhibit high porosity near the mountain slopes. However, as one moves away from the mountain edge, both the effective porosity of the fan deposits and the hydraulic gradients decrease. Consequently, this leads to a decline in groundwater potential and a deterioration in water quality.

Fissured and karst aquifers (marble) – The entire thickness of the marble body is covered in fissures where groundwater is stored. Karstification along certain of these fissures might increase their permeability. The control of solution phenomena and karstification in the underground drainage of carbonate rocks is determined by the base level. This base level can be represented by a perennially draining stream and/or an impervious formation within the carbonate aquifer, such as graphite schist or intrusive rocks. It can also exist outside the carbonate rocks. The base level influences the interaction between the water table and the carbonate aquifer, as well as the processes of solution and karst development. A carbonate rock surface covered in soil or another relatively permeable, less soluble material is preferable to bare rock for the start of karstification. The area where the water table is located

between its highest and lowest points is where the rock is likely to dissolve the fastest.

Fissured aquifers (sandstone and volcanic rock) – The groundwater is held in joints and fissures across the entire thickness of lava flows, as well as in pores and fissures throughout the entire thickness of sandstone and conglomerate layers. The structure that is primarily present in stratified sedimentary rocks is the one that is most conducive to groundwater accumulation. Sandstone has a porosity range of less than 5% to as much as 30%.

The hydrogeological characteristics of volcanic rocks are significantly influenced by geological time. With the passage of geological time, porosity and permeability both tend to decrease. Young lava flows may have high porosity, but the permeability is mostly determined by a mix of primary and secondary rock formations. The main vertical barriers in young volcanic rocks are dykes. While usually, porous, pyroclastic rocks connected to lava flows are not extremely permeable due to poor sorting and an excess of fine particles. Large-scale volcanic ash layers could provide semi-horizontal impediments to water circulation. The aquifers are expressed in the hydrogeological map in light green.

Fissured aquifers of low potential (some non-carbonate metamorphic and intrusive rocks) – The primary storage of groundwater in these hard rocks occurs within fractured zones and the weathered mantle, also known as the overburden or regolith. Fractured aquifer zones are typically located at shallow depths, around 50–70 meters below the surface. However, as depth increases, the fractures tend to close. In igneous rocks, faults and joints are predominantly vertical, except for minor fractures, sheeting, and exfoliation that align parallel to the rock surface.

Among partially decomposed rocks, the subsoil zone exhibits the highest permeability. Wells that access this zone yield nearly ten times more water compared to tapping into unweathered (fresh) rock. The hydrogeological map

(Figure 3.7) depicts the representation of these aquifers.

Aquitards– consisting of non-carbonate metamorphic and intrusive rocks, are present in the study area. The fractured zones and the weathered mantle known as overburden or regolith are where the majority of the groundwater in hard rocks is essentially stored. Mafic mineral-rich rocks are more likely to weather in a clayey manner. Because the fractures are sealed by clay particles, they will also tend to close as the depth increases.

3.1.9. Classification of aquifer

Quantitative classification of the aquifer is carried out based on the value of transmissivity and/or yield of water points as follows:

3.1.9.1. Extensive and highly productive fissured and karstic aquifers

Precambrian marbles- it found in the southern and northwestern parts of the study area, specifically near the Bullen-Wombera boundary and in the Guba woreda, southeast of Mankush town. These marbles exhibit jointing in certain areas and contain solution holes. The spring located in this formation, southeast of Mankush town, experiences limited production during the peak of the dry season, as noted in the GSE Abu Ramla report. However, locals have reported an increase in yield during the rainy season. Geomorphologically, this outcrop is situated in the lowlands, characterized by poor recharge potential. The entire thickness of the marble body's fractures is thought to be where groundwater is stored, and karstification along portions of these fissures has made them more permeable.

South of the study area, there is elevated well-jointed marble with significant solution holes, as observed in GSE Asosa-Kurmuk sheets NC36-7 and NC36-8. This region features multiple cold springs, with a maximum discharge exceeding 15 liters per second, indicating excellent recharge. Based on field observations and spring output, the fractured and karst aquifer within the marble can be considered moderately productive.

Quaternary Basalt: - it extends from the quaternary basalt of Bahir Dar in the northeastern portion of the research region, showing high discharge for small drawdowns in general, while in Dangila showing high drawdown for small discharges, indicating that the productivity decreases southward. This rock unit includes young lava fields characterized by aligned spatter cones and lava flows originating from volcanic centers. These lava fields exhibit fractures and high temperatures. The aquifer potential of these rocks has increased due to the interconnected pore spaces formed through the fracturing process. Considering all these factors, Precambrian marbles and Quaternary basalts are typically classified as highly productive aquifers.Taking into account all of the aforementioned factors, Precambrian marbles, and Quaternary basalts are typically categorized as an aquifer with high production.According to the GSE, this formation has aquifer parameters within the following ranges: transmissivity (T) greater than 100 square meters per day, specific capacity (q) exceeding 1 liter per second per meter, and discharge (Q) surpassing 5 liters per second.

3.1.9.2. Aquifer with moderate to high productivity

The GSE report indicates that this formation comprises a fractured and intergranular aquifer with average values of transmissivity (T) ranging from 100 to 10 square meters per day, specific capacity (q) varying from 1 to 0.1 liters per second per meter, and discharge (Q) ranging from 5 to 1 liter per second.

The Ashangi Basalt, which is found in the northeastern highlands and along the northern border of the research area, is a type of fissural flood basalt. This basalt formation is often intruded by dolerite dykes and sills. It is characterized by its fractured nature, considerable thickness, and significant weathering, as cited in Merla (1979).This unit's spring discharge can range from 0.5 liters per second to 10 liters per second, but it typically exceeds 2 liters per second. As a result, this unit is regarded as a moderately to highly productive aquifer.

3.1.9.3. Extensive and moderately productive fissured aquifers

Tertiary volcanic rock: - The Tarmaber Basalt and Aiba Basalt are two tertiary volcanic rock formations that are mostly found in the eastern, northeastern, and northern parts of the study area.

Tarmaber Basalt: - this unit encompasses the northernmost region of North Achefer, a sizable portion of Jawi, and the lowlands surrounding the escarpments of the Dangur and Balaya Mountains. It typically lies in a variety of topographic regions. It is fairly worn and joined. Tarmaber basalt is typically categorized as a moderately productive aquifer.

Aiba Basalt: situated in the northeastern part of the region, occupies a relatively small area. This rock unit exhibits jointing and is highly weathered. As a result of the fracturing and weathering processes, the Aiba Basalt can serve as a suitable aquifer, containing moderately productive zones with a satisfactory water yield.

3.1.9.4. Extensive and Low productive fissured aquifers of basement

This particular aquifer is present in certain non-carbonate metamorphic and intrusive rocks. The aquifer system primarily consists of Precambrian basement rocks, which encompass a combination of high-grade and low-grade metamorphic rocks along with granitic intrusions. Regrettably, the less economically viable rock unit of crystalline basement rocks dominates the research area, as depicted in Figure 3-9. The groundwater potential in this region is considered poor due to the extremely low permeability of these hard rocks and the limited recharge at this level.

The formation extends across the southern and western parts of the research area, encompassing valley slopes, escarpments, and a significant portion of the lowlands and escarpments in the Mandura and Dangila woredas. These areas consist of metabasalt, meta-andesite, and green schist. The structure of this formation leads to rapid drainage of groundwater, and recharge is virtually absent at lower

elevations.

Groundwater in the crystalline basement rocks is limited to fractures and weathered zones. However, proximity to volcanic aquifers provides some recharge contributions, especially for basement rocks near the volcanic plateau. These units are generally classified as a low-production aquifer. The aquifer parameters for this formation range from T=10-1 square meters per day, q=0.1-0.01 liters per second per meter, and Q=1-0.5 liters per second.

3.1.9.5. Minor and Local Aquifers

Ignimbrite (Nig), and rhyolite with minor tuffs (Nrt) represent minor local aquifers. The productivity of these aquifers is mainly governed by their capacity to transmit, store and yield water. These parameters are directly or indirectly controlled by the topographic setting, both primary and secondary porosity, the amount of recharge, and areal extent. Although scoria has sufficient primary porosity, its small areal extent and dome nature determine its storage capacity as an aquifer. Both ignimbrite and rhyolite have low primary and secondary permeability; however, the small areal extent also affects their storage capacity.

3.1.9.6. Aquitards

This aquifer is composed of specific non-carbonate metamorphic and intrusive rocks, namely meta-tonalite and gneisses, which are predominantly located in the lower western and southern parts of the study area. These rocks exist as extensive outcrops with very limited permeability, classifying them as either an aquitard or a regional aquiclude. However, in their slightly weathered state, they do exhibit localized aquifer characteristics.The aquifer parameters for this formation are as follows: transmissivity (T) ranges from 0.1 to 1 square meters per day, specific capacity (q) varies from 0.001 to 0.01 liters per second per meter, and discharge (Q) ranges from 0.5 to 0.05 liters per second.

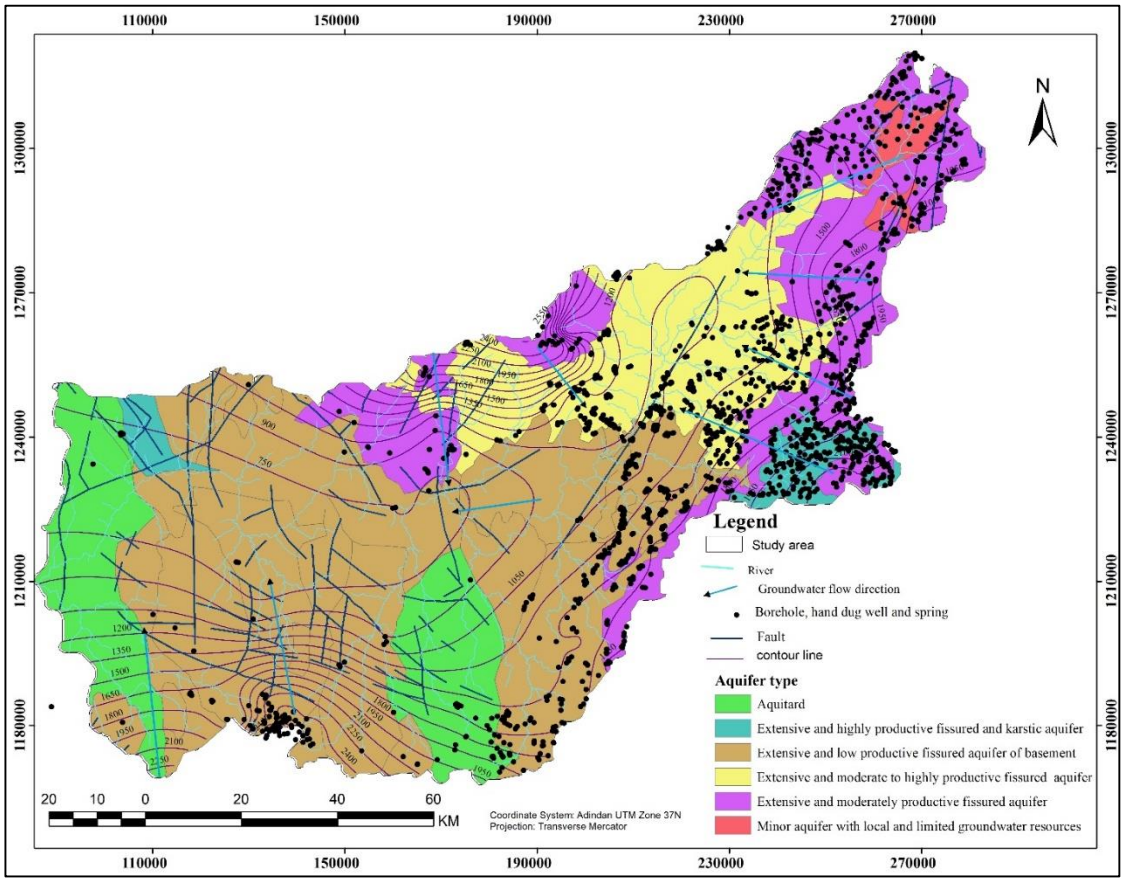

Figure 3. 6. Simplified hydrogeological map of Beles basin (modified from GSE, 2005 and 2017)

3.1.10. Water Points and existing water supply

Based on information gathered from various organizations and water-related specialist agencies in various years, 105 springs, 350 hand-dug wells, 25 shallow wells, and 6 boreholes had been constructed and drilled. Due to the abundance of shallow groundwater, particularly in Chagni town and its adjacent areas with minimal discharge, there are a lot of hand-dug wells in the area. In comparison to springs and manually dug wells, there are surprisingly few boreholes in the area. In the study area, Dig Dams also services for irrigation for downstream communities.

Boreholes

Governmental, non-governmental, and private drilling companies have both drilled deep and shallow boreholes in the research region. There are 25 shallow boreholes with a depth range of 27–50 meters and roughly 6 deep boreholes with a depth range of 50–196 meters.

The information from some of the boreholes is incomplete, which is important for hydrogeological research. They lack information on depth, hydraulic conductivity, transmissivity, and static water level. The Ashangi Formation is located in the Faguta Lekuma area, and the maximum depth of the well, according to the available data, is around 196 m. The Bulen woreda in the Bakuji region is home to Gaze, a well that is about 27 meters deep and drilled into a marble formation. The main aquifers are found in basaltic layers that have been strongly, moderately, and mildly fractured and weathered. While the majority of the boreholes driven into Quaternary basalt are shallow, those into the Tarmaber-Gussa and Ashangi Formations range in depth from medium to deep.

As seen by the borehole log data, distinct strata, and aquifers are intercepted by deep well boreholes in particular. A single well intercept unconfined, semi-confined, and confined aquifers, demonstrating the presence of multilayer aquifers despite the lack of information regarding the vertical and lateral variations of the aquifers with restricted data sources. The hydrogeological map and general information about the boreholes presented in annexes 1 and 2 both show the hydraulic characteristics of the wells.

Hand-dug wells

Within the research region, there are numerous hand-dug wells used for livestock and human consumption as well as for washing. These hand-dug wells are abstracted manually, and their depths range from 5 to 21 meters with a static water level of 1 to 3 meters. In most highlands and alluvial deposits in the lowlands, thick

overburdened soil is recognized to constitute the predominant aquifer formation. Hand-dug wells can also be successfully constructed on highly worn volcanic rocks found in the lowlands of the Mentawuha and Bulen woreda. The majority of dug wells offer a consistent source of water, although, during the dry season, production significantly decreases.

The direct recharge condition from precipitation into the well, which internally reflects the unconfined character of the aquifers, is responsible for the seasonal variation of the static water levels in the majority of wells. The yield, depth of penetration, and recovery of the hand-dug well development option may be limited in some circumstances, and motor pumps may not be useful to abstract water from the hand-dug wells, as has already been seen in several villages. According to estimates made using user data, the yield of many hand-dug wells is less than 1 l/sec, and this low yield will have a restricted ability to water the farmer's plots. Details about the hand-dug wells are listed in Annex 2.

Springs

Springs in the study area emerge from the hillside, depression, and slope break of the topographic setting. In the study area about twenty-six Contact, depression, and fracture-type springs are the dominant types of springs. These springs from quaternary volcanic rocks on the other hand are located in flat topographic terrain and have better discharge. Most springs produce less than 2/s but three springs produce more than 2 l/s on fractured volcanic rocks in the study area. Springs are generally evenly distributed in volcanic rocks but are rare in lacustrine and alluvial deposits. The highest discharge of spring in the study area is elaborated below.

Ali Spring

Ali Spring is located east of Pawe town right at the border of Metekel Zone and Awi Zone of Amhara Regional State. The spring has high discharge (Estimated yield of 36 l/s). The great majority of the population within the Pawe woreda depends on

Ali Spring. Ali Spring is a gravitational spring and has been developed and diverted by a pipeline to the different villages and towns it was established in 1980 and the overflow of the spring discharge around 15l/sec of water used for small-scale irrigation downstream of the spring, especially for wobo kebeles, in Jawi woreda.

The reservoirs are not functional for a long year and now after rehabilitation conducted in 2008, the main pipeline that connects the spring with towns (Pawe and Almu) is functional. The reservoir is far 2 kilometers from the spring. Even the existing pipeline has substantial leakage problems. This spring has a great sanitation problem. Because the dam is unprotected and has no treatment mechanisms. According to the information from the community, the spring discharge is decreasing from time to time.

Figure 3. 7 . Ali spring. The left-hand side picture is a reservoir, the middle one is the water body of Ali Spring, and the right-hand side was an overflow of the spring (taken from Pawe water office).

2. Abatachin Spring

The Abatachin Spring originates along a large regional fault that runs from north to south, tucked at the base of the magnificent Kar Mountain Ranges, about 1.5 km to the east of the charming village of Genete Mariam. An adjacent river that flows

in a meandering direction toward the Beles River originates from this spring. Notably, the spring's 7.5 liters per second discharge rate demonstrates how much water is flowing through it. The spring operates as a mechanized pump, providing a vital water supply to the towns of Gente Mariam (Mandura) and the regional hub, Gilgel Beles town. Remarkably, over 75 percent of the water consumed within these two towns originates from this very spring. The water is efficiently pumped to a reservoir situated in Genete Mariam town, from where it gracefully cascades by the force of gravity to reach Gilgel Beles town, located approximately 12 kilometers away. Despite this system in place, both towns continue to face challenges related to water scarcity.

3. Daphily spring

Daphily Spring is a gravitational spring situated 2.5 kilometers northeast of the small town of Mandura. It emerges from the foot of the Kar Mountains. The spring diverted by a pipeline to the kebeles of Daphily and services for communities.

4. Gisa spring

This spring is located in Dangila Woreda, 20 kilometers to the west of Dangila town. According to the Woreda water office, the spring has 11 locations with a combined area of roughly 0.05 km2 and an average discharge of 30 l/s. A heavily fractured and weathered porphyritic basalt geological formation can be seen in the vicinity. To provide water to nearby small towns and rural communities via pipes, three of these springs are now being built. According to data from the woreda water bureau, the three-spring discharge rises from 5 l/s during the summer rainy season to 8 l/s during the winter dry season. However, following development, its average discharge has increased to almost 10l/s. Its recharging region may be far from the discharge/spring, which is the likely cause of this increase in discharge during the dry season.

5. Littles Beles Dam 1243 (Diga Dam)

The Beles River basin has drawn a lot of attention as a focal point for massive development projects since the 1980s. Notably, the Tana Beles project has been carried out primarily to support irrigation operations and capture the potential of hydroelectric power generation. The Diga Dam has been built close to the town of Pawe as a result of this project. The Tana Beles Project's development was consequently momentarily stopped. Creating hydropower and using the dam for irrigation are the main goals behind its construction. This river water source is abstracted by a conventional concrete gravity Dam provided with steel logs to enable raised crest for water storage. The dam top is provided with an electrically driven hoisting mechanism that places and dismantles the steel logs to be placed across the spillway crest for storage during the dry season.

It has not yet been completely appreciated how Diga Dam might be used for water supply needs. The Pawe woreda settlement now has a water delivery system in place; however, it is only operational during the dry season. It is crucial to remember that this system does not have a treatment facility, and its drainage system is inoperable. In the long run, the Diga Dam has bright prospects for providing a crucial water source for sizable rural and urban settlements located downstream.

The basic problem at the dam is the malfunctioning of the electromechanical system provided for the hoisting mechanism and illumination purposes. Also, the siltation behind the dam that covered the intake ports is the other crucial problem. Silt has been deposited behind the dam in all areas except across the crest of the spillway.

Figure 3. 8. Littles Beles Dam 1243 (Diga Dam)

3.2. Methods

3.2.1 Data collection

To conduct this research, an extensive collection of meteorological data spanning a remarkable 30-year period was obtained from the esteemed National Meteorological Agency of Ethiopia (NMAE). This comprehensive dataset encompasses monthly records of precipitation, minimum and maximum temperatures, relative humidity, sunshine hours, and wind speed. Furthermore, river gauge data concerning the Main Beles and Gilgel Beles Rivers, along with water point inventory data, were diligently gathered from the Ahmara Water and Energy Office, the Ministry of Water and Energy, and various other organizations, in addition to the meteorological data. In order to facilitate the application of the Wetspass model, which computes groundwater recharge for the research area, essential input data of a physical nature were procured from the region. These

encompassed a 30-meter-resolution SRTM DEM (Digital Elevation Model) and served to drive the analysis of land use, land cover, and soil textural type. These valuable resources were obtained from the esteemed Ministry of Agriculture and Food.

The collected data underwent thorough analysis employing a range of software tools, including MS-Excel, Arc-view GIS 3.2, GIS ArcMap 10, Global Mapper 11, Surfer 10, USGS GW Toolbox, and WetSpass-M software. These diverse and specialized software applications were instrumental in extracting valuable insights from the collected data.

3.2.2. Methods of recharge estimation

3.2.2.1 Wetspass model

To conduct this study, the Python-based WetSpass model (WetSpass-M) was employed. Originally developed by Batelaan and De Smedt (2001) and later modified by Batelaan and De Smedt (2007), the WetSpass model—abbreviated for Water and Energy Transfer in Soil, Plants, and Atmosphere under quasi Steady State was adapted to suit the specific climatic and land conditions found in the tropical region under investigation. Notably, certain adjustments were made to account for variations in the length and timing of seasons between temperate and tropical areas. While temperate regions typically experience six-month summers and winters, in Ethiopia, summer spans four months while winter extends over eight months. Furthermore, disparities exist in the timing of rainfall seasons and land use/land cover patterns. Therefore, to apply the WetSpass model to the Beles catchment, modifications were made, including the use of an eight-month winter and four-month summer input for the meteorological grid map, as well as adjusted summer and winter land-use parameter tables. The WetSpass model itself is a numerical tool designed to simulate the average spatial distributions of hydrological parameters and processes over the long term, specifically at the basin scale, while operating under a quasi-steady state condition. This implies that the model considers

variations solely within seasonal or monthly time scales, wherein years of seasonal or monthly data are condensed into single seasons or months for analysis.

The model subdivides the precipitation into the runoff (to refer only to the surface component of the river flow in this paper), evapotranspiration, and groundwater recharge, and estimates long-term seasonal values as distributed spatial maps.

$$P = S + ET + R \quad (1)$$

Where P is precipitation [L], S is runoff [L], ET is evapotranspiration [L], and R is groundwater Recharge [L].

$$S = f1 * Pn \quad (2)$$

Where f1- is a runoff factor that depends on land use and vegetation characteristics, soil texture, and slope.

Pn- is the net precipitation reaching the ground surface (total precipitation minus interception by the plant canopy).

$$ET = f2 * EP \quad (3)$$

Where f2 -is an evapotranspiration factor that depends on land use and vegetation characteristics and soil texture, and EP is the potential evaporation of open water [L].

The estimation of groundwater recharge is accomplished by deriving the above equation 1.

The WetSpass-M model computes hydrological components for each pixel by subdividing it into open water, impervious surfaces, bare soil, and vegetated areas. The model assigns percentage values for these subdivisions based on the parameter table, with some adjustments made by local experts for specific land use classes.

In this research, the model is developed at 1000 m x 1000 m grid resolution. Hence, all nine input parameter grid maps are resampled to the same grid size. The model area is equally meshed and has 198 columns and 152 rows. WetSpass has parameter tables as an input besides the grid maps. Some land-use parameter values and the number of rainy days are modified into local contexts based on measured data and our expert knowledge whereas the default values of soil-related parameters have been kept. For instance, the root depth for forest land use is changed from 2 m to

5.5 m because eucalyptus (the dominant forest tree in the area) is deep-rooted. A similar modification was made by Yenehun et al. (2020) for the highland part of the Gilgel Abay catchment.

The developed WetSpass model is calibrated manually by adjusting the global model parameters, such as rainfall intensity, soil moisture alfa coefficient (α), LPa calibration parameter for adjusting the potential evapotranspiration depending on the soil moisture, interception parameter (a), and runoff delay factor (x). In the calibration process, the goodness of fit between the simulated and measured runoff for major rivers was checked and has been used for further model optimization. Moreover, the comparison of point recharge values derived from the baseflow separation method and the extracted recharge from the spatial map generated by WetSpass serves as a validation of the obtained result.

3.2.2.2. Baseflow separation methods

Stream discharge records offer insights into the water yield of the Beles basin at the stream gauging site.The exchange between the stream and groundwater system can be inferred from analyses of both short- and long-term discharge records. The baseflow component of a stream flow is assumed to represent the groundwater recharge of an area. However, base flow separation proves useful when estimating annual, or event, groundwater exchange (effluent conditions). In this study, a detailed analysis of the baseflow using different methods will be employed to determine the amount of water flowing from the groundwater system to surface water bodies or vice versa (Woessner, 2020).

3.2.2.3. Chloride mass balance (CMB)

The CMB method, based on the principle of mass conservation, assumes that there is a balance between atmospheric chloride input and chloride flux in the subsurface. The suitability of the chloride ion for chemical recharge studies stems from its conservative nature, as it does not leach, adsorb to sediment particles, or participate

in chemical reactions (Cooper et al., 2013). However, there are certain conditions under which the method may fail. For example, if the soil contains sources of chloride other than those present in rainwater, such as halites, the accuracy of the results can be compromised (Huang and Pang, 2010). Additionally, factors like wind-induced salt recycling, unaccounted runoff, and uptake by harvested plants can also introduce distortions to the outcomes.

The chloride mass-balance method has another limitation related to the uncertainty in determining atmospheric deposition, including both wet deposition from rainwater and dry deposition from aerosols and dust (Naranjo et al., 2015). The accuracy of these determinations is primarily affected by the deposition of sea-salt particles on vegetation, such as leaves, fine stems, and branches. The CMB approach, in comparison, offers a cost-effective benefit since it just needs information on the yearly precipitation, the concentration of chloride in the precipitation, and the concentration of chloride in the groundwater of the particular aquifer under study (Bazuhair and Wood, 1996).

To estimate groundwater recharge in the Beles basin using the CMB method, several assumptions were made:

1. Precipitation is the sole source of chloride in the groundwater.

2. Chloride acts as a conservative component within the system.

3. Steady-state conditions exist with regards to long-term precipitation and chloride concentration.

4. Chloride does not undergo recycling within the watershed.

In this study, a total of 13 groundwater samples were gathered from hand dug wells and boreholes across the study area. The sampling sites were statically distributed within the study site. Furthermore, during the rainy season of July 2023, four rainfall samples were collected and analyzed to determine their chloride concentration. The average chloride concentrations in both precipitation and

groundwater samples were calculated using the measured values over the entire study period. The chloride content of the samples was analyzed using the titration method, which involved the use of AgNO3 (silver nitrate).

3.2.2.4. Limitation of the methods

The assumptions made when using these base flow separation methods are that factors such as diversion of upstream river water, water extraction, effluent from treatments, inter-basin groundwater transfer, and channel losses are negligible. However, as cited in Hautet et al. (2006) and Prove et al. (2006), the presence of deep-seated geological structures, ancient fluvial deposits, and multiple episodes of volcanism in the Tana area may facilitate interbasin groundwater flow from the Tana basin to the Beles basin. It is important to mention that physical characteristics such as geology, hydrogeology, unsaturated zone properties (soil moisture), elevation differences, and climatic and meteorological factors are not taken into account when estimating recharge.

Base flow analysis is useful for understanding how groundwater inputs change over time along a stream, but it does not provide information on their spatial distribution between gauging stations. Additionally, this analysis is only applicable to gaining streams, as noted by Brodie and Hosteler (2005). In the study area, as the river flows downstream, the discharge decreases, indicating a Losing River phenomenon. This limitation is one of the constraints of the study basin.

The fact that the rainfall samples were only obtained during a single rainy season presents another obstacle to using chloride mass balance techniques in this study location.

CHAPTER 4

4. RESULT AND DISCUSSION

Numerous different results relating to the hydrological component were attained in this chapter and then examined. In particular, the catchment's yearly water balance component was examined in light of the results produced by the WetSpass model. Additionally, the regional distribution of seasonal and annual groundwater recharge generated from the WetSpass data was carefully evaluated and elaborated. The average recharge brought on by the separation of base flow was also carefully assessed and discussed. The objective was to clarify the complex elements and significance of these findings within the framework of the investigation..

4.1. Hydrometeorological data analysis

Numerous meteorological components, such as atmospheric pressure, temperature, humidity, wind, and rainfall, are included in climate. It represents the average over the course of time for various components in the given area. There are many variables that affect climate features, but latitude, altitude, vegetation cover, density, and rainfall patterns stand out. These variables interact intricately, causing a chain reaction that starts a number of connected processes in motion. Rainfall, runoff, recharge, stream flow, and groundwater dynamics are all examples of hydrological processes that result from this dynamic interaction between climate factors and physical characteristics. Estimating these hydrological processes within the Beles basin involves computing the values of meteorological variables and river hydrographs. Fortunately, the region has a sizable number of meteorological stations that help with the gathering of important data.

The researcher received monthly meteorological data from a total of 12 sites from the National Meteorological Agency of Ethiopia (NMAE). It is significant to note that the characterization of hydrometeorology was impacted by the limited and imperfect climatic records that were available. Most of the meteorological stations are located in a small number of urban areas. On the other hand, daily river discharge statistics for two rivers with gauging stations**,**the Main Beles and Gilgel Beles rivers were solely received from the Ministry of Water Resources. These data show large discharge level oscillations due to a variety of topographical features, precipitation patterns, vegetation cover differences, and infiltration conditions that vary across the study area.

4.1.1.Precipitation

Precipitation plays a significant role in the hydrological system, particularly in influencing the spatial and temporal distribution of recharge. The amount of rainfall experienced in a specific region is influenced by various factors, including the physiographic and geomorphological characteristics of the area, the circulation patterns of moisture, the proximity to moisture sources, and the temperature of the basin. In the study area, the rainy season spans from June to September, exhibiting a uni-modal character that aligns with the hydrograph of the Beles catchment (see Figure 4.1). Furthermore, the basin can be predominantly categorized into two seasons based on the Intertropical Convergence Zone (ITCZ) (see Figures 4.1a, b).

As a consequence, the dry season, known as Bega, prevails from October to May as a result of the southward movement of the Intertropical Convergence Zone (ITCZ) in the eastern part of Africa. During these months, the region is primarily influenced by the northeasterly trade wind originating from Arabia. Consequently, a minuscule rainy season, referred to as Belg, occurs from March to May, although it is not considered a separate season within the sub-basin. In March, the ITCZ gradually shifts northward, leading to the development of low pressure in Sudan and Arabia while high pressure systems form over the Gulf of Aden and the Indian Ocean.

The primary rainy season, known as Kiremt, commences in June and extends until late September. This season coincides with the northward migration of the Intertropical Convergence Zone (ITCZ) during the spring and, more significantly, the summer in the northern hemisphere. As a result, the study area receives the majority of its monsoon precipitation from both the Atlantic and Indian Oceans during this period.

The highest recorded annual rainfall in the region is 2367mm at the Injibara station, while the lowest minimum is 1035mm at the Mankush station (see Annex 5). To ensure the suitability of the WetSpass model, the meteorological data were categorized into two seasons: summer (encompassing the months from June to September) and winter (encompassing the period from October to may). These data were then interpolated separately to generate input maps for further analysis.

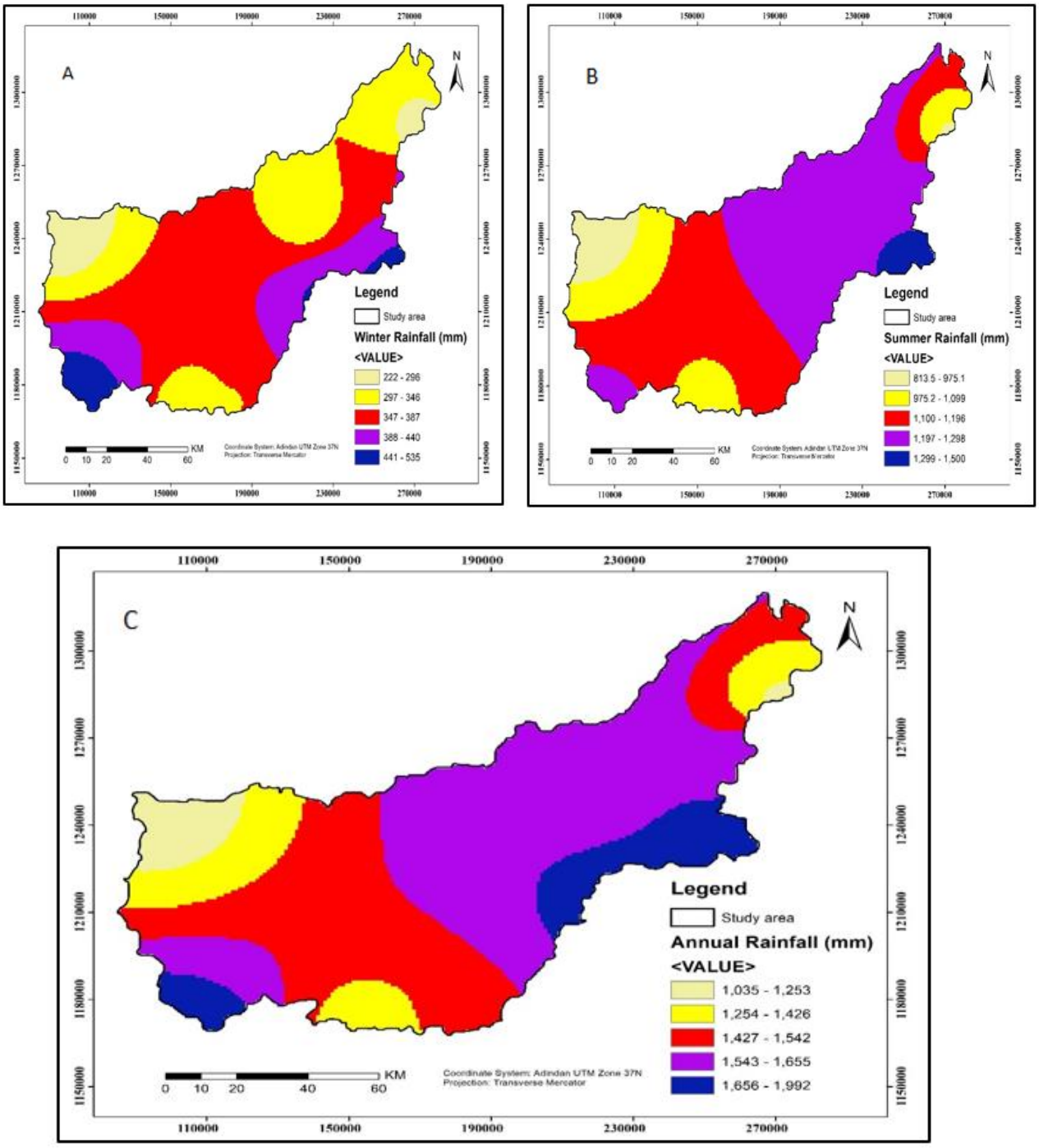

Figure 4. 1. Seasonal and spatial distribution rainfall in Beles basin a).Dry season precipitation. b). Rainy season precipitation c). Annual precipitation

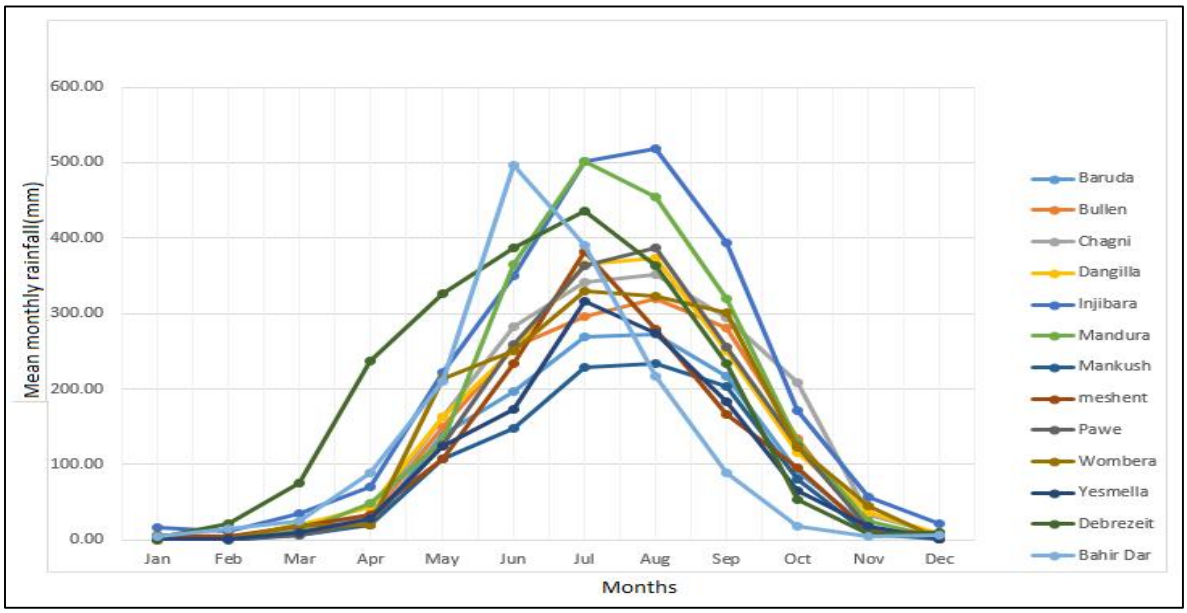

Figure 4. 2. Uni-modal rainy Seasonal distribution of rainfall in Beles basin

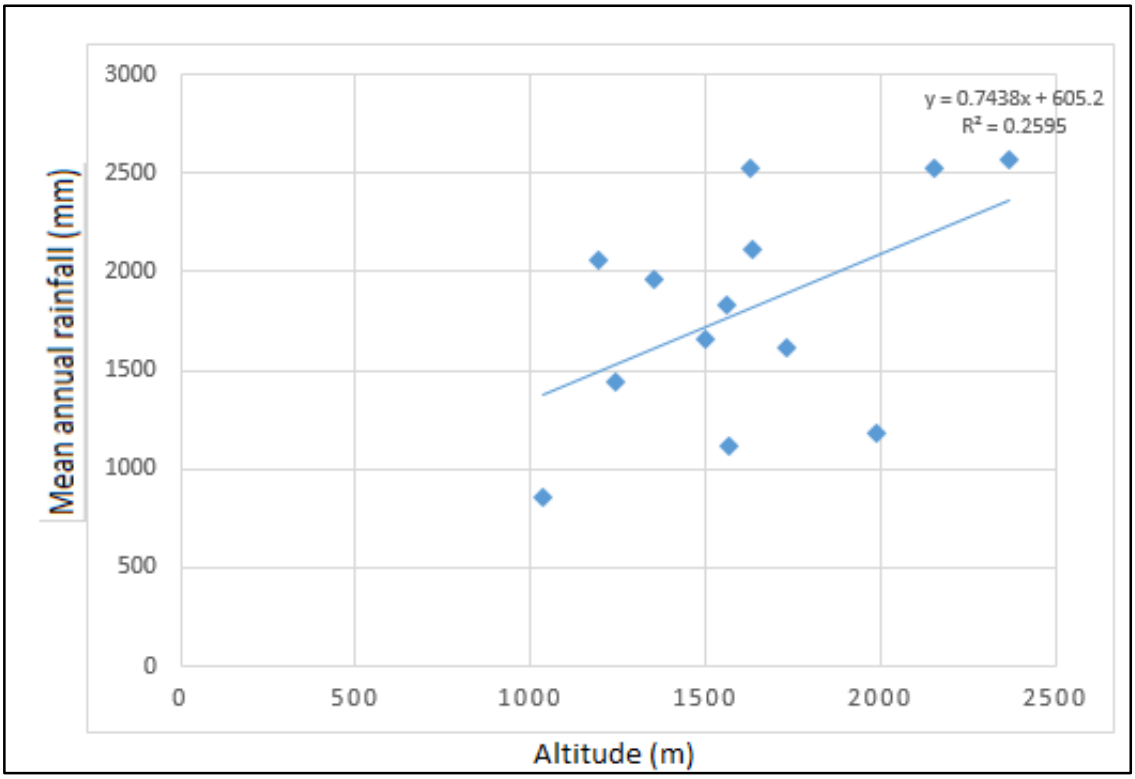

Figure 4. 3. Relation between Mean annual precipitation and altitude (NMA)

As per the findings by Daniel Gamachu in 1977, the primary rainy season in the study area occurs from June to September, when moist winds from the Atlantic and Indian Oceans converge over the Ethiopian highlands. As displayed above figure 4.3, the observed amount of rainfall at the meteorological stations, as provided by the National Meteorological Agency, indicates a weak correlation ($r^2 = 0.2595$) between altitude and precipitation. Typically, mean annual rainfall tends to increase with higher altitudes, but in the study area, the correlation value ($r = 0.509$) suggests a poor relationship between precipitation and altitude. This discrepancy can likely be attributed to the orographic effect. The presence of the Wombera plateau and nearby mountains such as Belaya Northwest of Pawe, Dangila East of Pawe, and Kar southeast of the basin may influence the distribution and quantity of rainfall. The evident influence of orography on rainfall distribution suggests that the precipitation in the Beles basin is not predominantly determined by altitude.

Determination of aerial depth of precipitation

Rainfall measurements obtained from rain gauges provide data at specific points. However, precipitation exhibits significant spatial variability within the study area due to its physiography. Various methods, such as arithmetic, isohyets and Thiessen polygons, can be used to compute areal rainfall from point data. In this case, the isohyetal method is chosen as it yields accurate results in areas with pronounced topographic contrasts, where the influence of topography on precipitation is expected to be substantial. By utilizing rainfall depths from different stations within the study area and the surrounding region, the average rainfall depth over the entire area is determined. The isohyetal method is selected to account for the non-uniform spacing of stations and the topographic variations across the area. For illustrative purposes, the average of these values is used. The computed annual average aerial precipitation, based on the average of isohyets, is determined to be 1399.50mm.

A. Isohyetal method

Considering the unevenness of the land and the diverse topographic characteristics of the Beles basin, the isohyetal method is chosen. This approach involves connecting areas with equal rainfall depths across the region of interest. To create a precipitation map, the Kriging interpolation technique within the Arc GIS spatial analyst tool is employed, utilizing data from the 12 stations located within and near the basin. This process generates an isohyetal map, as depicted in Figure 4.4.

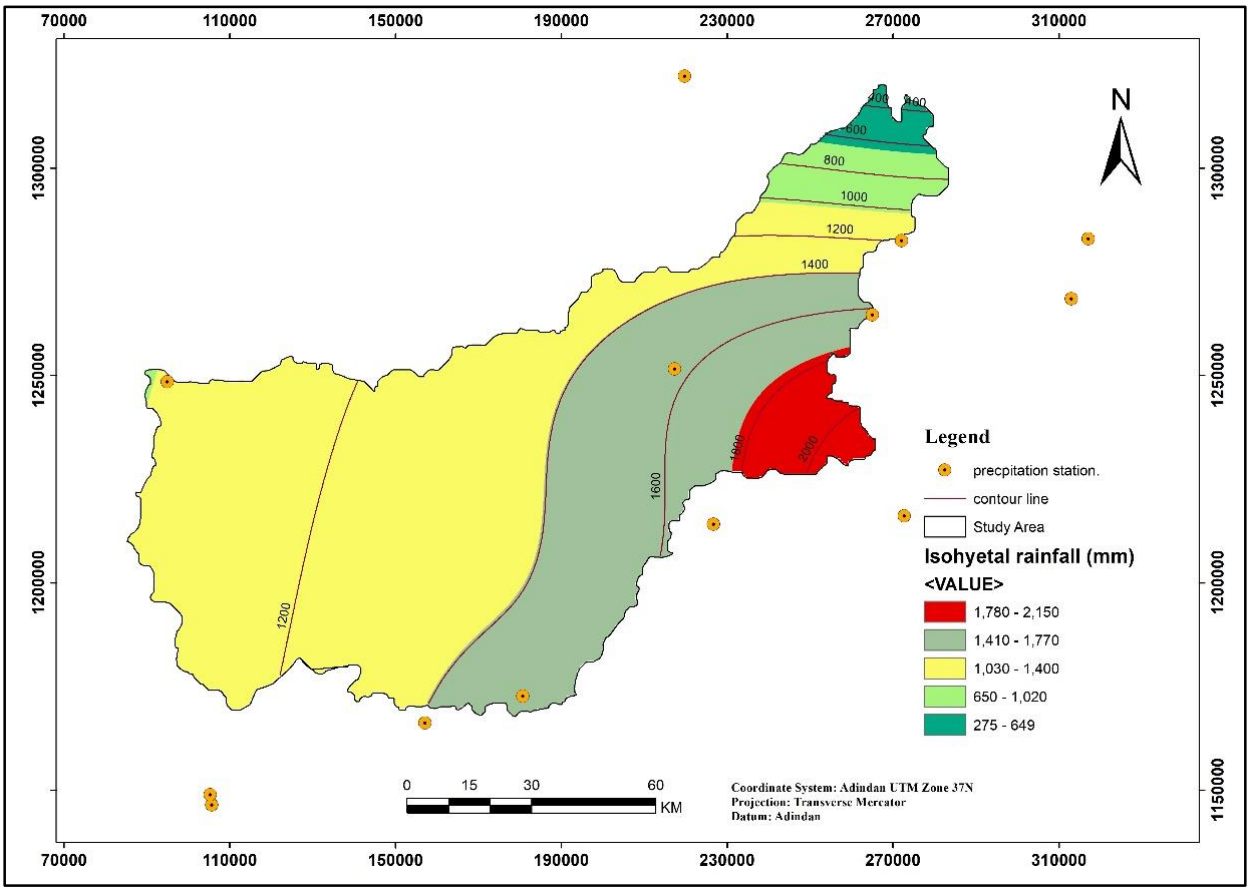

Figure 4. 4. Isoheytal map of Beles basin

$$P_a = \underline{p_{12}A_{12} + p_{23}A_{23} + \ldots\ldots\ldots\ldots\ldots + Pn\text{-}1.n.\ An\text{-}nn}$$

$$At$$

Where p12 –rainfall depth between isohyets 1 and 2,

A12 –Area enclosed by successive isohyets 1 and 2

At –total area, therefore, the estimated average rainfall depth over the Beles basin is about 1399.50mm

The findings from these methods reveal a significantly higher amount of rainfall compared to the average elevation. In contrast to the southern, northwestern, and eastern lowlands of Ethiopia, which receive less than 600 mm of rainfall annually, the Beles basin experiences notably higher precipitation. Despite the dominance of the lowland system in northwestern Ethiopia, the basin stands out with its elevated rainfall levels. This can be attributed in part to the moisture source. Ethiopia primarily receives its main rainfall from the Atlantic Ocean during the period from June to September.

The study area, along with much of Ethiopia, receives Belg (summer) precipitation originating from the Atlantic Ocean. However, the amount of Belg precipitation gradually decreases when moving from southwestern to northwestern Ethiopia. The Beles basin serves as a transitional zone between these two extremes.

4.1.2. Temperature

Temperature, as another significant hydro-meteorological factor, can have a notable impact on evaporation processes, whether from surface water bodies, bare soil, or leaves. The temperature of a specific environment is primarily influenced by its geomorphological configuration, altitude, and geographic location. In the study area, a total of nine stations monitor the daily maximum and minimum temperatures, which are then averaged to obtain the mean monthly values. These stations are strategically located in both the highland and lowland regions. Among the recorded data, the highest mean monthly temperature of 32°C was observed in Mankush during the month of April, while the lowest temperature of 14°C occurred in Wombera during the month of August. These variations in temperature provide valuable insights into the thermal characteristics of the study area throughout the year.

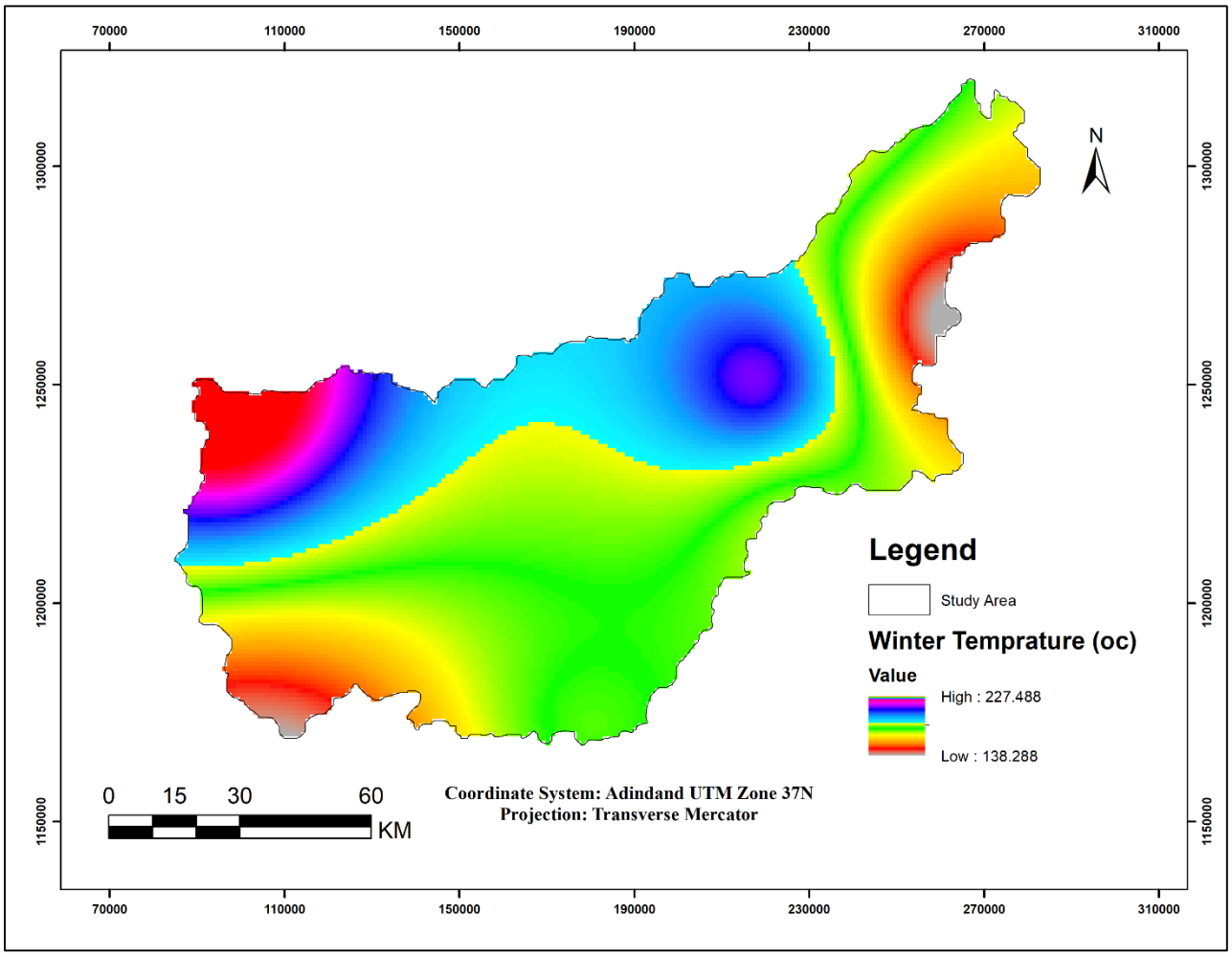

Figure 4. 5. Winter temperature

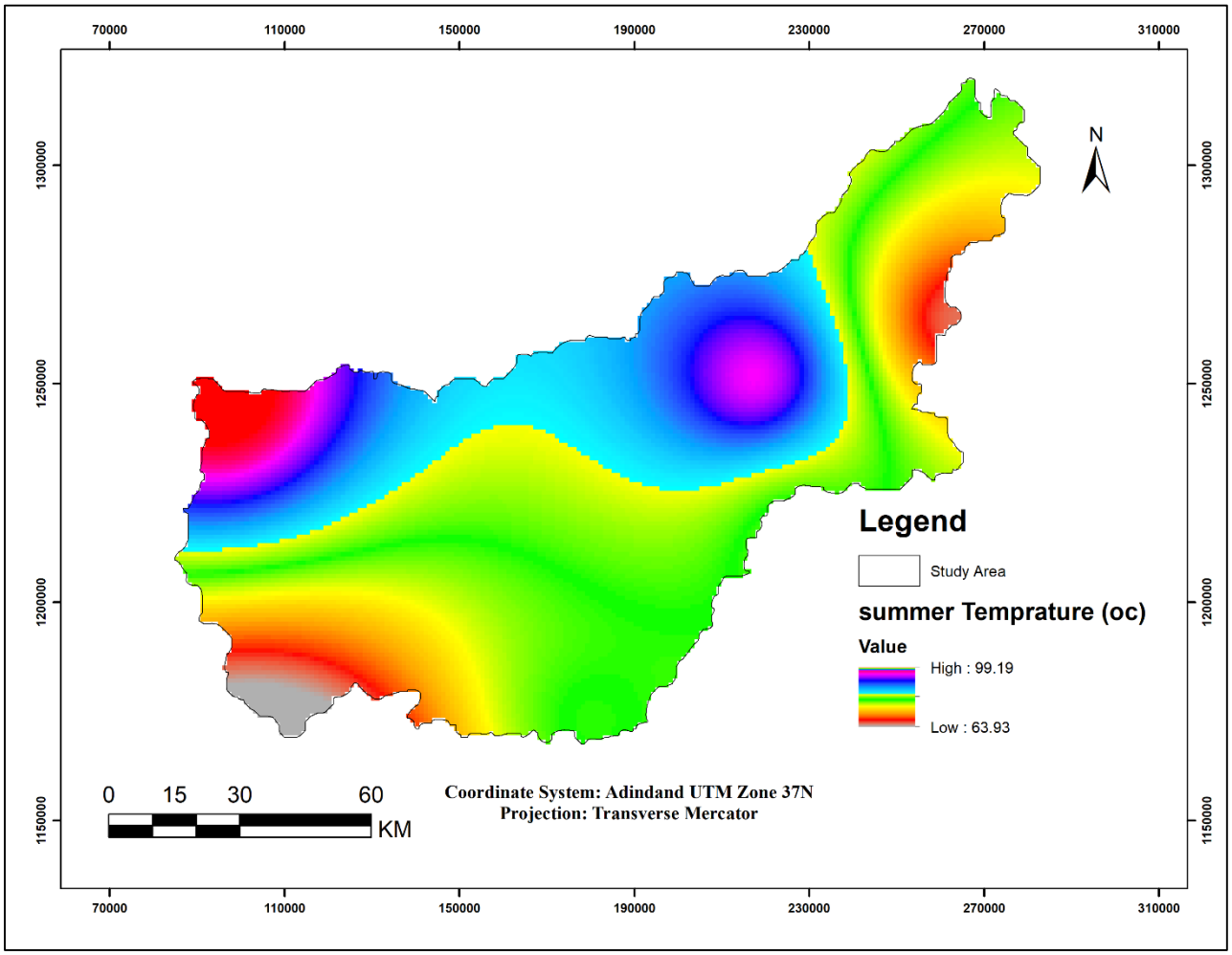

Figure 4. 6. Summer temperature

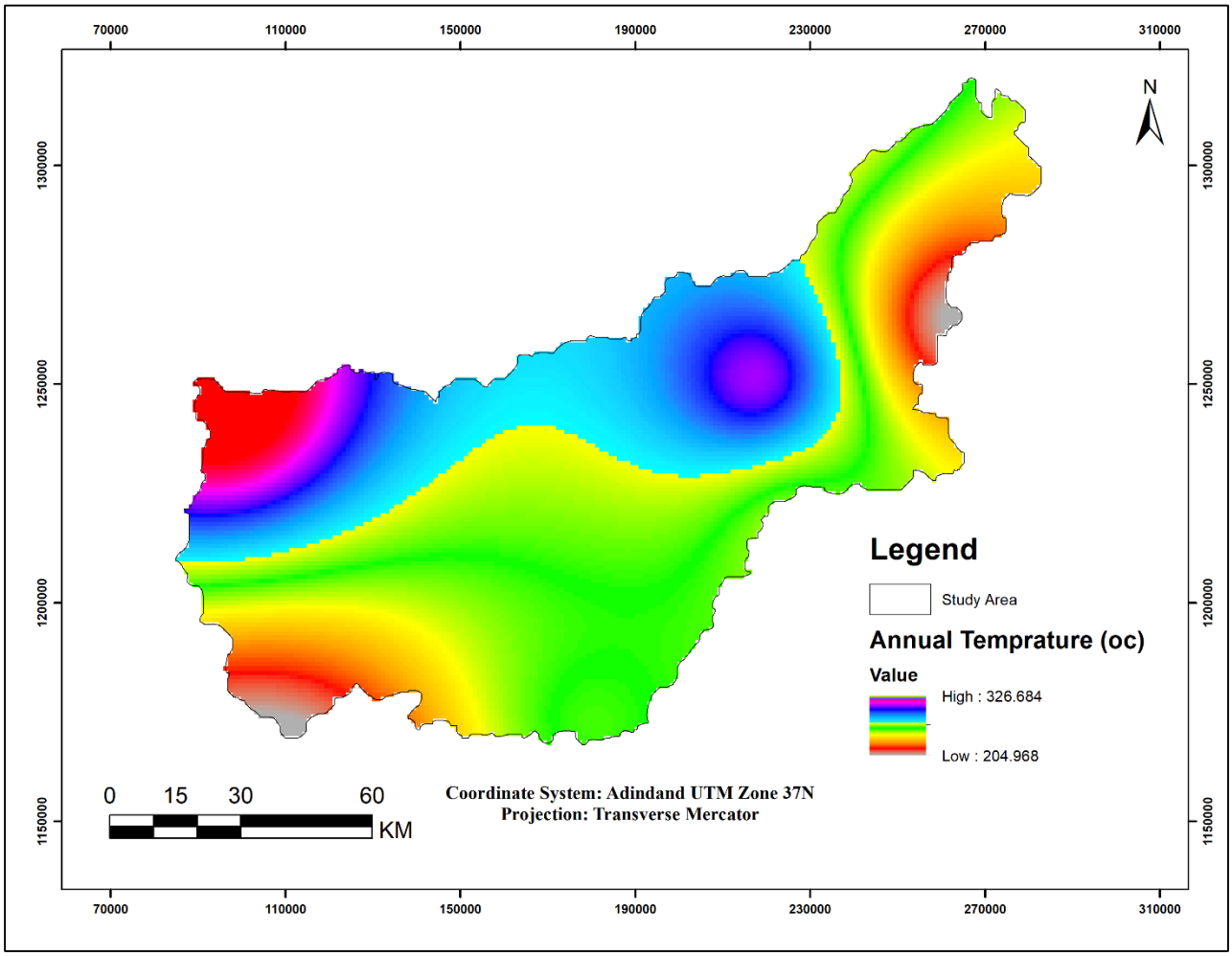

Figure 4. 7. Annual temperature

4.1.3. Sunshine hours

Sunshine hours refer to the duration during which the ground surface is exposed to direct solar radiation, specifically the sunlight that reaches the earth's surface directly from the sun.

In the Beles basin area, the sunshine hours are assessed based on data collected from five stations. The analysis reveals that the maximum duration of sunshine occurs between the months of November and March, while the minimum values are observed in July and August. This information sheds light on the seasonal variations in sunlight availability within the Beles basin area.

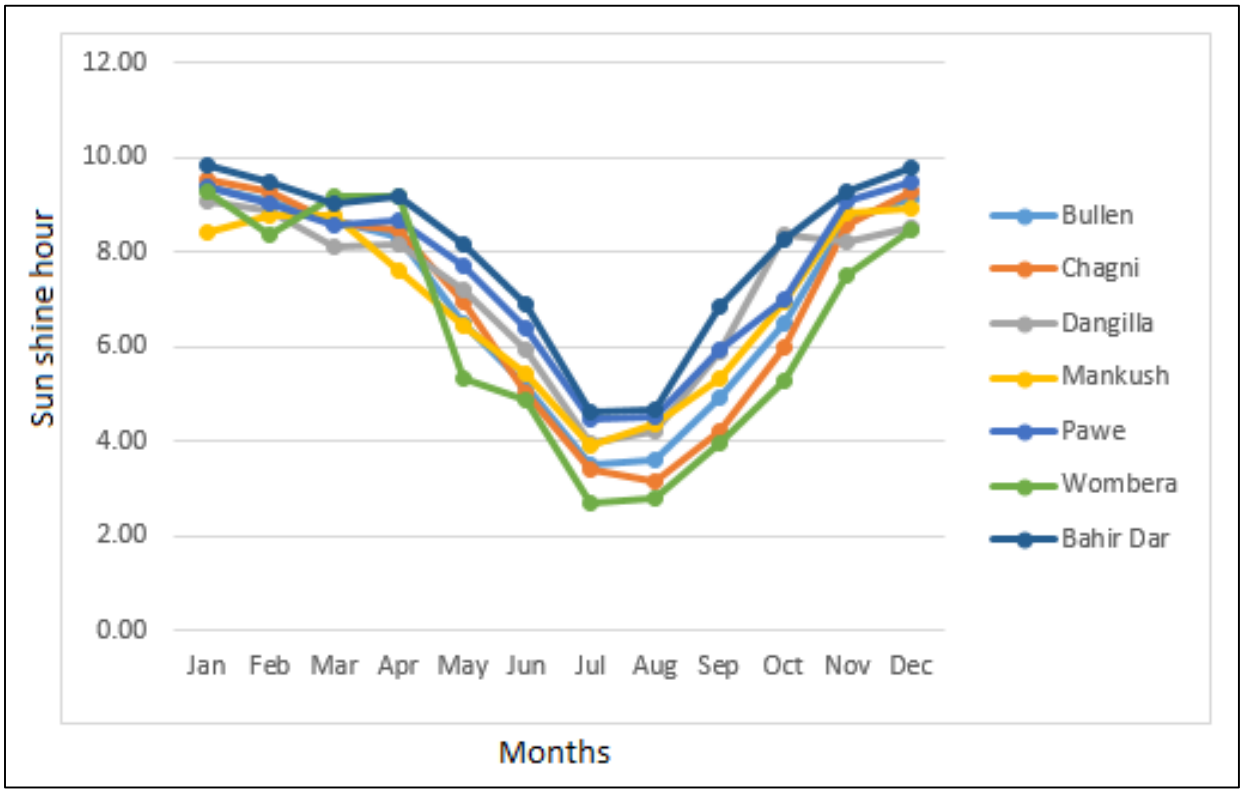

Figure 4. 8. Mean Monthly pattern of sunshine duration in (hour) from (NMA)

4.1.4. Wind speed

Wind speed is a significant factor influencing the process of evaporation. When wind speed decreases, it hinders the removal of saturated vapor, which in turn affects the rate of evaporation. Data on wind speed is obtained from a limited number of meteorological stations. These wind speed measurements are applied uniformly across the entire watershed to ensure consistency in the analysis of evaporation. By considering this data, we can gain insights into the impact of wind speed on evaporation rates within the study area.

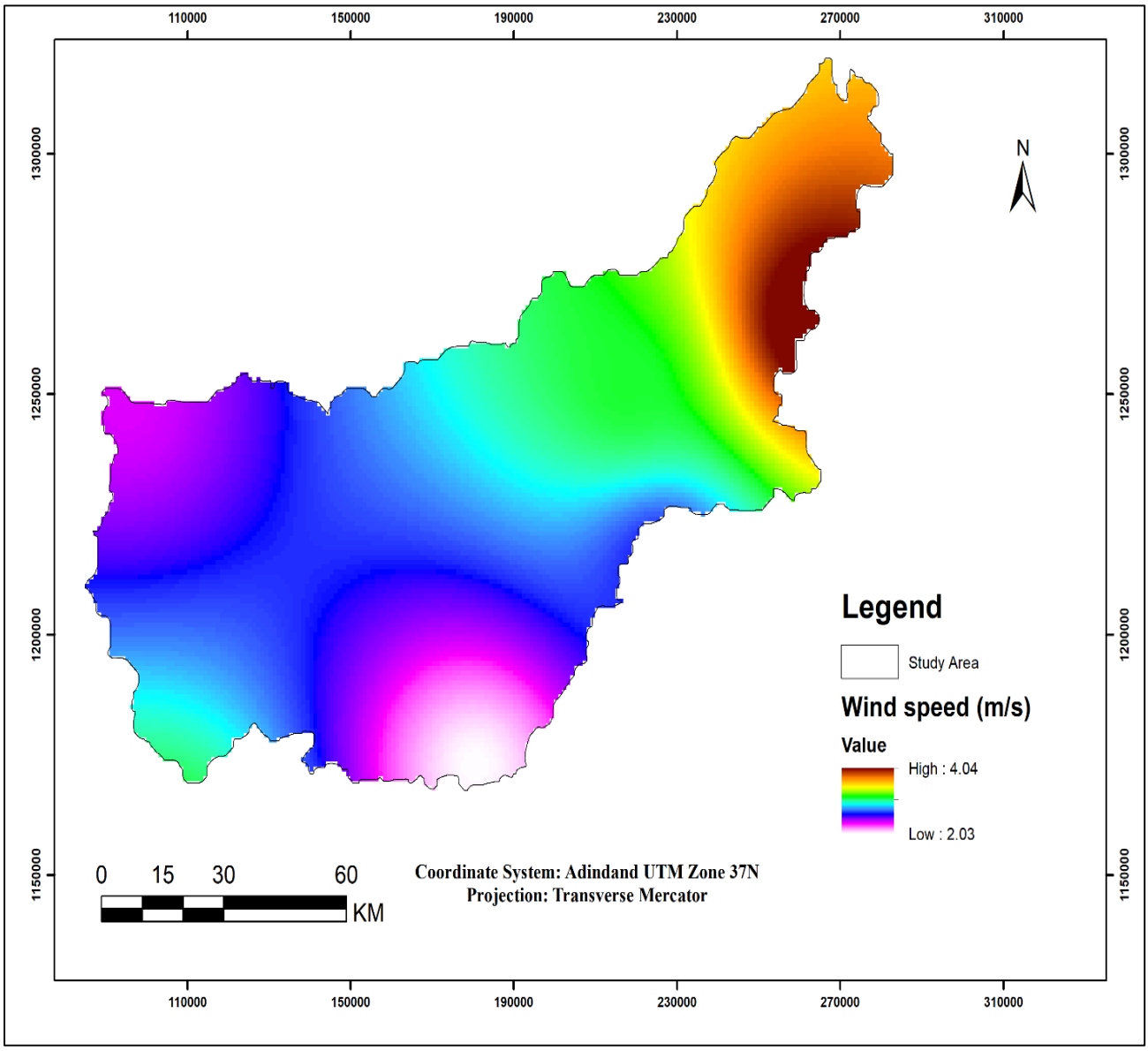

Figure 4. 9. Winter wind speed

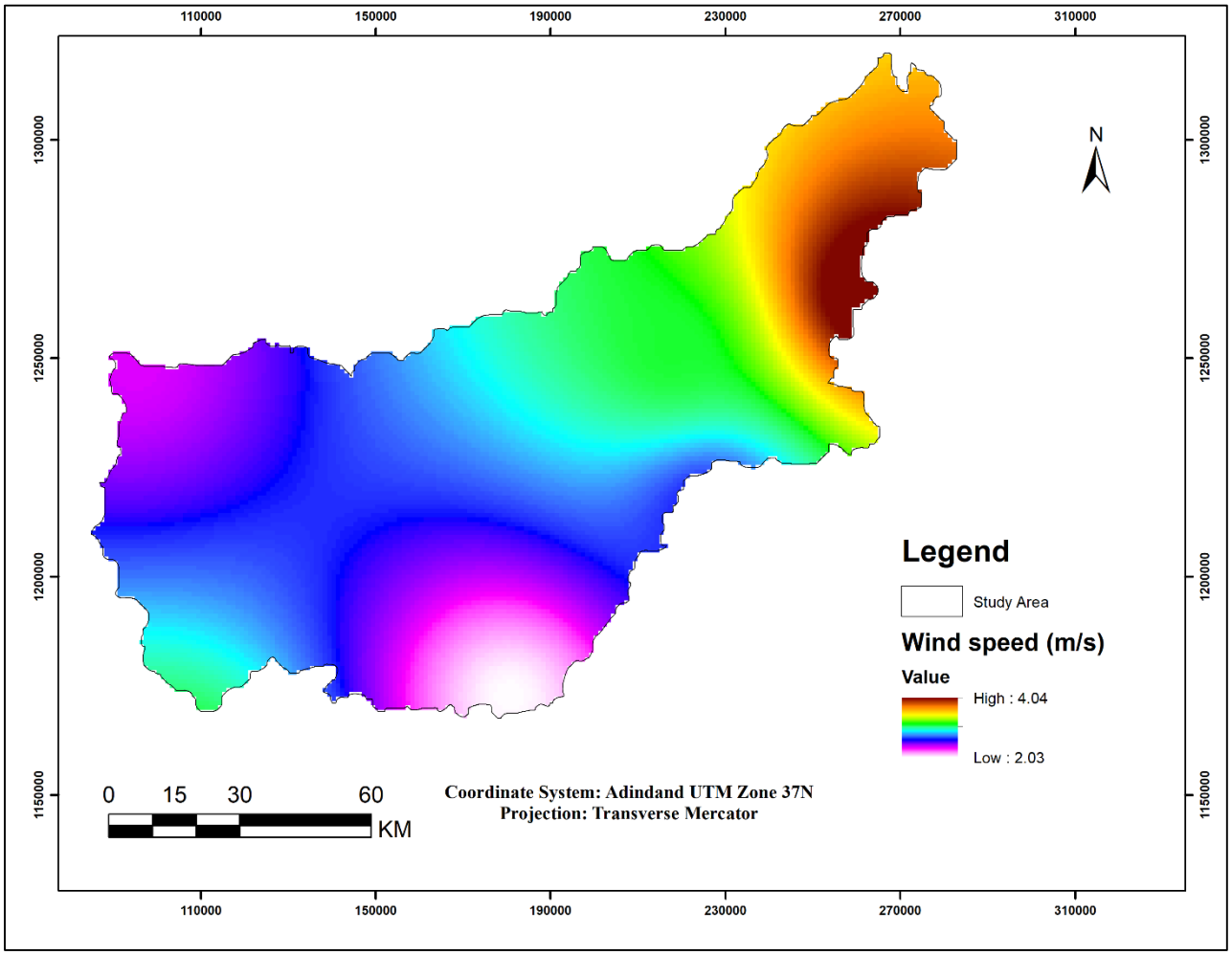

Figure 4. 10. Summer wind speed

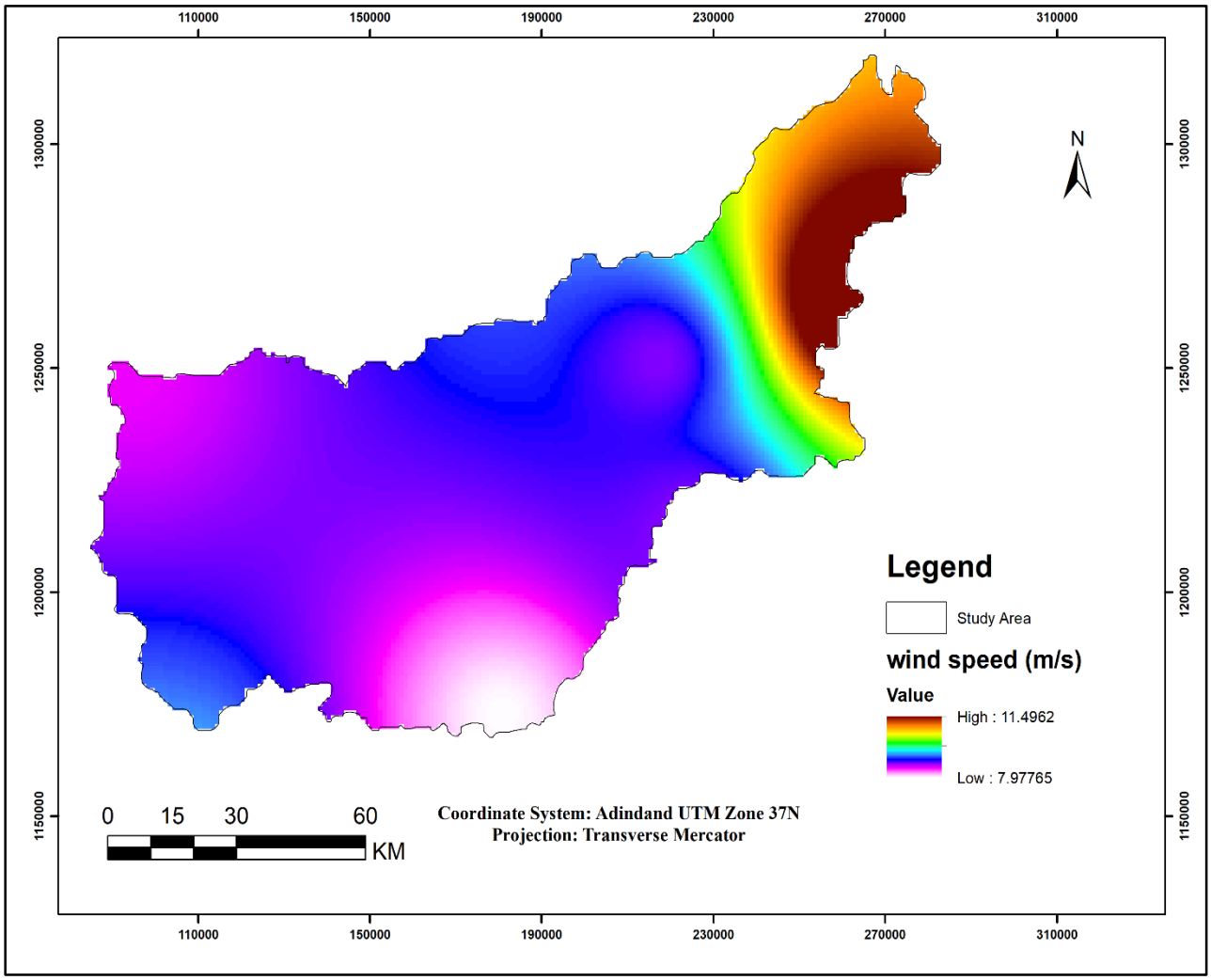

Figure 4. 11. Annual wind speed

4.1.5. Relative humidity

Relative humidity is a measure of the moisture present in the air in relation to the amount needed to fully saturate the air at the same temperature. It is primarily influenced by temperature and rainfall. As Shaw (1985) explains, relative humidity is expressed as a percentage, representing the ratio of the actual water vapor pressure (ed) to the saturation water vapor pressure (ea) at a given temperature. RH= (ed/ea)100

Where: - RH is relative humidity,

-ed is actual vapor pressure at the dew point, Td

-ea is saturated vapor pressure at air temperature, Ta.

When the humidity of the air increases, its ability to hold water vapor decreases, resulting in a slower evaporation rate. In order for evaporation to occur, there needs to be a difference in humidity, as noted by Tenalem Ayenew and Tamiru Alemayehu (2001) and Fetter C.W (1994).

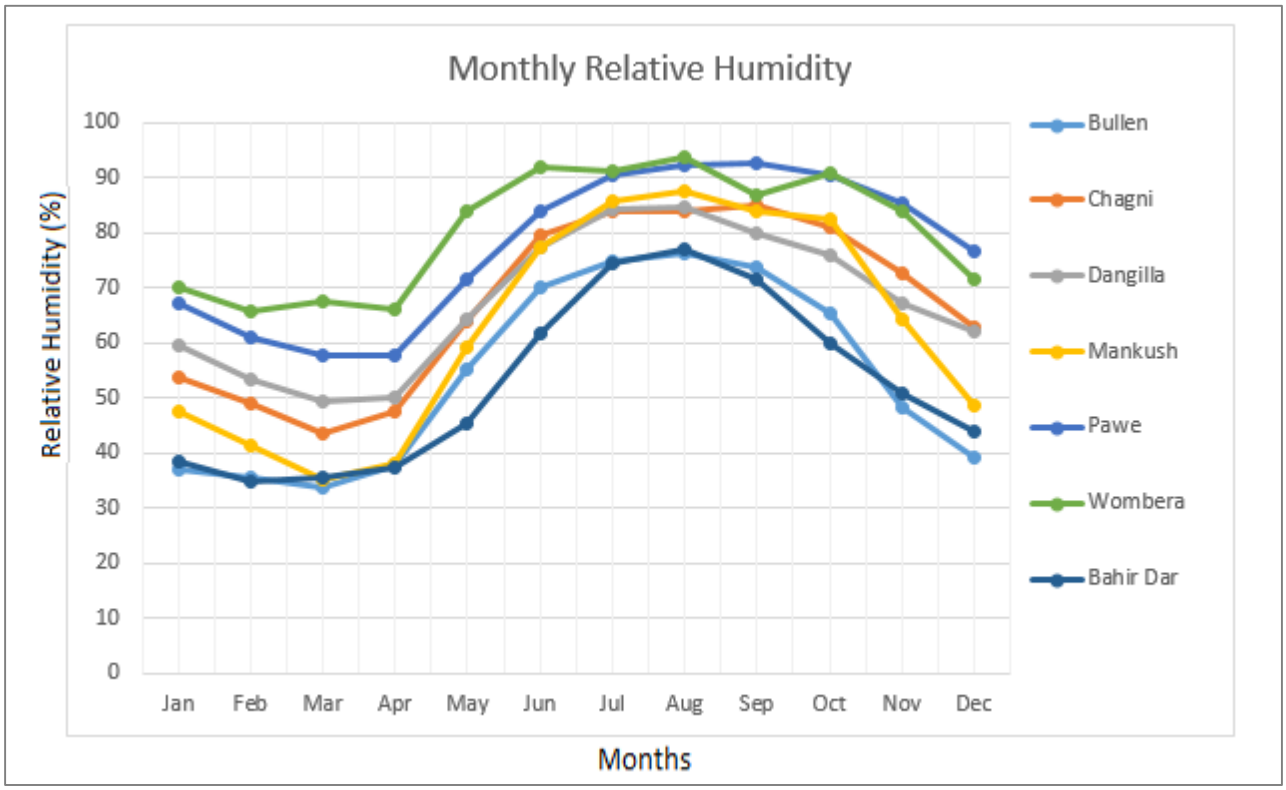

Figure 4. 12. Graph of Mean Monthly Relative Humidity (%)

Hence, the aforementioned findings indicate that the relative humidity of the air is primarily influenced by rainfall and temperature. Specifically, the Wombera meteorological station records a maximum monthly relative humidity of 93.75% in August, while the Bahir Dar meteorological station experiences a minimum relative humidity of 34.76% in February. These variations in relative humidity provide valuable insights into the moisture content of the air at different locations and times within the study area.

4.1.6. Potential evapotranspiration

Evapotranspiration is an important parameter in the water budget which abstracts water from the system and controls the soil moisture content, groundwater recharge,

and stream flow components of a certain basin. The monthly Potential evapotranspiration of the Beles basin is calculated using the Thorenthwaite method. The monthly results are subdivided into two main seasons (4 months of summer and 8 months of winter). Finally, the summed PET values of each season are converted to spatially distributed grid maps. The grid maps of PET for both seasons are incorporated with other input parameters in the WetSpass model to estimate the recharge as well as actual evapotranspiration (AET).

This approach utilizes air temperature as an indicator of the energy accessible for evapotranspiration. It operates under the assumption that air temperature is correlated with the combined impact of net radiation and other factors influencing evapotranspiration. Furthermore, it assumes that the available energy is distributed in a consistent proportion between heating the atmosphere and evapotranspiration. To compute potential evapotranspiration, average air temperature data spanning twenty years is collected from the Ethiopian Meteorological Agency. The following formula is then employed to calculate potential evapotranspiration.

$Et = 16b\,[10Ta/I]^a$ ……………………………………………………………………….(1)

Where: Et- is the potential evapotranspiration in mm/month

Ta -is the mean monthly air temperature in (°C)

I -is the annual heat index

b- is latitude correction

The value of heat index (I) can be calculated as:

$I = \sum im = \sum (Tmi/5)^{1.514}$

$a = 6.75\times10^{-7}I^3 - 7.71\times10^{-5}I^2 + 1.79I + 0.49239$

The latitude of the study area is estimated to be around 10° N. Consequently, the latitude correction (b) required for computing potential evapotranspiration can be obtained from the table provided below.

Table 4. 1 . Latitude correction values of 100 N Latitude

Month	Jan	Feb	Mar	Apr	May	Jun	Jul	Aug	Sep	Oct	Nov	Dec
b	0.97	0.98	1	1.03	1.05	1.06	1.05	1.04	1.02	0.99	0.97	0.96

Potential evapotranspiration is calculated using the Thorenthwaite formula while taking into account the previously mentioned factors. The calculated values are shown in Figure 4.13 and Annex-8.

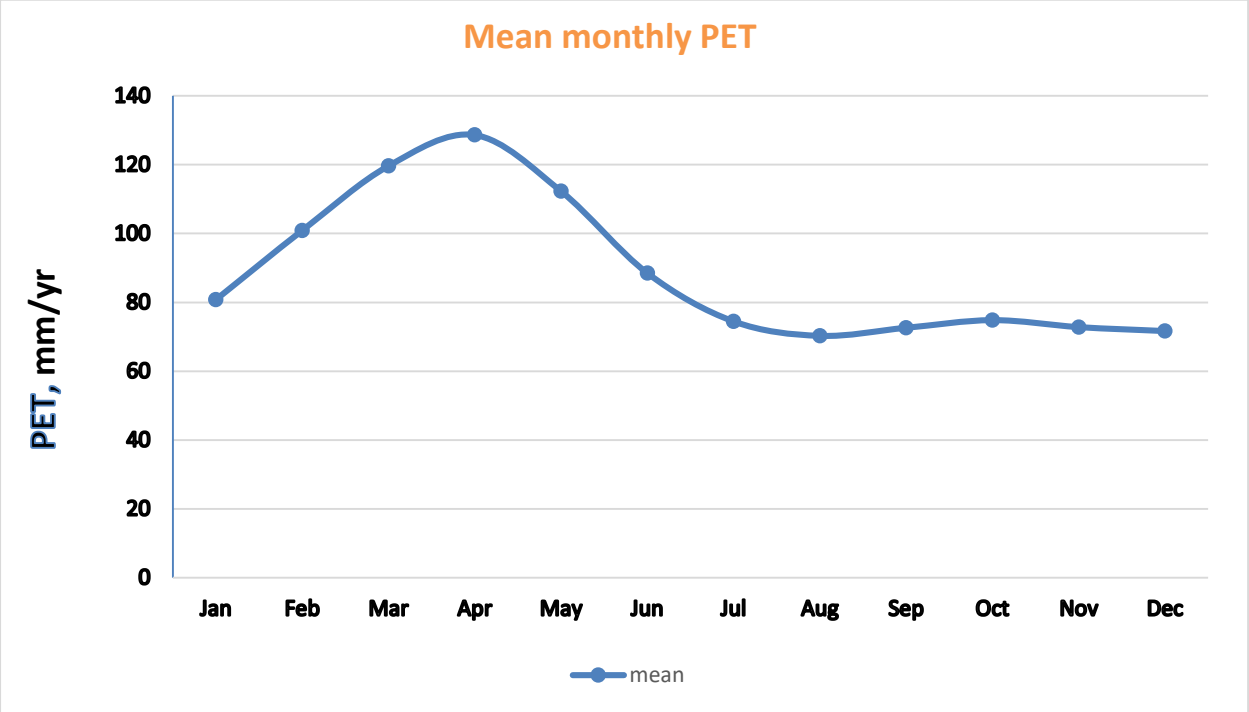

Figure 4. 13. Mean monthly distribution of potential evapotranspiration

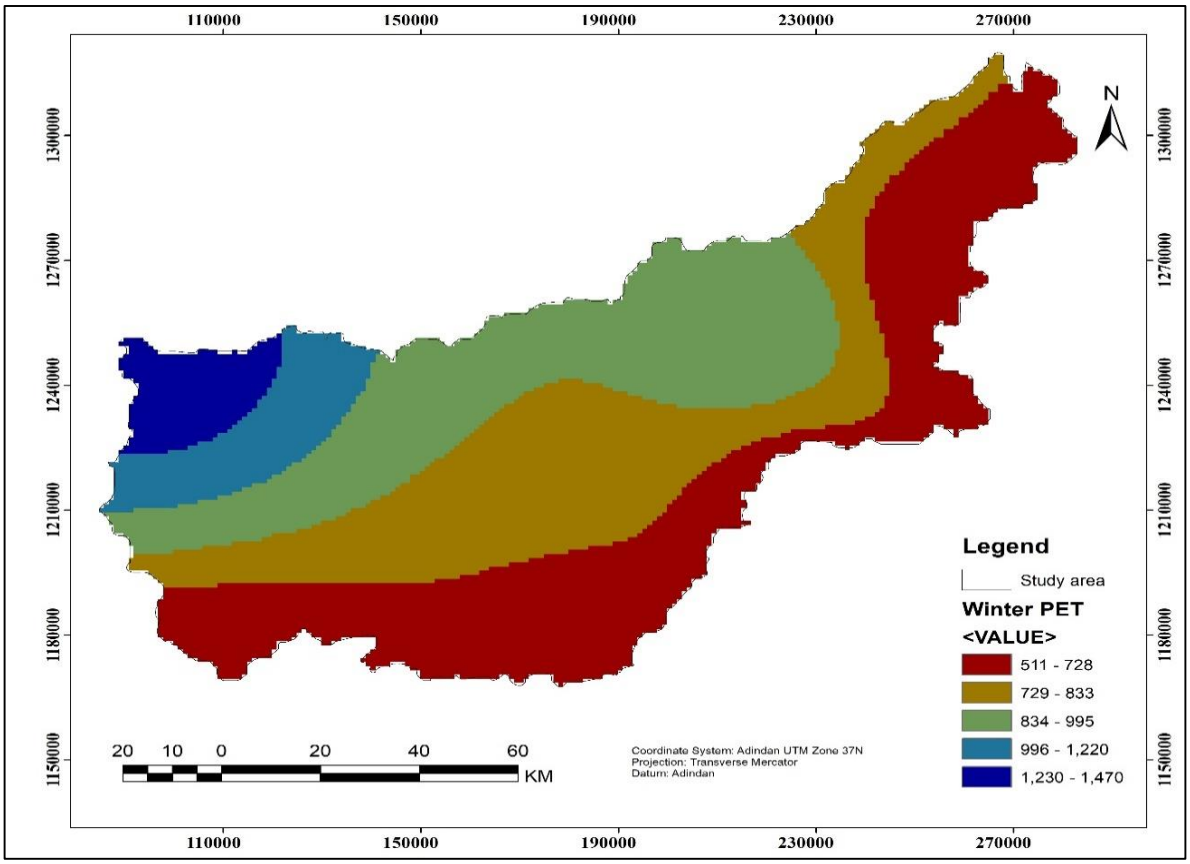

Figure 4. 14. Winter potential evapotranspiration

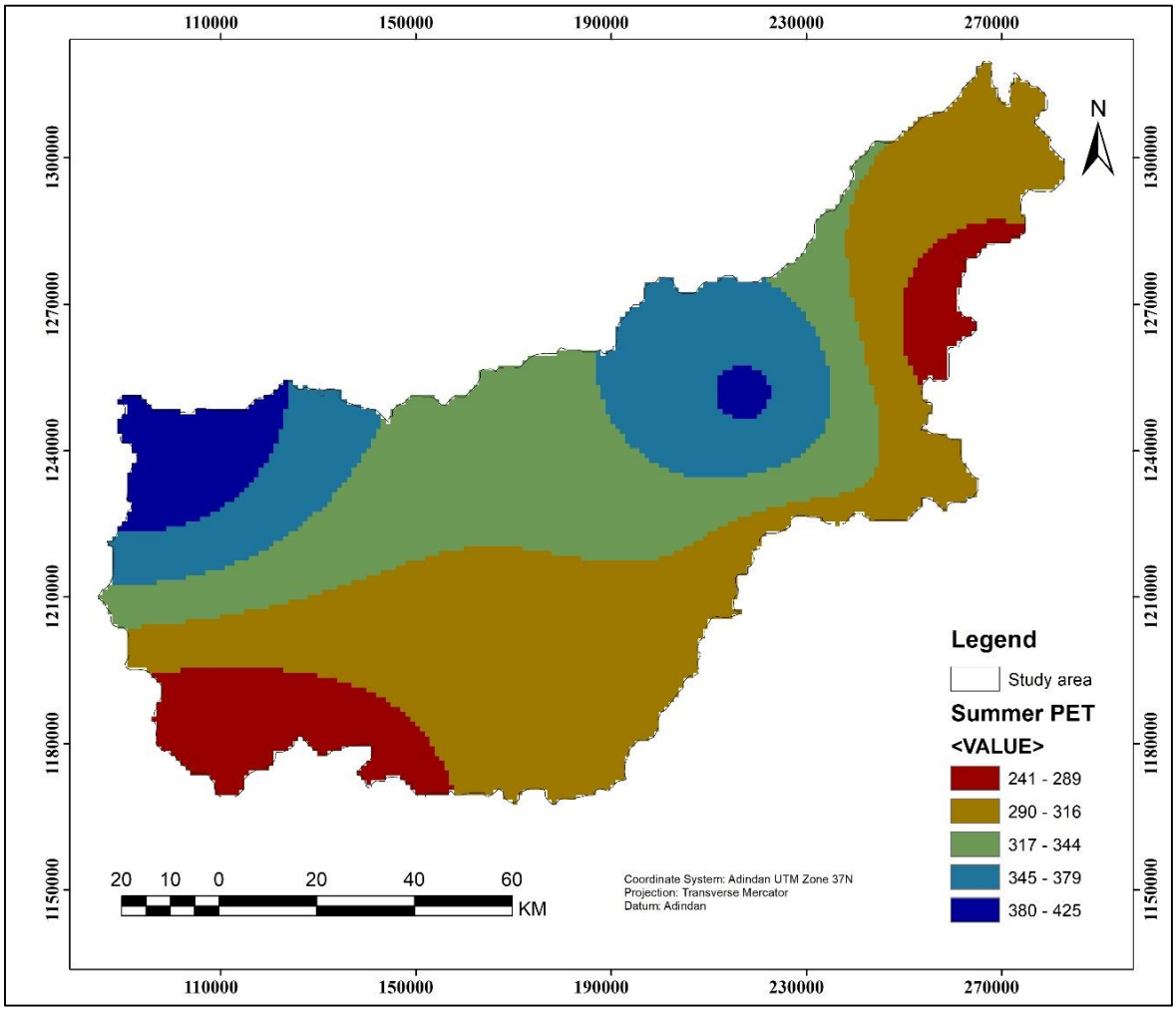

Figure 4. 15. Summer potential evapotranspiration

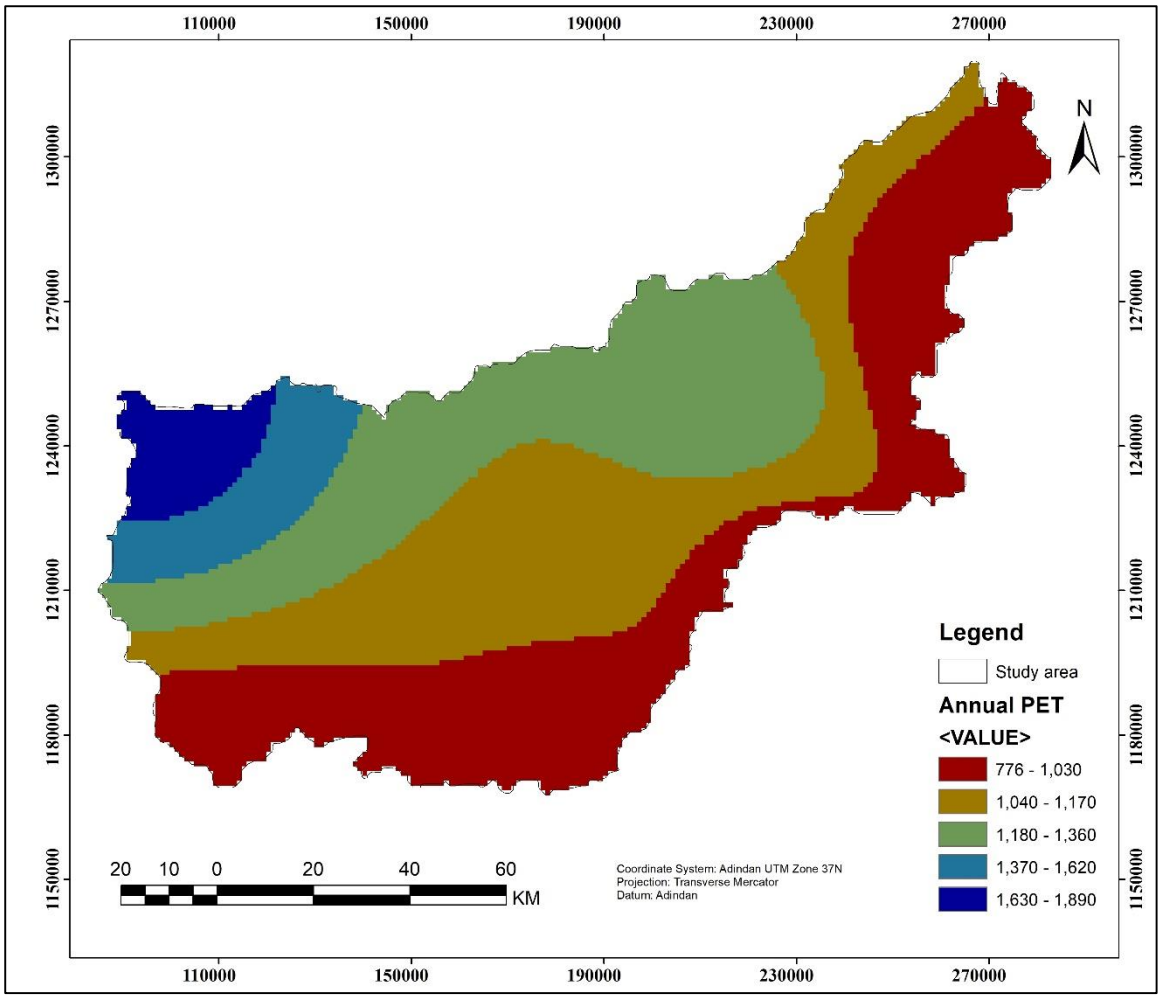

Figure 4. 16 . Annual potential evapotranspiration

4.2. Elevation and slope

To ensure uninterrupted flow within the watershed of the research area, all sinks and peaks were filled in the digital elevation model (DEM) prior to estimating various parameters. This process results in a depressionless DEM, which has been modified to eliminate all sinks. The filled DEM was then utilized to extract important terrain characteristics such as elevation, flow direction, flow accumulation, stream network, and stream order within each grid cell. Figure 4.17a provides a visual representation of these features derived from the processed DEM.

The USGS's Shuttle Radar Topography Mission (SRTM) dataset's DEM, which can be downloaded, was used to create the topography (elevation) map of the watershed.

The watershed's mean elevation is 1189 m, with the lowest (minimum) elevation point located in the downstream portion at 542 m and the highest in the highland portion at 2595 m.

Due to their relative flatness and high infiltration rate, the flat and gentle slope locations were thought to have a very high potential for groundwater recharge. These locations also make up the biggest portion of the basin when compared to other classes. By employing the 'slope' module within ArcGIS 10.8, a slope map of the watershed is generated using the digital elevation model. The slope values range from 0.020 to 21.780, with a mean of 9.80 and a standard deviation of 7.19, as depicted in Figure 4.17b. This map provides valuable information about the terrain's steepness within the study area.

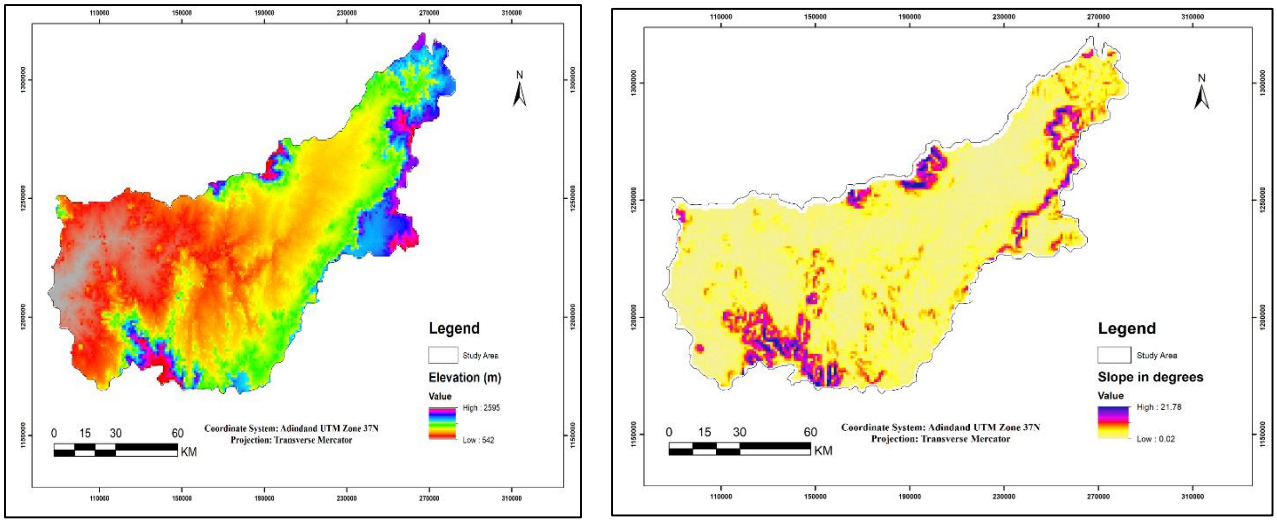

Figure 4. 17. (a) Elevation (b) Slope map of Beles watershed

4.3. Soil texture

The soil map of the Beles basin has been generated by utilizing a raster map with a resolution of 30 meters obtained from the Ministry of Agriculture. To classify the soil texture within the respective catchments, the United States Department of Agriculture (USDA) classification system has been employed. This classification is crucial for the WetSpass model, as it relies on accurate soil texture data during simulation. In the research region, the predominant soil type is loam, encompassing

approximately 67.23% of the total catchment area. Following loam, clay and sandy loam constitute 18.51% and 14.26% of the catchment, respectively. These soil texture proportions offer valuable insights into the composition of the soil within the study area.

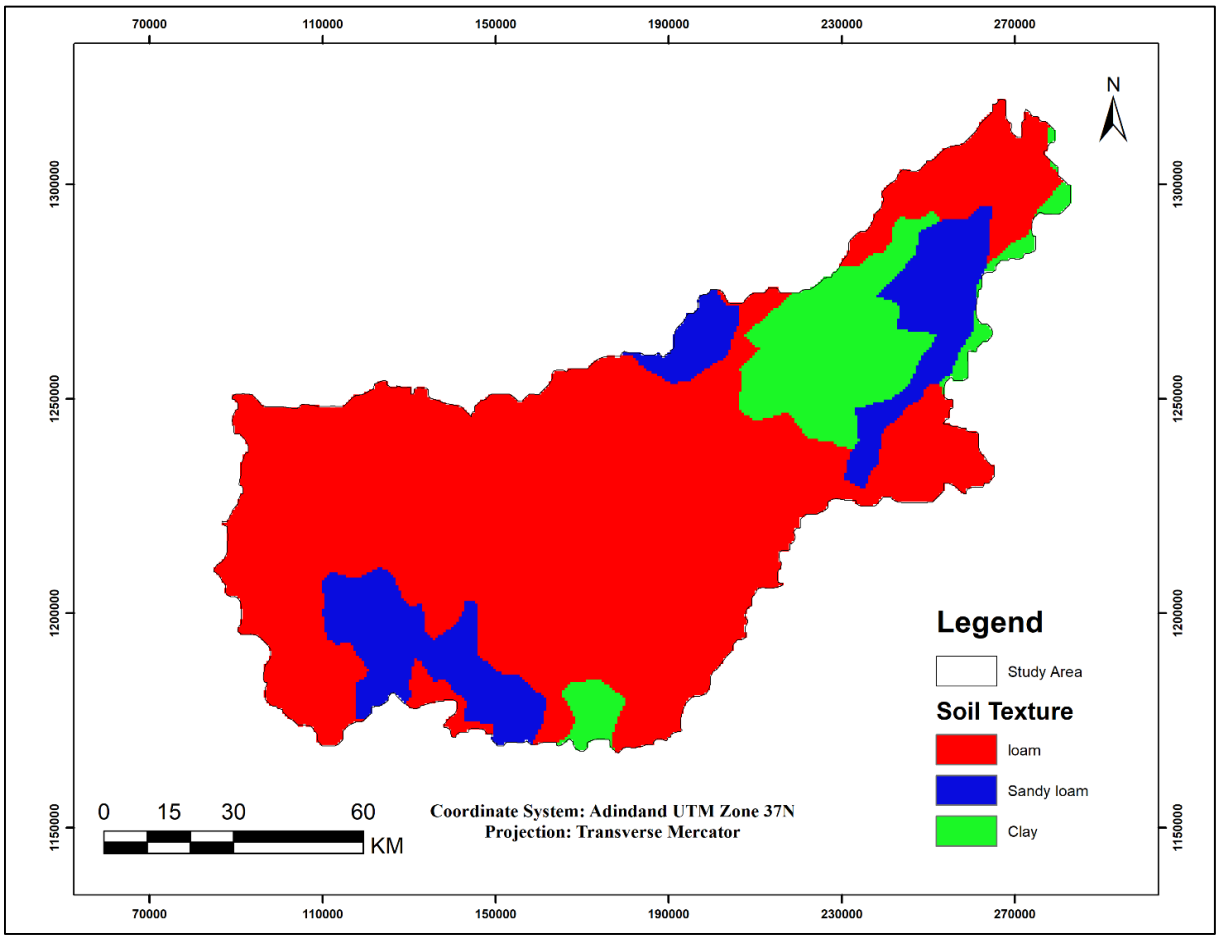

Figure 4. 18. Soil texture

4.4. Land use and land cover

According to Achu et al. (2020), vegetation cover contributes to the enhancement of the recharge mechanism by reducing surface runoff and limiting percolation to impervious surfaces.

The modification of land use and land cover has a significant impact on hydrological processes such as evapotranspiration, surface runoff, and infiltration, as cited by Kirubakaran et al. (2016). Therefore, it plays a crucial role in

determining the groundwater recharge zone. The land use land cover map was analyzed and classified into seven distinct categories: bare soil (3.23%), agriculture (12.75%), grassland (4.08%), deciduous forest (0.05%), mixed forest (0.28%), water bodies (0.11%), shrub grass (30.08%), and coniferous forest (49.42%). The spatial distribution of these land use classes is illustrated in Figure 4.19. It should be noted that water bodies consist primarily of seasonal rivers and ponds. The highest-ranking land use class, coniferous forest, and the second-ranking class, shrub grass, are assigned to agriculture and grass, respectively, due to their ability to retain water, facilitate infiltration into the subsurface formation, and support recharge in the study area.

Naturally occurring deciduous leaf forest covers the plateaus. In low-lying places, where scattered trees and the amount of trees reduces. Along stream and river courses, there is some dense vegetation can be found. Due to ongoing local building and yearly burning, the forest cover is declining as the population grows. On the Wombera, Dangur, and Belaya Mountains, the natural vegetation is a moisture-loving mountain forest, composed of Hagenia abyssinica and Podocarpus gracilior. The majority of the area has a crystalline basement that makes it appear unsuited for agriculture. In the highland areas, agriculture is practiced on the Tertiary basalt plateau. Additionally, the gum obtained from various types of trees is utilized in the production of incense. Along the stream valleys, a specific species of palm tree flourishes, which is known for its abundance. The leaves and fibers of this palm tree are skillfully woven to create baskets and home furnishings. A substantial portion of the terrain is covered in deciduous trees and woodlands. The local population relies on the forest to gather honey, make charcoal, and harvest materials for incense. Both the forest and the wild animals that live there are in danger due to improper forest management.

Generally, agricultural activities are practiced mostly in the highland of Dangur, and Dangila areas and rarely in the Wombera highland, lowland, and central part of

the study area. They grow teff, selit, raise, dagusa, and also in the highland of Wombera they grow coffee. The dominant crops in this study area are sorghum and sesame. Ginger, finger millet, teff, and maize are grown especially around Mandura.

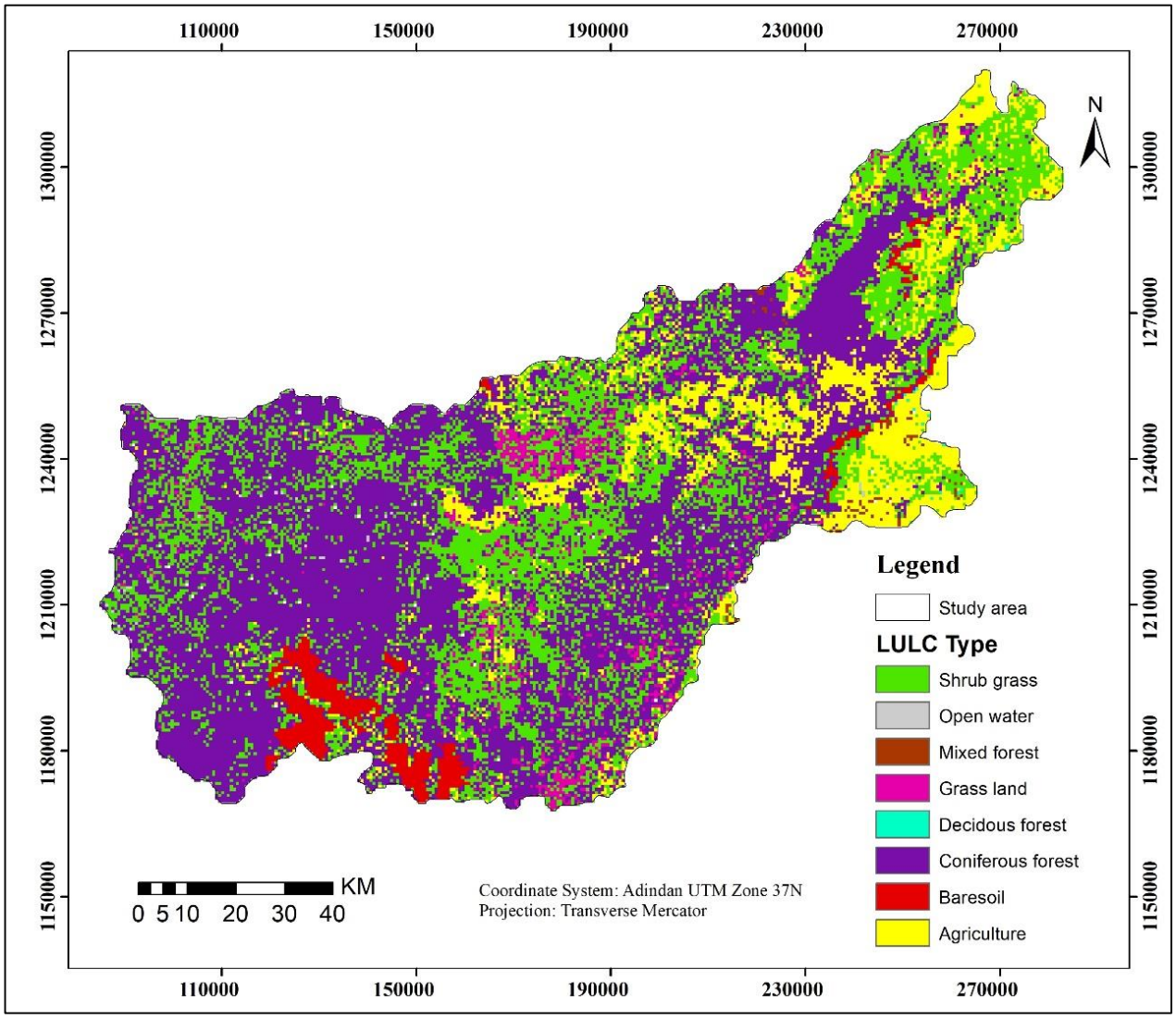

Figure 4. 19 . Land use and land cover

4.5. Groundwater flow dynamics

Groundwater is in constant motion, flowing from areas of higher hydraulic head in recharge zones, which typically receive more precipitation, to areas of lower hydraulic head in discharge zones such as wells, springs, rivers, lakes, and wetlands. This movement is driven by a change in hydraulic head or a hydraulic

gradient present in the potentiometric surface of the groundwater system. The force behind this movement is gravity.

Groundwater levels loosely follow topographic contours and flow follows these gradients. The fractured rock aquifer is a large regional aquifer, with little known about its groundwater movement and behavior. Groundwater movement occurs from the fractured rock aquifer to the alluvial aquifer, either through direct pathways or via the colluvial aquifer. The flow dynamics within the alluvial aquifers are intricate, consisting of both local and regional flow cells. Kovalevsky et al. (2004) emphasize the significance of groundwater as a vital water source. It serves as the source for baseflows in rivers and acts as an underground reservoir that can be tapped for water supply or drainage purposes. Hence, it is crucial to thoroughly examine the flow of groundwater.

Groundwater flow directions were determined by analyzing groundwater contours derived from groundwater elevations. These contours, also known as flow nets, connect points with the same groundwater elevation. The groundwater elevation is obtained by subtracting the static water level from the surface elevation. The patterns formed by these contours play a crucial role in identifying the flow directions of groundwater in the area under investigation. Consequently, groundwater flow lines are perpendicular to the equipotential lines (contours). By examining the groundwater contour map, narrow spacing between contours indicates high hydraulic gradients, suggesting rapid changes in water level elevations. On the other hand, wider spacing between contours indicates the presence of localized aquifers within the regional aquifer domain. Therefore, in Figure 4.20, the contour map of the study area in the North Highland of Dangur and Southwest of Wombera Highland shows a high hydraulic gradient.

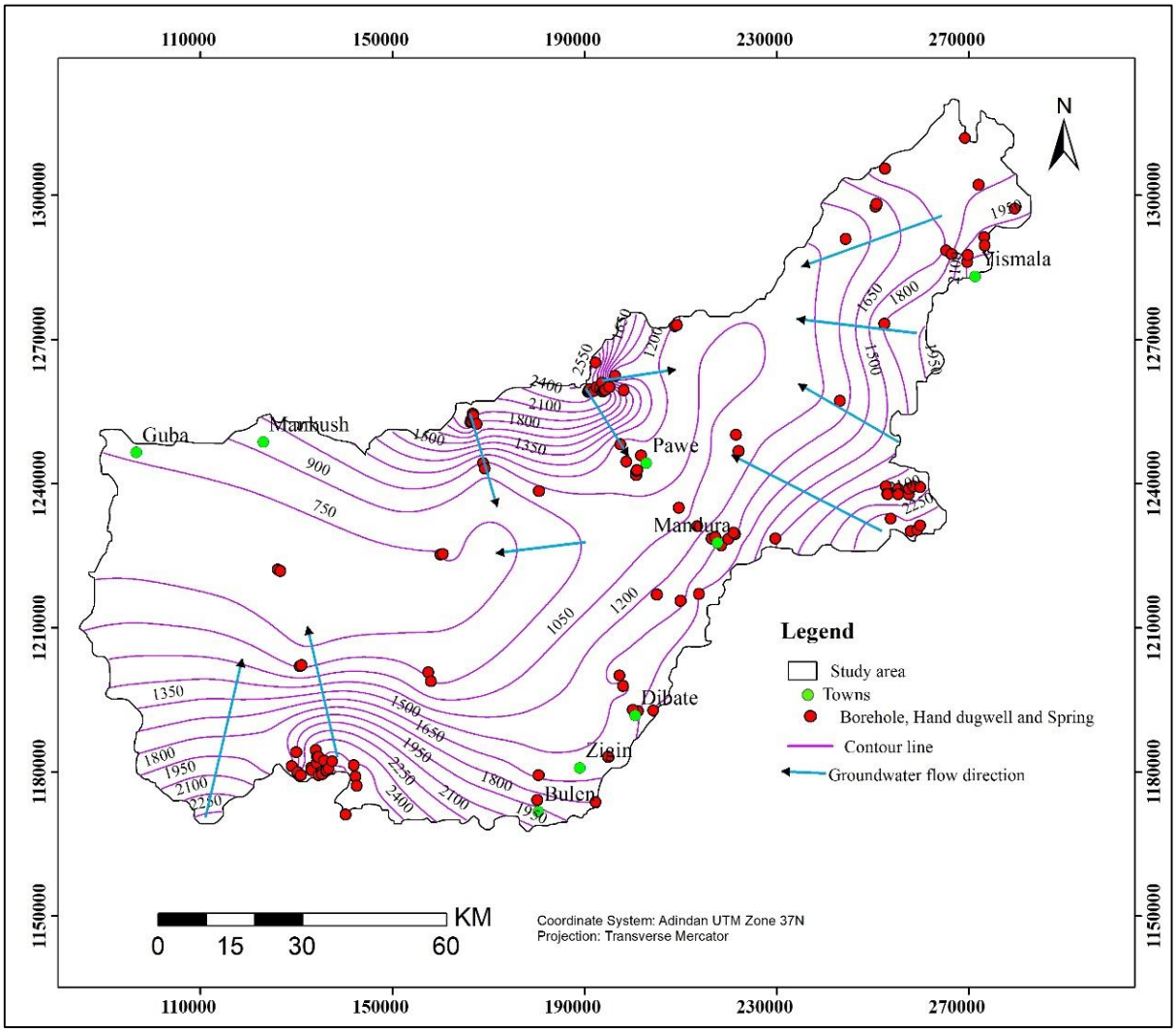

Figure 4. 20. Groundwater level contour map showing the groundwater flow direction

In the Beles basin, the flow direction of groundwater is influenced by the surface topography, surface water flow, and the presence of geological structures. The alignment of perennial and intermittent rivers, which contribute to local aquifers, follows these lineaments, and groundwater flow tends to follow a similar pattern.

The locations of spring points in the tertiary volcanic rocks are structurally controlled, indicating the influence of geological structures on groundwater flow.

Additionally, springs can be found at the contact points between different geological formations.

In terms of depth, the flow of regional groundwater generally occurs at greater depths compared to the local flow system. Both local and regional subsurface flow systems can have a boundary known as a groundwater divide, which acts as an impermeable layer vertically. This divide restricts the flow of water across it. Similarly, in the case of surface water divides, the principle remains the same, but it pertains to topographically elevated areas that act as boundaries for surface water flow. Hypothetically, if groundwater flow aligns with the slope of the surface morphology, the surface and groundwater divides often coincide or overlap with each other.

Groundwater discharge refers to the removal of water from saturated zones near the water table surface, while the water table in discharge zones is either close to or at the land surface. Consequently, a water table contour map can effectively identify groundwater recharge and discharge zones.

Discharge of groundwater is indicated as springs, seepage zones, and base flow of rivers. Groundwater discharge areas are frequently found in the lowlands, local and regional depressions, and along the banks of rivers. The presence of geological structures and groundwater flow lines are directly related to discharge areas. In accordance with the topographic slope, the regional flow of groundwater predominantly occurs towards the western and southwestern directions. The contours of groundwater resemble topography features in a more muted way. The appearance of springs and an increase in base flow are signs that groundwater is being discharged in the area. Many springs are concentrated at significant regional faults and where volcanic rocks meet basement rocks. About all of the Basin's high discharge springs are controlled by faults. No large seepage zones exist. On the contrary groundwater recharge from rivers is dominant in the lowlands.

In general, the highlands have a higher input of groundwater to rivers. Rivers that

flow into lowlands are predicted to lose a significant amount of water through porous quaternary sediments and fractured rocks into the groundwater system (both the volcanic and the basement). As revealed from field observations and cited in Ayenew Tenalem and Addisu Girma's (2010) study, it has been observed that the discharge of the rivers in the study area decreases from upstream to downstream. In the lowlands to the southwest, the perennial rivers' discharge reducesIn the lowlands, several small rivers experience a cessation of flow, despite having significant volumes of water in the upper peaks. In larger streams with a notable sand bed, water continues to flow beneath the sand even during the dry season. However, as the streams move downstream, completely dry sand becomes visible, indicating that water infiltrates back into the permeable streambed. Often, groundwater flowed perpendicular to the water-level altitude contours and in the direction of decreasing water-level elevations from regions of recharge to regions of discharge.

Generally, groundwater flows from higher contour value to lower contour value hence as displayed above map groundwater of the Beles basin flows from N-E to the west-flowing Beles River.

4.6.Model calibiration

To calibrate the model, various parameters such as the alfa coefficient, "a" interception, Lp coefficient, and runoff delay factor "x" were manually adjusted within their specified range values. This process continued until a satisfactory level of agreement was achieved between the simulated and observed stream discharge data recorded at the Beles river gauge station. The calibration of the model was carried out by simulating volumetric runoff and base flow values. The combined flow in a river or stream within a watershed is determined by the sum of Q base flow and Q surface runoff, representing the long-term monthly average river discharge from the watershed. These values, simulated by the WetSpass model, were used to calibrate the model with the observed stream flow data obtained from the

Beles gauge station.

The Nash-Sutcliffe model efficiency coefficient (NES) has been employed to evaluate the accuracy of the simulated outcomes. This statistical metric serves as a means to assess the predictive capability of a hydrological model. The formula for calculating the NES is as follows:

$$NSE = 1 - \frac{\sum_{i=1}^{N}(Qs_i - Qo_i)^2}{\sum_{i=1}^{N}(Qo_i - \overline{Qo})^2}$$

Where: NSE= Nash –Sutcliffe Model Efficiency

N= Number of time step

Qo = Observed discharge [MCM]

Qoi= Simulated Discharge [MCM]

Qo = Mean of Observed Discharge [MCM]

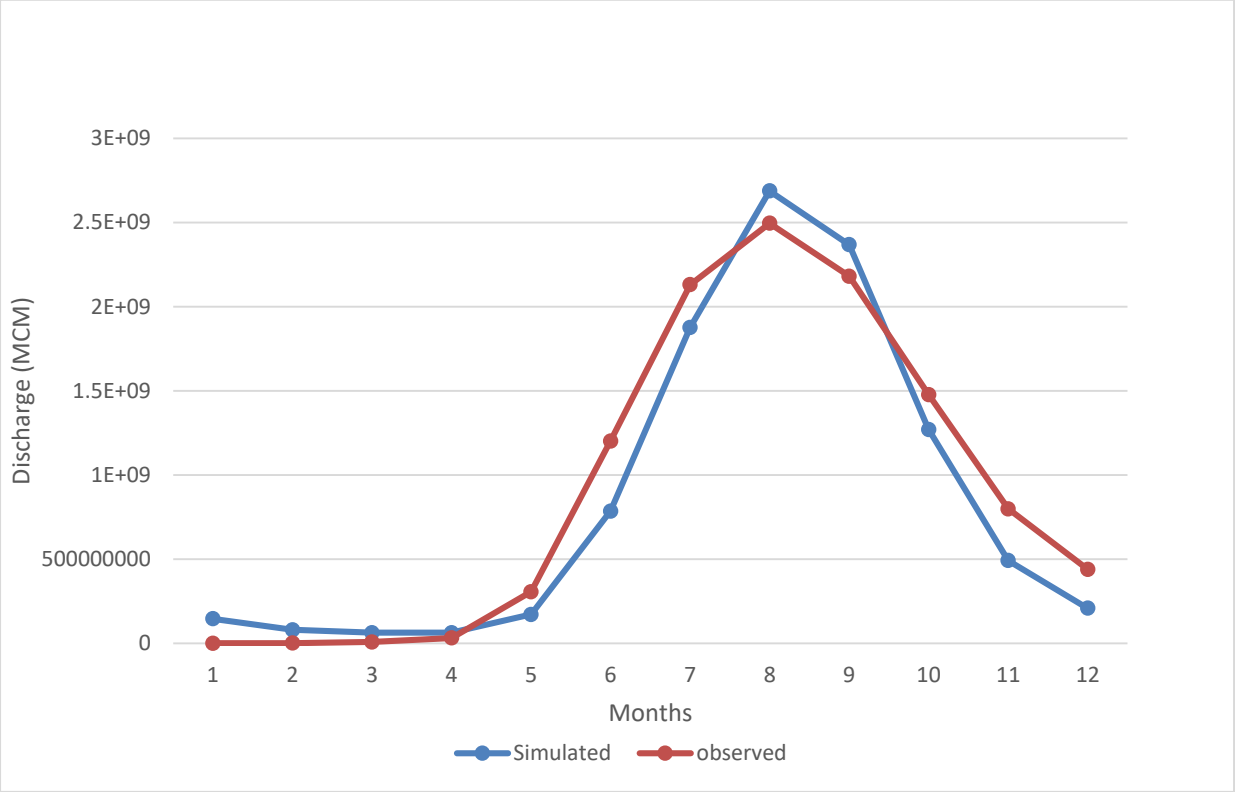

Figure 4. 21. Graphy of long-term Simulate and observed discharge

4.8. Outputs of WetSpass of Model

The WetSpass model generates grid maps of various hydrological parameters on a seasonal and annual basis. These parameters include groundwater recharge, actual evapotranspiration, surface runoff, interception loss, evaporation, and more. The main outputs of the WetSpass model are annual groundwater recharge, annual actual evapotranspiration, and annual surface runoff. A concise description of these outputs is provided below.

4.8.1. Actual Evapotranspiration (AET)

Actual evapotranspiration is the evapotranspiration from a vegetal cover under the natural or given conditions of supply of moisture or the actual amount of vapor which might be transferred to the atmosphere, depending also on the availability of water to meet the atmospheric demand.

The annual evapotranspiration was calculated by WetSpass as a sum of evaporation from bare land, transpiration of the vegetated cover, interception loss by vegetation,

and evaporations of the open water body. Actual evapotranspiration is one component of water balance to determine the groundwater recharge of the Beles basin using the WetSpass model. The WetSpass model has provided simulated results for the long-term actual evapotranspiration, which have been presented on a monthly basis and categorized into two seasons for the catchments (refer to figures 4.21, 4.22, and 4.23). The analysis reveals that approximately 941 mm of water is lost through evapotranspiration from the catchment, accounting for 58.38% of the annual precipitation. Out of the total annual evapotranspiration of 518mm, 32% occurs during the winter season, while the remaining 68% (equivalent to 423 mm) takes place in the summer season. This variation can be attributed to soil moisture deficit resulting from limited precipitation, leading to decreased evapotranspiration in winter. During the dry season, there is an increased demand for water due to the water requirements of crops and vegetation. Conversely, the summer season experiences higher precipitation duration, intensity, and distribution, along with healthy vegetation and other land covers, which contribute to accelerated evapotranspiration. Furthermore, the WetSpass model provides simulated results for the long-term annual transpiration, bare soil evaporation, and interception of the catchments (see figures 4.24, 4.25, and 4.26).

The Beles catchment exhibits an average annual interception ranging from 0 mm to 270 mm, with a mean value of 103 mm and a standard deviation of 57. Transpiration within this catchment varies from 0 mm to 453 mm, with a mean of 276 mm and a standard deviation of 58.5. The range of bare soil evapotranspiration in the catchment extends from 0 mm to 623 mm, with a mean value of 31.7 mm and a standard deviation of 102. Actual annual evapotranspiration with catchment, its value ranges from 574.8 to 1593 mm with mean and standard deviation 941 mm and 52.76 respectively. The output annual evapotranspiration grid map (figure 4.23) shows that low annual evapotranspiration is observed in north Eastern parts and southwestern parts of the catchment which receives lower annual rainfall.

High evapotranspiration value is observed in the north-western, western area and northern highlands of the Dangur area of the catchment because these areas are covered by cultivated crops, woodland, forest, grassland, and also the presence of high rainfall in highland areas. Generally, the value of annual evapotranspiration of the Beles basin varies with precipitation and land use/land cover. Hence, precipitation and land use land cover are the main controlling factors of evapotranspiration in the catchment.

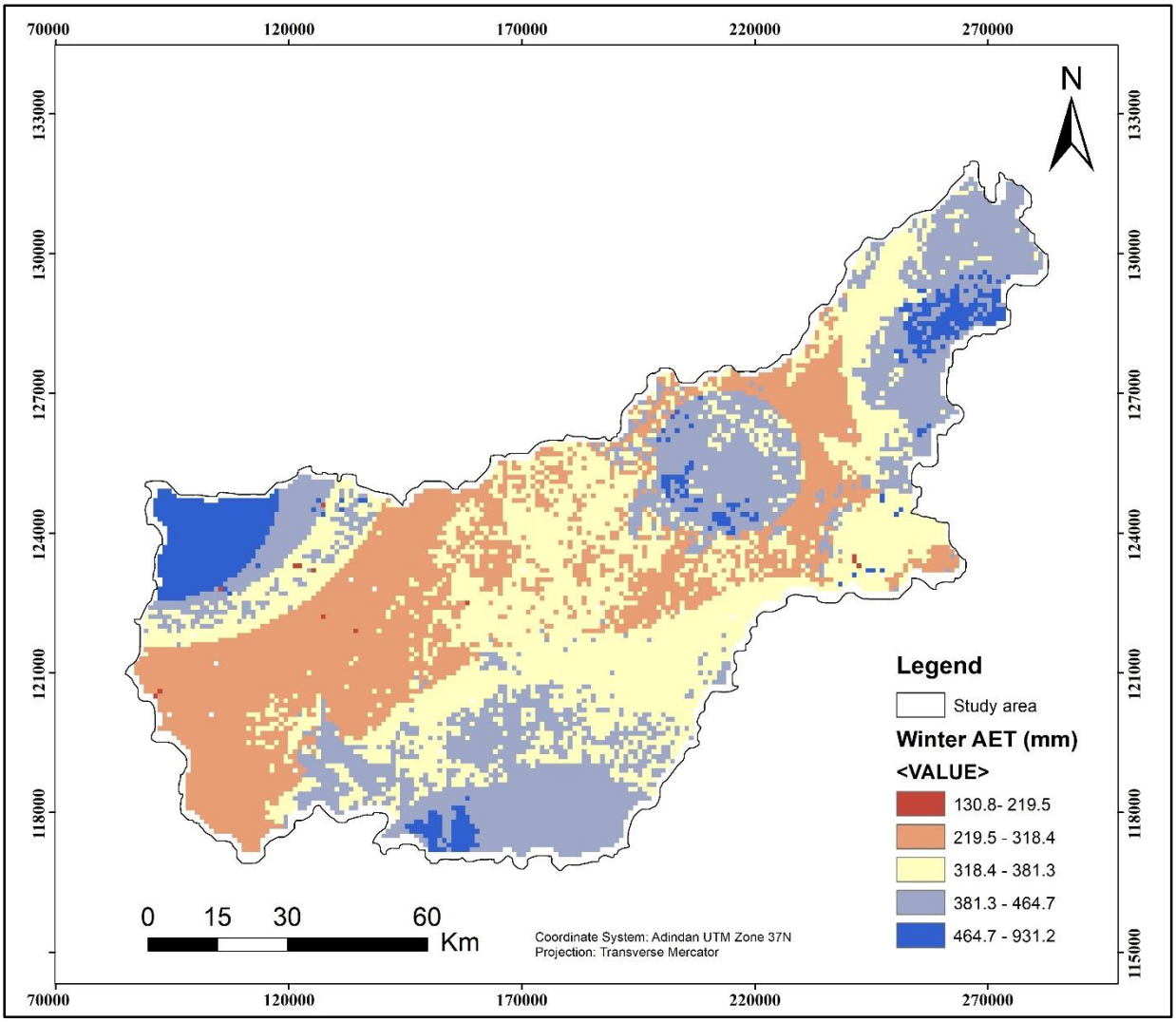

Figure 4. 22.winter Actual evapotranspiration

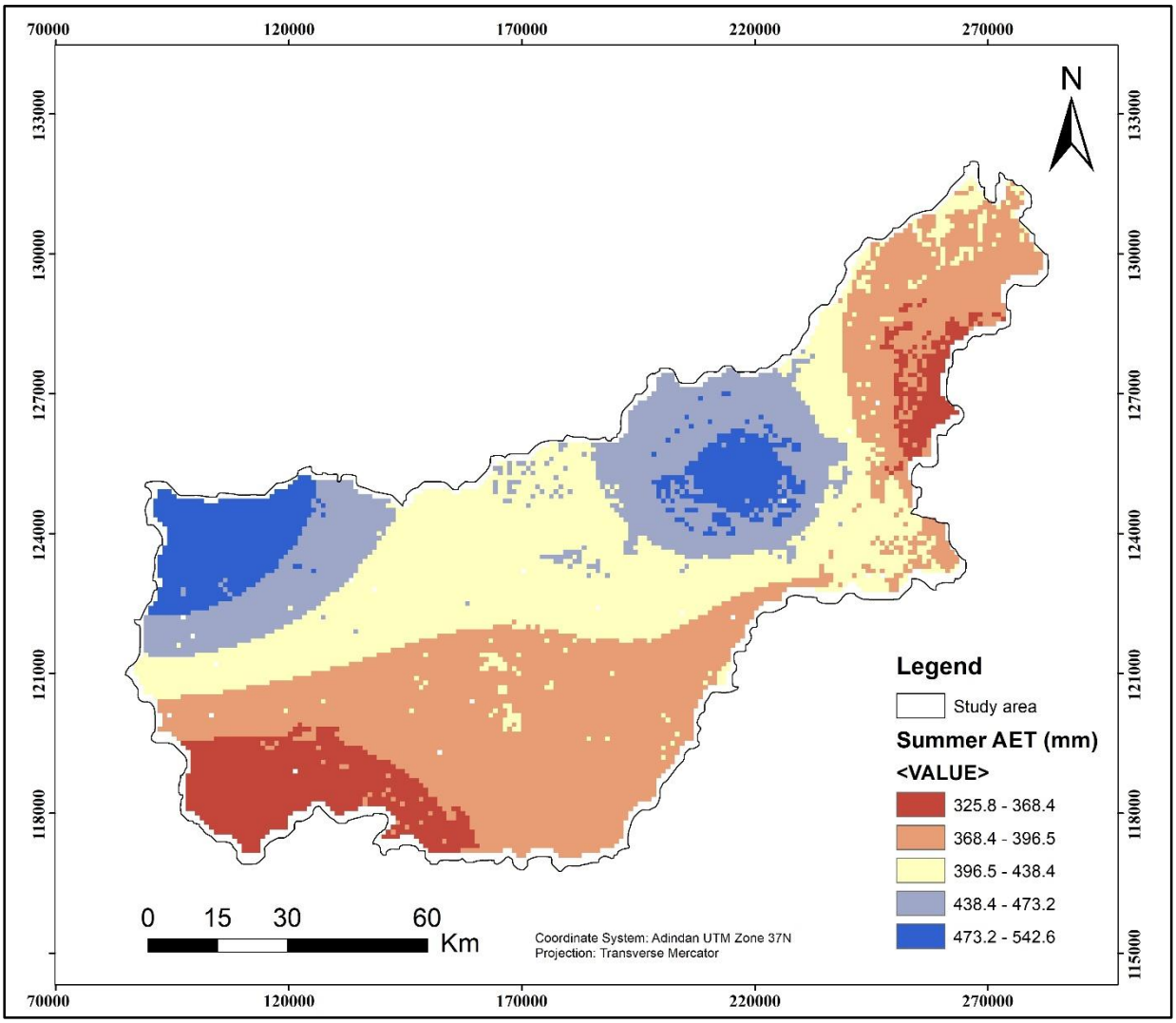

Figure 4. 23. Summer Actual Evapotranspiration

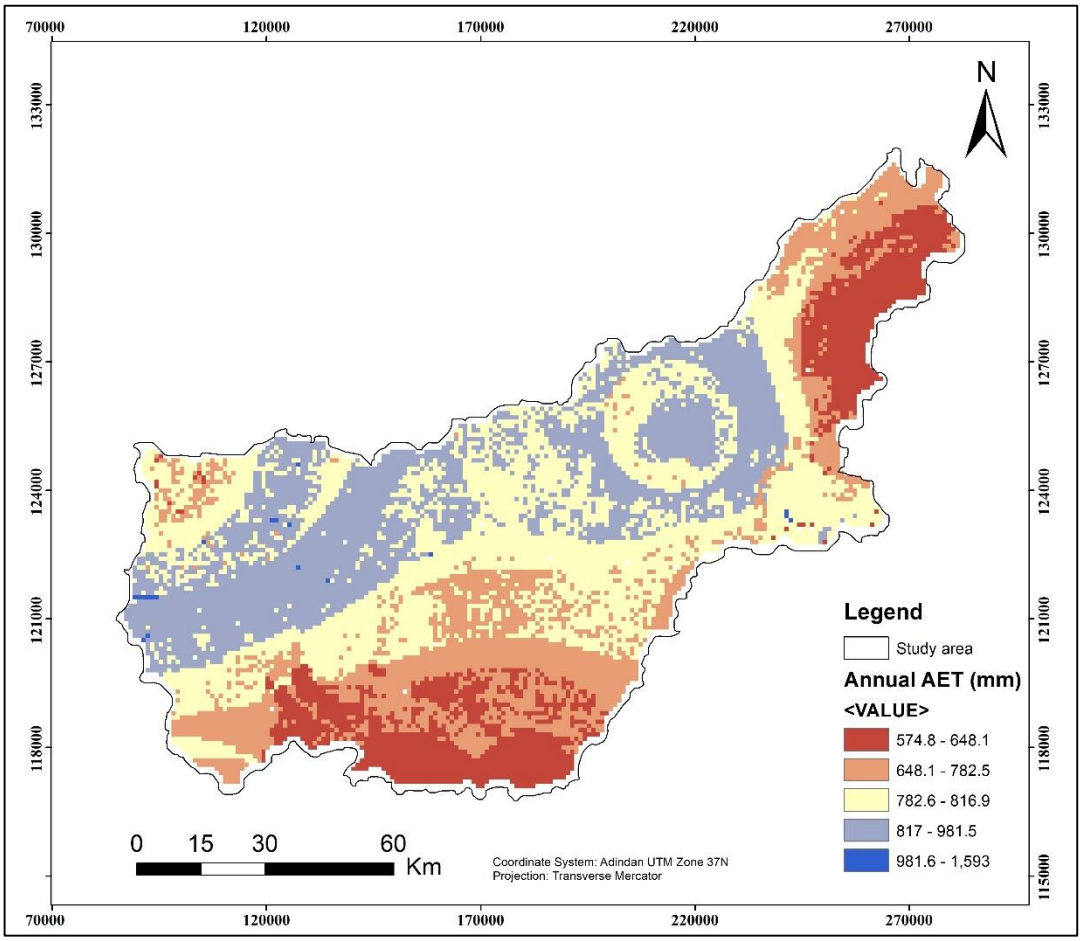

Figure 4. 24. Annual Actual evapotranspiration map of Beles basin

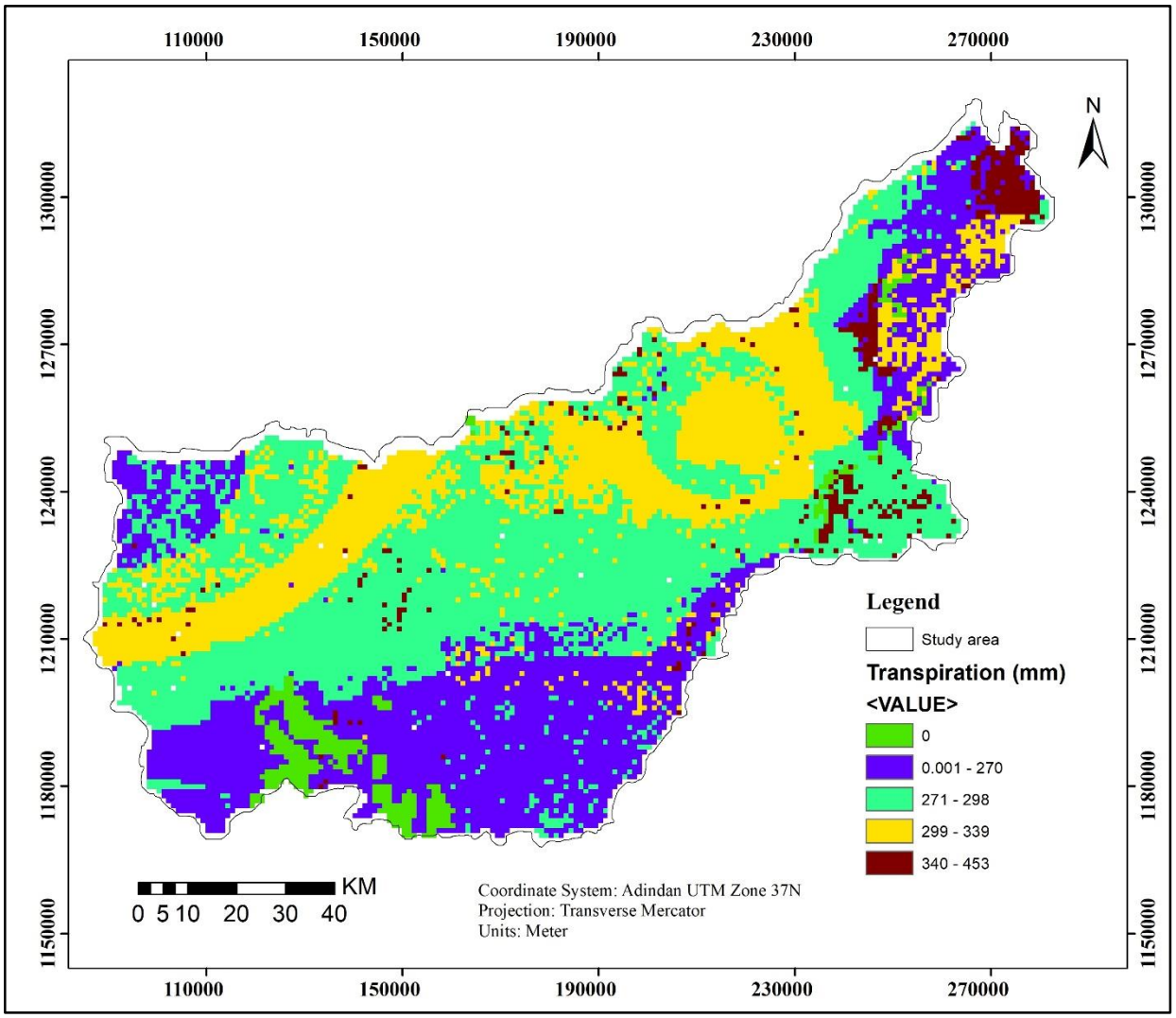

Figure 4. 25 . Transpiration map of Beles basin

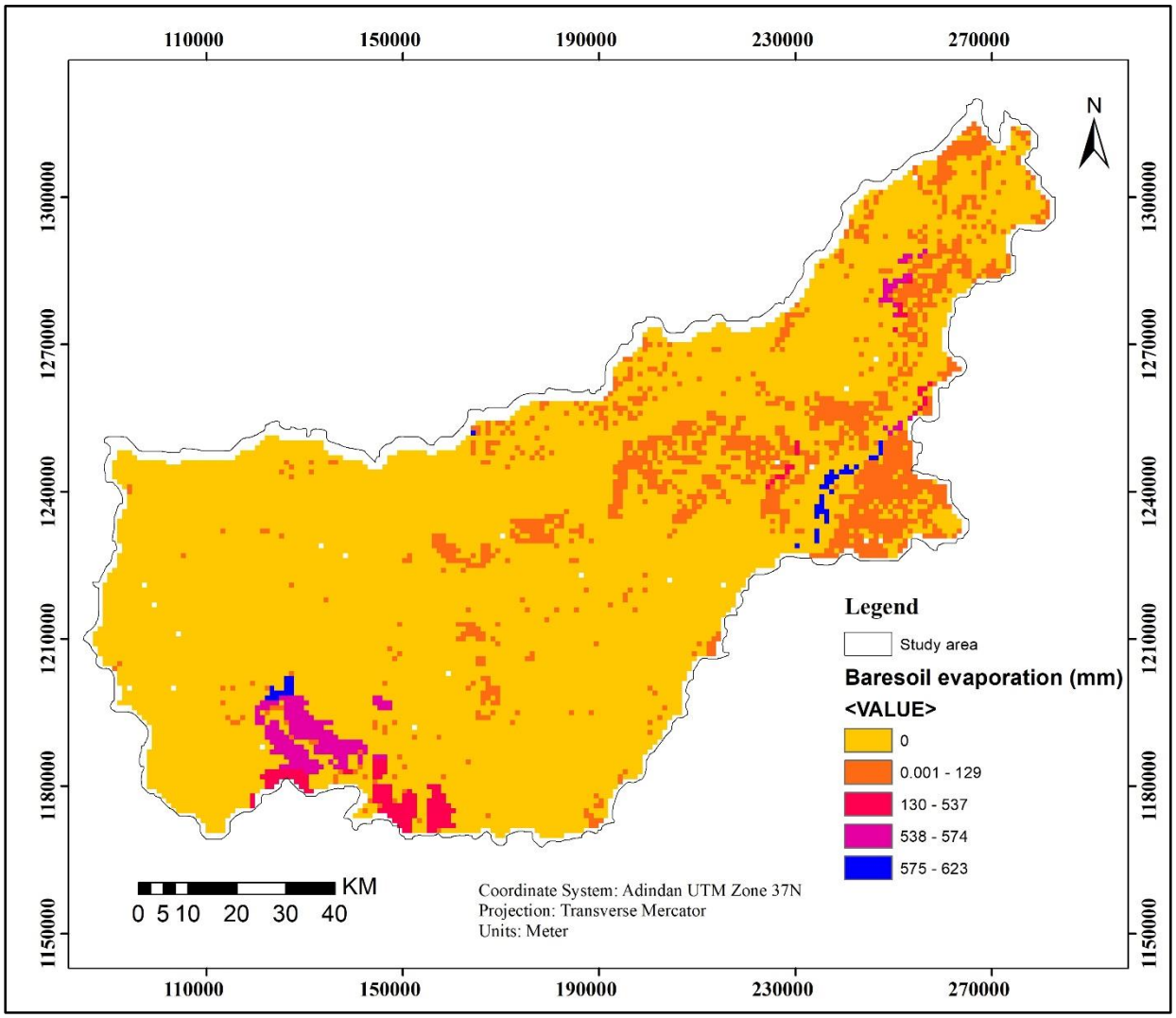

Figure 4. 26 . Baresoil Evaporation map of Beles basin

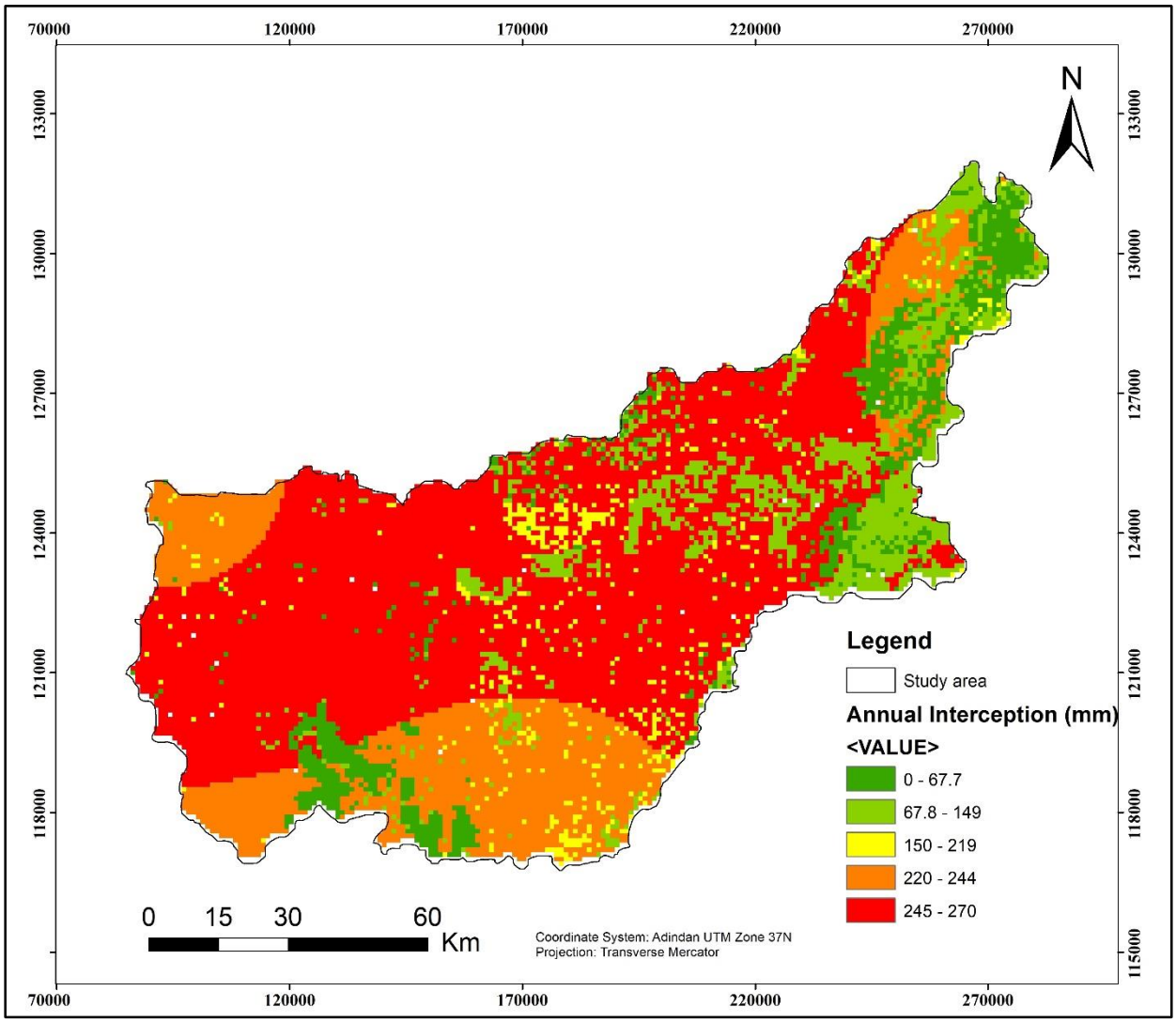

Figure 4. 27. Interception map of Beles basin

4.8.2. Surface Runoff

For estimating the surface runoff in the Beles catchment, the WetSpass model takes into account the runoff coefficient, which is influenced by factors such as vegetation type, soil type, and slope. The surface runoff within the Beles catchment exhibits variations due to diverse land use patterns, soil types, slopes, topography, precipitation levels, and other meteorological parameters. These variations can be observed and analyzed through figures 4.27, 4.28, and 4.29. The amount of surface runoff also shows variation in the summer and winter seasons. Surface runoff in the

Beles basin ranges from 186.4 to 1132mm with 586mm and 138 of mean and standard deviation values respectively. The mean value represents 36.35% of the total annual precipitations of the Beles basin. From this, about 86.47% of the surface runoff occurs during the wet season (June to September) while the remaining 13.53% occurs during the dry season (October to May).

This variation comes from rainfall differences in the two seasons. The rainfall exceeds the infiltration capacity of soil during the wet season which leads to high surface runoff. According to the annually simulated surface runoff of the catchment (Figure 4.29), the southwestern and eastern part of the catchment has the highest rates due to land use and land cover types in bare soil and agricultural area, which enhances surface runoff. Conversely, the western region of the catchment experiences lower surface runoff due to the presence of loam soil types, which enhance soil permeability. Additionally, this area is predominantly covered by forest and shrubland, further contributing to reduced surface runoff. This shows that soil types have a great impact on the annual surface runoff of the Beles catchment. Most of the rainfall in the Beles basin comes in the form of thunderstorms, whereby a thin impermeable layer at the ground surface increases the probability of surface runoff.

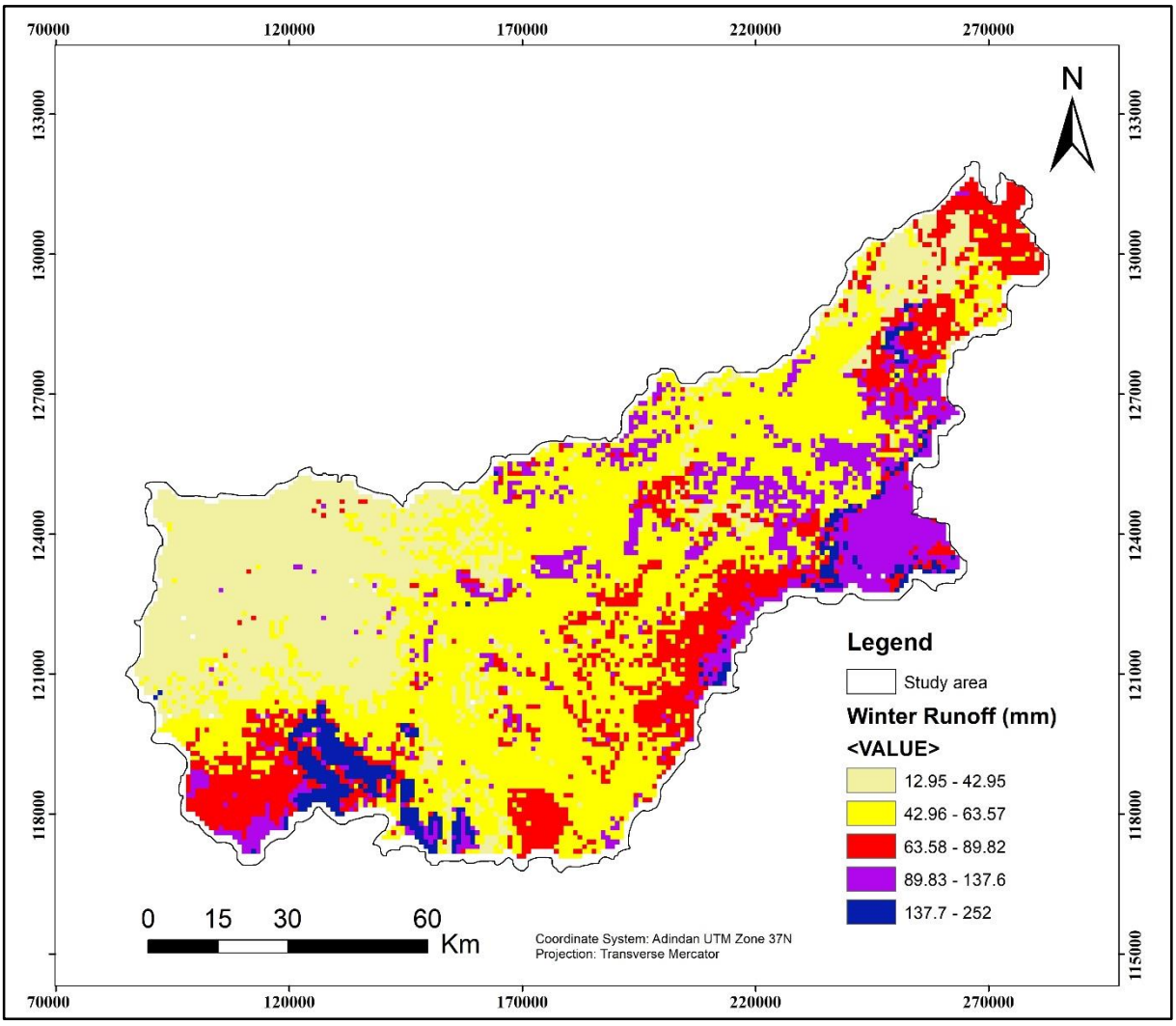

Figure 4. 28 . Winter surface runoff map of Beles basin

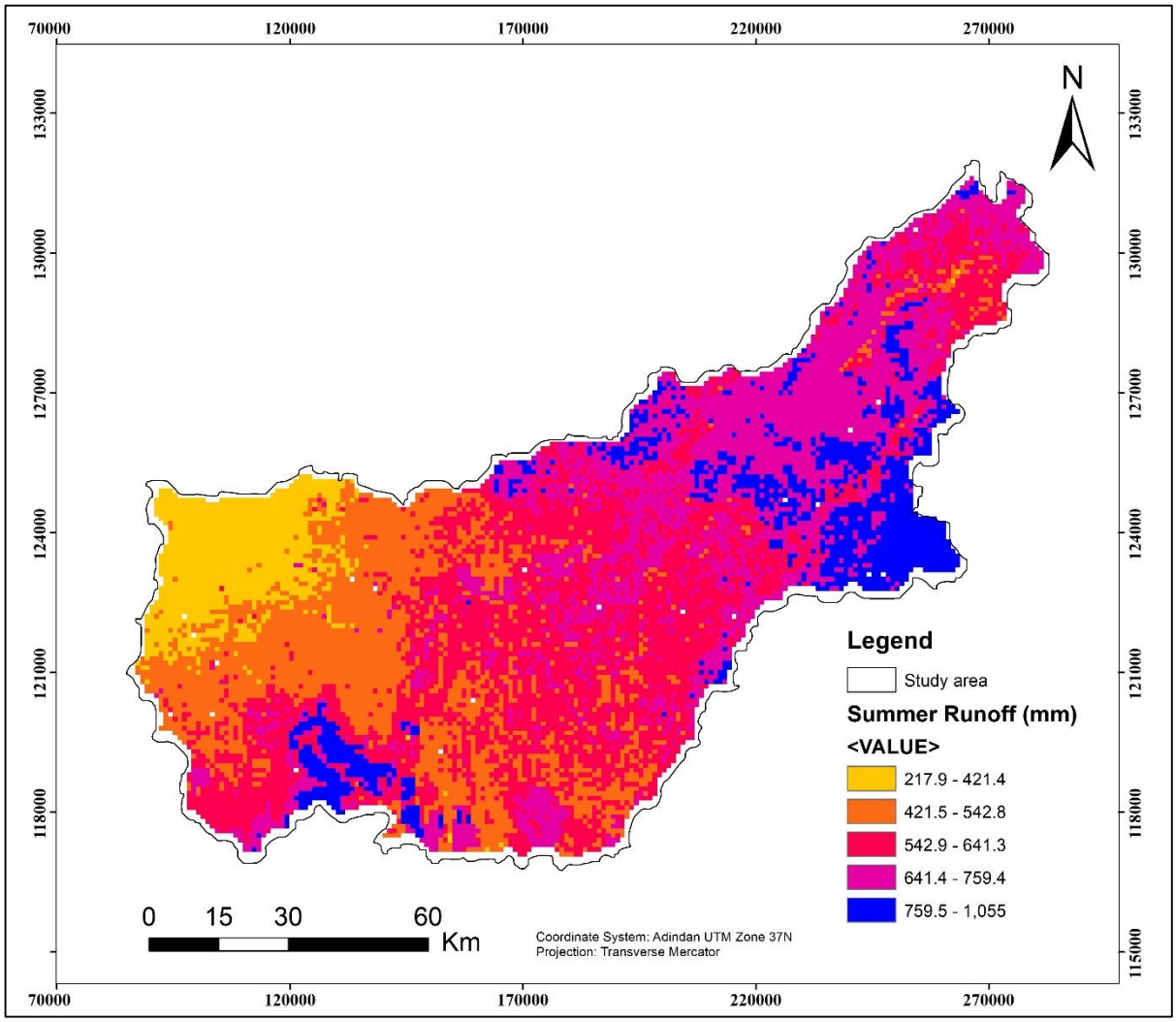

Figure 4. 29 . Summer surface runoff map of Beles basin

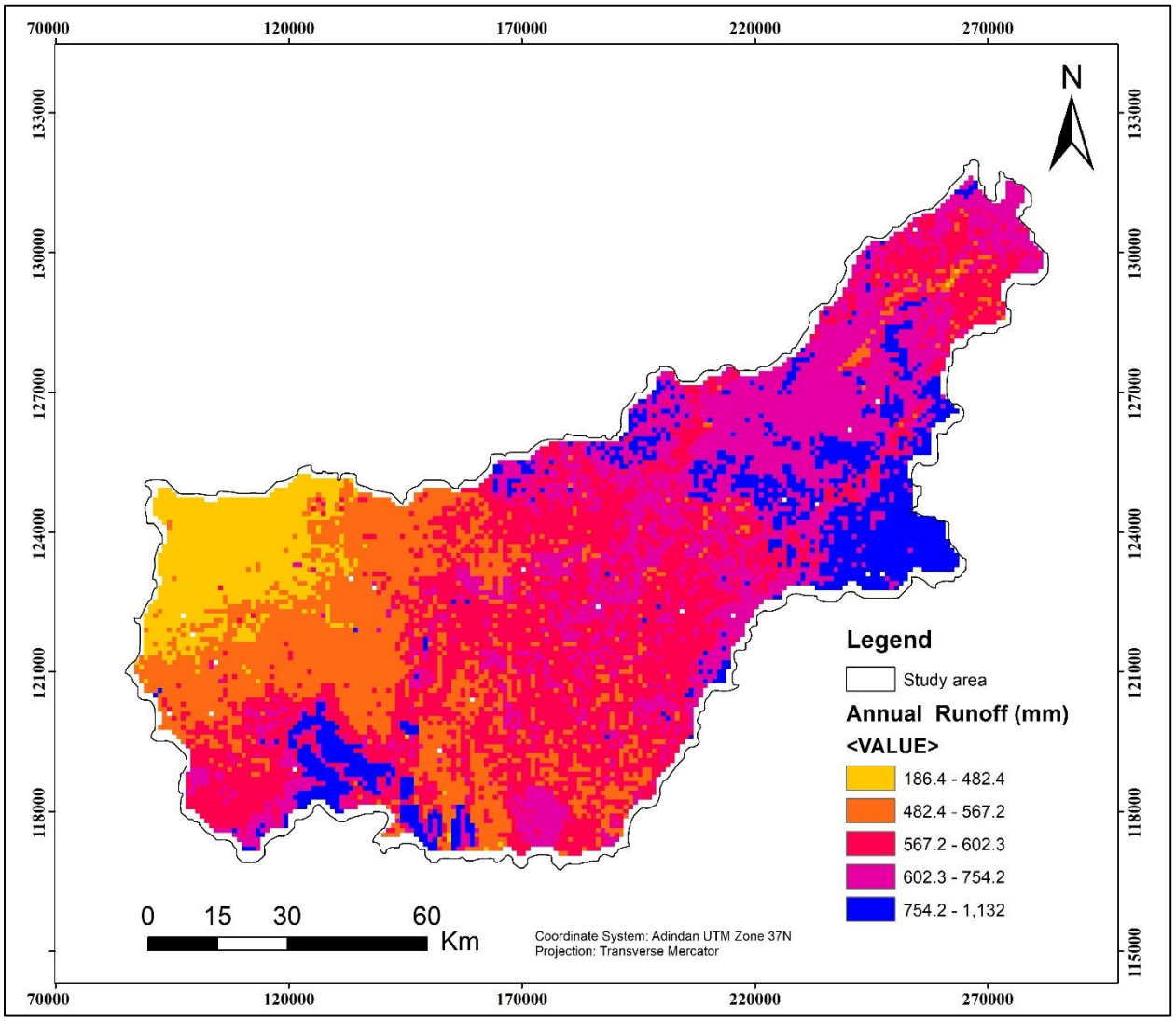

Figure 4. 30. Annual surface runoff map of Beles basin

4.8.3. Groundwater Recharge

Recharge refers to the process of replenishing aquifers with water from the surface, restoring them to their previous state. This natural process occurs as a crucial part of the hydrologic cycle, wherein rainfall infiltrates the land surface and percolates into the underlying aquifers. The rate of recharge in the Beles basin is influenced by various factors, including the physical characteristics of the soil, land cover, slope, water content of surface materials, rainfall volume, and the presence and depth of aquifers and confining layers.

Types of recharge.

Direct recharge - water added to the groundwater reservoir in excess of soil moisture deficits and evapotranspiration, by direct vertical percolation of precipitation through the unsaturated zone.

Indirect recharge: - it is percolation to the water table following runoff and localization in joints, as ponding in low lying areas or through the beds of surface water sources such as rivers, lakes and reservoirs.

Localized recharge: - the process of replenishing the groundwater reservoir through horizontal surface concentrations of water, typically occurring in areas where well-defined channels are absent. This localized recharge can be observed in various natural settings, such as depressions, low-lying areas, or regions with porous soils that promote the infiltration of water.

This endeavor seeks to provide a comprehensive overview of the recharge process at both regional and subregional scales. In the study area, all three types of recharge are present and identifiable. However, it is noteworthy that direct recharge from precipitation and indirect recharge from rivers hold the utmost significance in contributing to the overall recharge process.

Recharge from precipitation

The ultimate source of groundwater recharge in the study area is precipitation. The precipitation in the area varies significantly both in space and time. Generally precipitation increases with altitude. However, due to Topographic effects, this relation does not hold in these Basins. The total precipitation is in the study area used as shown in (figure 4.1).

The recharge to the groundwater is used as a parameter to be modified by trial and error so that the resulting hydraulic pressure fits the measured groundwater tables at known places in the basin because there is no data on the groundwater recharge at a regional scale.

Under favorable geological and topographic conditions, locations with significant precipitation typically experience greater groundwater recharge. The elevated mountain ranges and plateaus play a crucial role as recharge zones for groundwater. These include the Wombera plateau in the southwest, the Balay and Dangur mountains in the northeast, the highlands of the Dangila and North Achefer woredas in the north and northeast, and the Kar Mountain Ranges in the east. However, due to topographic limitations, the groundwater potential in these elevated regions is relatively low. On the other hand, the undulating and lowland plains, along with the permeable volcanic rocks, contribute to the continuous supply of water to the shallow and intermediate aquifer systems. Additionally, high-discharge springs originating from the base of the mountains also receive a consistent flow of groundwater.

In lowland areas, the potential evapotranspiration greatly exceeds the amount of precipitation, resulting in minimal direct recharge from rainfall. However, in regions with severely fractured rocks and permeable quaternary deposits, direct recharge can occur during exceptionally wet months such as July and August. Despite having remarkable rainfall, the Pawe Plains receive a lot of precipitation. They have fractured basalts and substantially thicker permeable quaternary deposits.

Recharge from Rivers

In addition to the very heavy precipitation, the area may experience significant direct recharge. The existence of perennial rivers and springs with high discharges is proof of this. In general, the highlands have a higher input of groundwater to rivers. Rivers that flow into lowlands are predicted to lose a significant amount of water through porous quaternary sediments and fractured rocks into the groundwater system (both the volcanic and the basement). As revealed from field observations and cited in Ayenew Tenalem and Addisu Girma's (2010) study, it has been observed that the discharge of the rivers in the study area decreases from

upstream to downstream. In the lowlands to the southwest, the perennial rivers' discharge reducesIn the lowlands, several small rivers experience a cessation of flow, despite having significant volumes of water in the upper peaks. In larger streams with a notable sand bed, water continues to flow beneath the sand even during the dry season. However, as the streams move downstream, completely dry sand becomes visible, indicating that water infiltrates back into the permeable streambed.

Large regional recharging zones can be found in the Dangur Mountains and the Wonbera plateau. Even though there doesn't seem to be much precipitation, there are heavily fractured basalts. All sides of this plateau in the highlands are surrounded by sheer escarpments. Along the ridge where the volcanic and basement rocks contact line, the recharged water creates a large number of springs. In the case of Wombera, the residual groundwater drains to the lowlands of Bullen and Wonbera Woreda, and the case of Dangur Mountain, it drains to the lowlands of Dangur Woreda, namely the Manbuk area. The Balaya Mountains, North Achefer's highlands, Dangila, and Kar Mountains are excellent local sources of recharge for the basin. These recharge areas produce numerous high-yield springs, the majority of which are aligned with local faults and lineaments. These springs include those in the lowlands of Pawe, such as Ali Spring, which is estimated to have a yield of more than 36 lit/s, at the escarpment of Kar Mountain (Abatachin Spring), daphily spring, and many others. (figure 3.8).

There are different models to estimate recharge in a given area depending on actual areal conditions. In this case, the WetSpass model estimates seasonal and annual long-term spatial distribution amounts of groundwater recharge of the Beles basin by subtracting the seasonal and annual surface runoff and evapotranspiration from the seasonal and annual precipitation, respectively. The annual groundwater recharge of the Beles basin varies from 0 to 540mm with a 223.40mm mean value (13.86 % of the annual precipitation).

The simulated groundwater recharge is highly dependent on land use and land cover of the study area (figure 4. 32). The degree of surface sealing of the ground surface depends on the type of land use. The rural area comprises different land-use types and covers the highlands of Beles. These areas have both positive and negative impacts on groundwater recharge. For agricultural areas, maize, sorghum, and teff crops there is a clear influence of the seasons. It is assumed that these lands are in the winter almost bare, which results in increased surface runoff, and reduced actual evapotranspiration. During the summer season, actual evapotranspiration increases, resulting in reduced recharge. Coniferous forests and wet grasslands, which retain vegetation during winter, exhibit relatively higher evapotranspiration and lower surface runoff. The groundwater recharge map, generated using WetSpass, illustrates that the distribution of recharge is primarily influenced by soil type in the highlands and land use in the lowlands.

In general, high values of groundwater recharge are observed in the coniferous forest and shrubland with loam soils and sandy loams and low evaporation. This phenomenon can be attributed to the favorable permeability of these soils and the gentle slope of the topography. However, areas with grazing land-use and various soil types exhibit lower levels of groundwater recharge. This is primarily due to the increased release of transpiration through plants and grass leaf stomata, resulting in reduced amounts of water infiltrating the soil to recharge the groundwater.

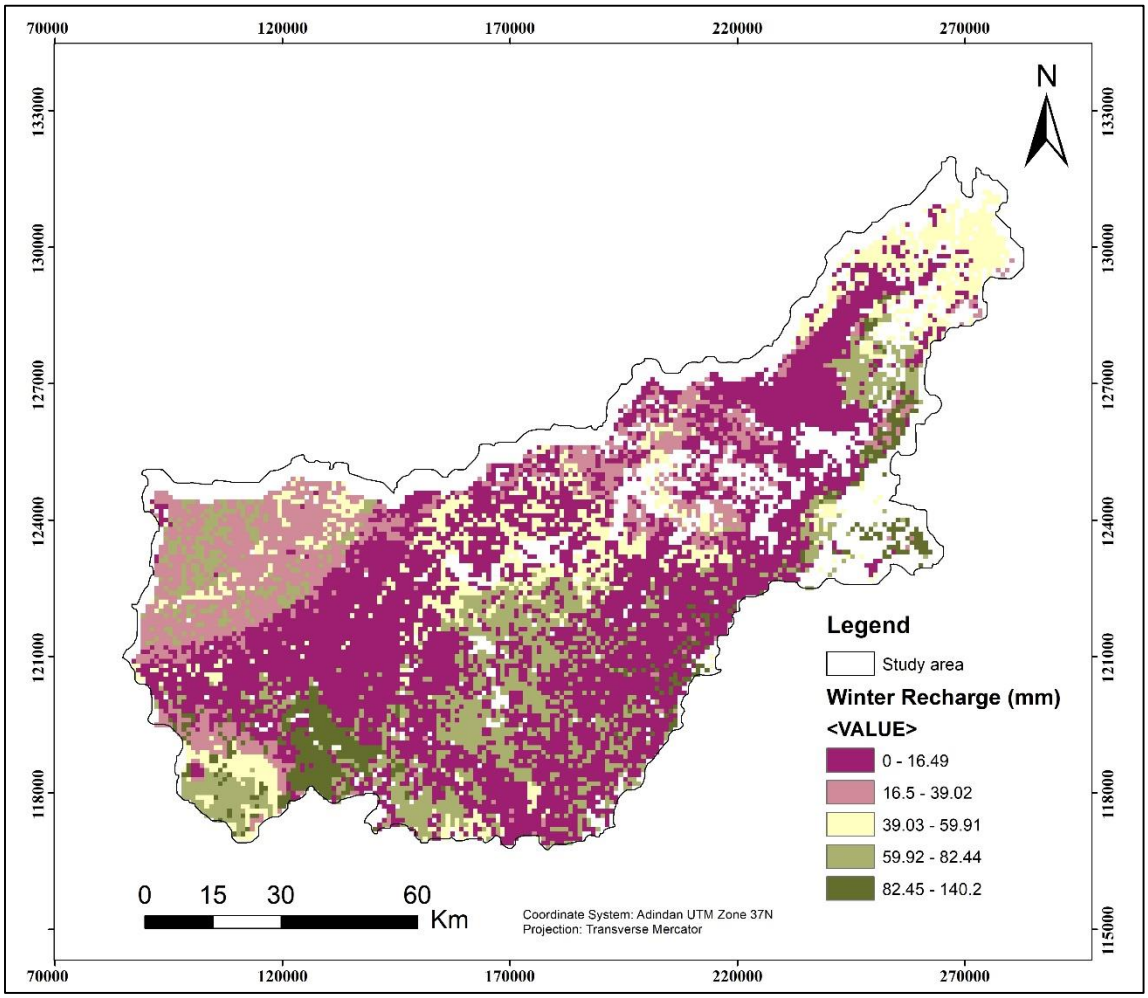

Figure 4. 31 . Winter groundwater recharge of Beles basin

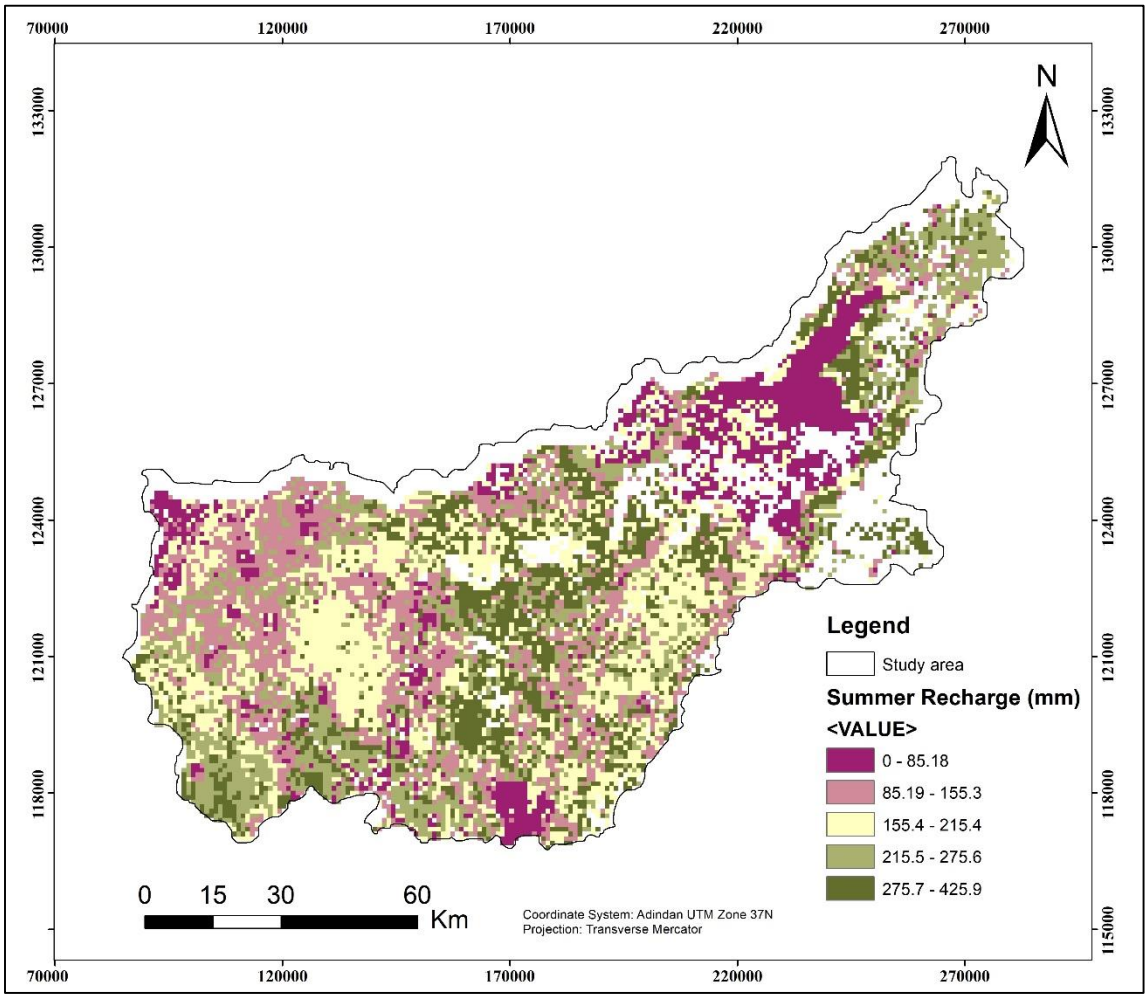

Figure 4. 32 . Summer groundwater recharge of Beles basin

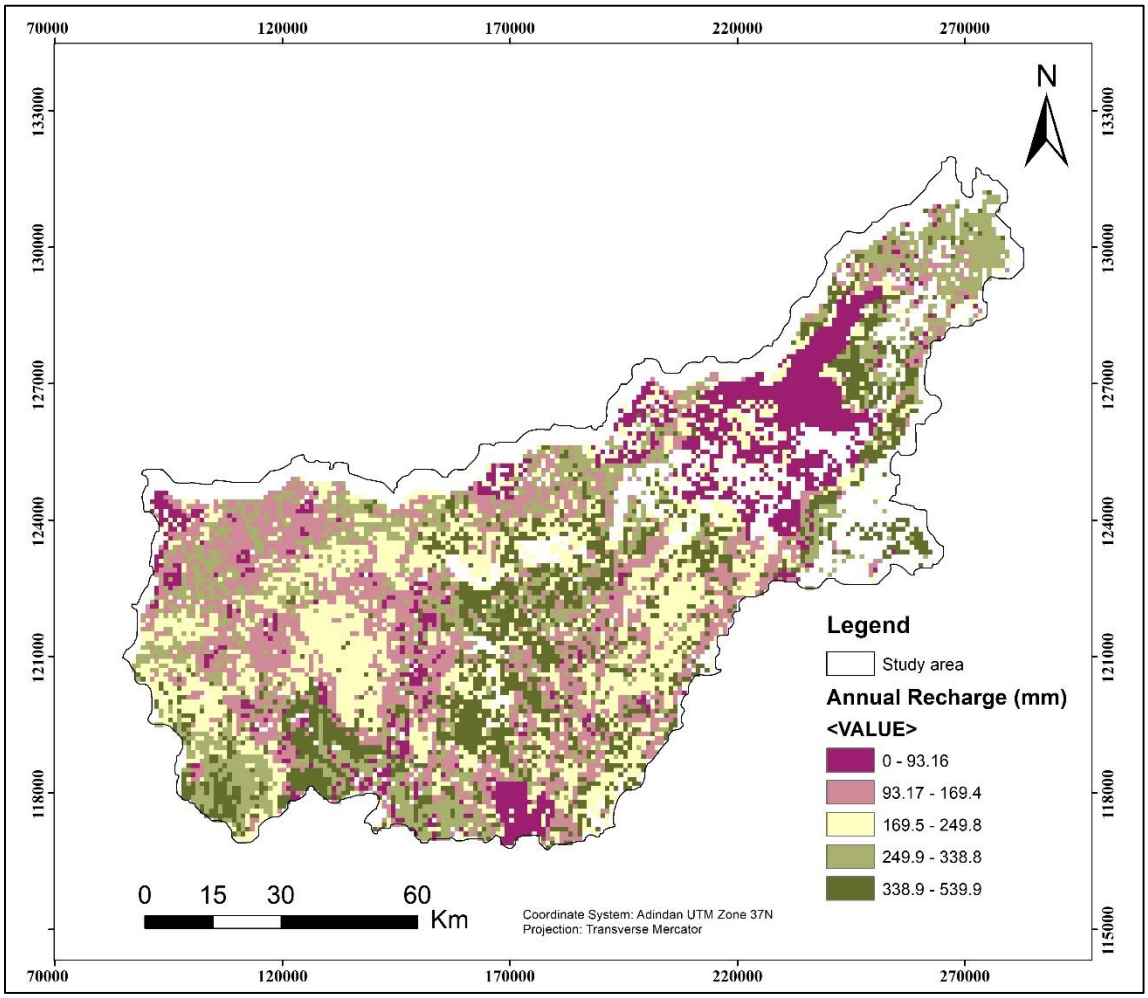

Figure 4. 33. Annual groundwater recharge map of Beles basin.

4.9. Baseflow recharge estimation methods

The most basic difference between base flow separation and the other recharge estimation methods is that this method is designed to quantify part of the stream flow hydrograph attributed to groundwater discharge, whereas, all the other methods estimate the amount of water added to the water table

In accordance with Balek's definition (1988), recharge is characterized as the downward movement of water through the saturated zone, driven by gravity or hydraulic conditions dictating its direction.

In certain cases, baseflow has been utilized as a means to estimate recharge, assuming that it is likely lower than the actual amount of groundwater recharge

(Chen and Lee, 2003). The drainage systems in a given area are influenced by factors such as climate, topography, land cover, and geological characteristics, including tectonic structures. In regions with steep mountains, the drainage systems are well developed and follow the natural slopes of the terrain. As described by Erickson and Stefan (2008), baseflow refers to the continuous discharge into a stream originating from natural water storage, predominantly groundwater, which helps maintain a consistent flow between rainfall events. Rivers that flow consistently throughout the year tend to have a significant baseflow component. Various techniques have been developed to assess baseflow as an indicator of groundwater discharge in streamflow hydrographs, albeit with subjective outcomes. Consequently, an analysis of long-term daily stream discharge data reveals that most streams exhibit flashy characteristics that are observed solely during the short duration of rainy seasons. Therefore, during summer rainfall events, the rivers exhibit a progressive flow towards the Beles River from the remaining watershed while remaining completely dry during the dry seasons.

In the Beles basins, there are two primary tributaries: the Main/Enat River and the Gilgel Beles River. The Main/Enat River has an average annual flow of approximately 577.44 mm/yr., while the Gilgel Beles River has an average annual flow of around 773.55 mm/yr. The Enat Beles River is the main river located upstream of the Beles catchment, whereas the Gilgel Beles River is a tributary that joins the main Beles River downstream of the basin. To better understand the dynamics and occurrence of groundwater discharge into streams, it is essential to closely examine the relationship between the various stream flow components and their connection with peak rainfall events. The daily time-series record of stream flow data has already been utilized to analyze and separate the hydrograph components of these two rivers. For a thorough examination, periods with complete daily discharge records are deemed most suitable for hydrograph separation and assessing groundwater recharge in the Beles basin.

To evaluate the indirect groundwater recharge or baseflow in the Beles basin, the baseflow separation Excel spreadsheet program was employed. This analysis utilized the daily river flow data from the Main Beles and Gilgel Beles River gauge stations (table 4.2).

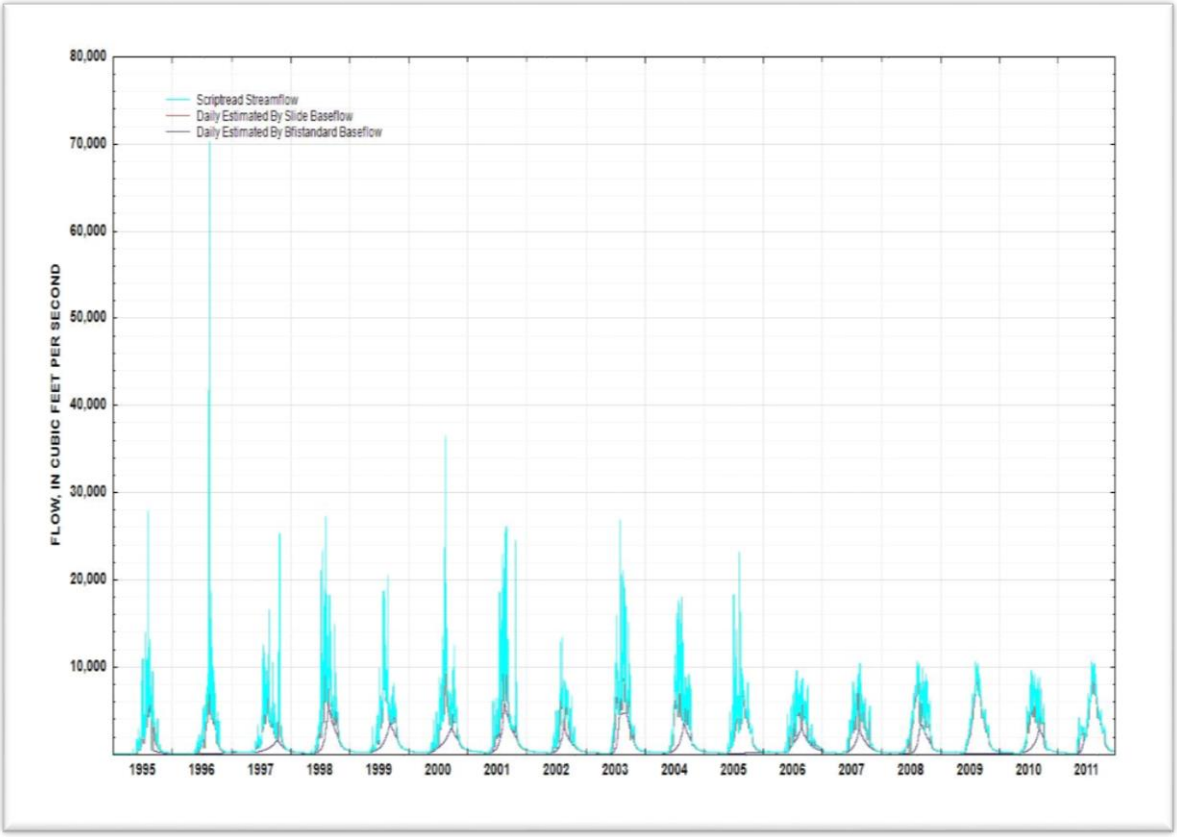

Figure 4. 34. Baseflow Separation of Main Beles at Bridge

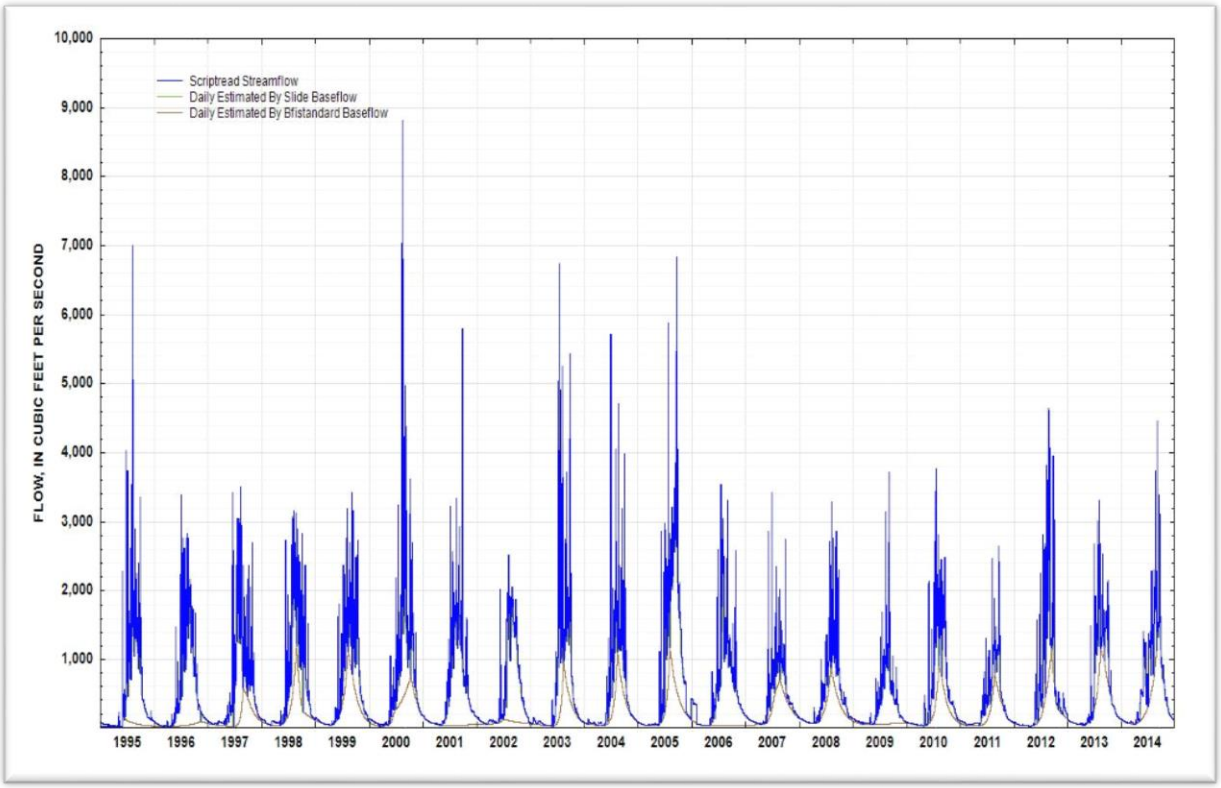

Figure 4. 35 . Baseflow Separation of Gilgel Beles near Mandura

The total annual recharge or base flow from the BFI Standard are 205.74mm/year which accounts to be 12.76% of the mean annual areal precipitation while Hydrograph Separation models average 201.29 mm/year, which accounts for 12.49% of annual areal precipitation. The total average annual recharge Beles basin of the two river catchment is 203.52mm/year which accounts12.63% of the mean annual areal precipitation of the catchment.

4.9.1. Seasonal dynamics of the baseflow index

The Base Flow Index (BFI) serves as a metric to assess the characteristics of baseflow in a basin. It is determined by calculating the ratio of base flow to total flow during the analysis. The BFI provides insights into the impact of factors such as soil type, land cover, slope, and geology on river flows, as highlighted by Gustard et al. (1992). Geology is the most important factor in influencing the BFI in the region as other catchment factors are more or less similar.

The average monthly baseflow index corresponds to the seasonal variation of baseflow, which is influenced by the seasonal patterns of precipitation. In this study, discharge data spanning nineteen years was utilized to examine the seasonal dynamics of the baseflow index in the Beles basin. Based on these findings, the rainfall pattern in the area was classified into two distinct seasons: rainy and dry. The groundwater component of the river was determined by analyzing the continuous and intermittent flows from aquifers that contribute to the river, taking into account varying levels of hydraulic connection. Table 4.2 presents the baseflow indices obtained through the BFI standard and hydrography separation sliding interval methods.

Table 4 2. Total flows, base flows, and base flow indices (BFI) for study area stations

watershed	Area km2	Measured Total Flow (mm/year)	BFI standard		HYSEP-Sliding	
			BFI	Baseflow (mm/year)	BFI	Baseflow (mm/year)
Gilgel Beles	675	769.77	0.31	238.76	0.29	226.06
Main Beles	3431	587.62	0.29	172.72	0.30	176.53

The average base flow indices (BFI) for the model period for BFI Standard and the HYSEP-sliding method, on a watershed basis, are 0.30 and 0.295, respectively (Table 4.2). The HYSEP method tends to produce more base flow than the BFI Standard. Moreover, the behavior of the BFIs of the two models was examined every month. The HYSEP method has higher BFI than BFI standard method the difference in others is insignificant or does not show a clear trend.

Higher BFI values for both methods occur in dry seasons, which are on average from 0.52 to 0.77. For wet seasons they are from 0.30 to 0.65. This shows that the watershed is mainly influenced by base flow contributions. The significant wet

season variations are likely in part attributed to rainfall distribution and land use patterns during wet seasons.

4.10. Chloride Mass Balance (CMB) Methods

The CMB (Chloride Mass Balance) method operates under the assumption that the amount of chloride tracer input at the surface is equal to the amount of tracer that reaches the groundwater table. Chloride ions are known for their conservative behavior, as they tend to remain chemically stable in solutions (Hem, 1985). This technique treats chloride as an inert element, which means it is not added or removed through water-rock interactions, unlike other inorganic ions. In the hydrological cycle, chloride is considered inert and originates from the atmosphere. One advantage of using chloride as a tracer is that atmospheric inputs are conserved during recharge processes, allowing for a mass balance approach to be applied. This distinguishes it from tracers involving water molecules.

According to the explanation provided by Somaratne and Smettem (2014), the fundamental equation used to estimate recharge using the chloride mass balance method is as follows:

$$R = (P.Clp)/Clgw$$

Where: R is the annual recharge (mm),

P- is the mean annual precipitation (mm),

Clp-is chloride concentrations of the precipitation (mg/ l),

Clgw-is chloride concentrations of the groundwater (mg/ l).

To ensure accurate results, the study excluded chloride concentration data from deep wells, as the vertical percolation of groundwater through clay layers and fault zones can lead to the retention and increased concentration of chloride ions. Only the average chloride concentration in groundwater from shallow wells was taken into account. In addition, the chloride concentrations of precipitation samples

collected from the Beles basin were used as a representative measure of the chloride concentrations in the basin's rainfall.

n this study, the chloride concentration in rainfall samples was analyzed at the Environmental Engineering and Testing water and wastewater quality testing laboratory. The groundwater chloride concentration data was obtained from hydrochemical and geological map sheets provided by the geological survey of Ethiopia. The findings revealed a chloride concentration of 0.74 mg/L in rainfall and 4.93 mg/L in groundwater. Based on these results, the recharge of the area can be estimated using the chloride mass balance method as follows:

R=1611.7mm/y*0.74mg/l/4.93mg/l

=241.9 mm/year

Consequently, in the Beles basin, an annual addition or recharge of 241.9 mm of water occurs within the groundwater system. This signifies that only 15% of the total annual precipitation infiltrates into the groundwater reservoir.

Table 4. 3. Summary of the results of recharge estimation by using the three methods

Methods	**AET(mm/yr)**	**SRO(mm/yr)**	**Recharge(mm/yr)**
Wetspass	1044	586	223.40
Base flow separation			203.52
Chloride Mass balance			241.9

In general, the estimation of groundwater recharge in the area yielded a relatively narrow range of values when using three different methods. The Wetspass, BFS, and CMB methods produced values of 223.40 mm/yr, 203.52 mm/yr, and 241.9 mm/yr, respectively. The variations among these methods can be attributed to their

inherent limitations, differences in data utilization, and potential analytical errors. Among the three methods, the result obtained through the Wetspass method is particularly appealing, as it incorporates various meteorological and physical parameters in its calculation.

CHAPTER 5

5. CONCLUSION AND RECOMMENDATION

5.1. Conclusions

The evaluation of groundwater recharge in the Beles catchment involved the utilization of three distinct methodologies: the Wetspass method, Base flow separation (BFS) method, and Chloride mass balance (CMB) method. These approaches were employed to assess the replenishment of groundwater in the study area. The Wetspass method considers various factors, such as meteorological conditions and physical characteristics, to estimate the recharge. The BFS method focuses on separating the base flow from the total streamflow, providing insights into the contribution of groundwater. Lastly, the CMB method analyzes the concentration of chloride in groundwater and precipitation samples to evaluate the recharge. By employing these diverse methods, a comprehensive assessment of groundwater recharge in the Beles catchment was conducted, enhancing our understanding of this significant hydrological process.

The WetSpass model's output indicates that the Beles catchment's evapotranspiration value ranges from 574.8 to 1593 mm/year. The simulated mean weight of 1044mm is equivalent to 64.77% of the basin's average annual precipitation. The region's annual surface runoff, which accounts for 36.35% of the area's precipitation, ranges from 186.40 to 1132mm with 586 mean values. Based on this, the rainy season (June to September) accounts for around 86.47 percent of surface runoff, while the dry season (October to May) accounts for the remaining 13.53 percent.

According to the WetSpass model results, the Beles catchment's annual groundwater recharge ranges from 0 to 540 millimeters, with a mean value of 223.40 mm (13.86% of the annual precipitation). With loam and sandy loam soils, agricultural land shrub grass and coniferous forest areas encourage the highest groundwater recharge in the basin. The diverse distributions of climatic parameters,

influenced by factors like land use, soil type, topography, and slope, contribute to variations in the water balance within the catchment. To separate the base flow of the Gilgel Beles River and Main Beles River from long-term daily flows, the study employed the USGS Tool Box software. The results from the software indicate that the average base flow indices (BFI) for the model period, using the BFI Standard and HYSEP-sliding methods, are 0.30 and 0.295, respectively, on a watershed scale. Consequently, the base flow separation methods estimate that the study area experiences a recharge of 203.52 mm per year, accounting for 12.63% of the annual precipitation.

The chloride mass balance (CMB) approach was employed as the third method to evaluate recharge. It involved calculating recharge based on the chloride concentrations in rainfall and groundwater samples. The chloride concentrations in rainfall were analyzed in the Environmental Engineering and Testing water and wastewater quality testing laboratory, while the groundwater chloride concentration data was obtained from hydrochemical and geological map sheets of the Beles basin prepared by the geological survey of Ethiopia. The results revealed chloride concentrations of 0.74 mg/L in rainfall and 4.93 mg/L in groundwater. Consequently, the CMB method estimated a groundwater recharge of 241.9 mm/year for the Beles catchment. Although all three methods were used to calculate groundwater recharge, the Wetspass method stands out as the most reliable estimate. This is because it incorporates all meteorological and physical parameters, considering both spatial and temporal distribution in its calculation. The variations in recharge amounts among the methods can be attributed to the limitations of each method and potential errors during analysis.

The allowable difference demonstrates that the WetSpass and Baseflow separation and chloride mass balance methods accurately estimate the catchment's water

balance state. The base flow separation method's various assumptions and constraints may be the cause of the differences, which led to a lower value estimate

than that of the WetSpass model and chloride mass balance because it was unable to take into account deep groundwater flows beneath the river channel and upstream channel loss.

In the study area the ultimate source of groundwater recharge is precipitation. Additionally, river recharge is another significant factor contributing to groundwater recharge in the study area. River recharge occurs when water from rivers and streams infiltrates into the ground and replenishes the groundwater reservoirs. As the river flows from upstream to downstream, it supplies water to the underlying aquifers along its path, thereby recharging the groundwater.

In the study area, the process of groundwater recharge is significantly impacted by the rainfall patterns that originate from the highland areas of North Achefer's and Dangila, as well as the Balaya and Kar mountains, with a notable exception in the Pawe lowlands.

Groundwater flow dynamics in the Beles catchment were characterized by using groundwater level measurements of 3 boreholes, 12 shallow wells, and 16 hand-dug wells, and from 89 springs data. The borehole data, hand-dug wells and shallow well, and springs data were collected from the Ministry of Water and Energy, and Water, Mines, and Energy offices of the Amhara Region and the rest was collected during fieldwork by the researcher. From the groundwater level data, a groundwater contour map was produced and the flow lines were also indicated. Static water level data provided crucial information about groundwater dynamics in the study area.

The groundwater table contour map showed that groundwater dynamics of flow converges towards discharge areas. In areas where the groundwater table is nearer to the surface (small gradient), the groundwater contour lines (equipotential lines) were widely spaced. Whereas; in areas of the higher gradient (deep water table), the groundwater contour lines were narrow spaced as it is shown in the map (Figure 4.20) in theNorthern Highland of Dangur and Southwest of Wombera Highland part of study area. Generally, the groundwater flow system is controlled by surface

morphology, structures (E-W,N-S,NE-SW, NW-SE and groundwater flows is from the northeast towards the west, aligning with the flow of the Beles River.

5.2. Recommendation

Planning for the sustainable management of the groundwater resource depends on an accurate assessment of the groundwater recharge and identification of the groundwater flow dynamics. Further study could improve the precision of the groundwater assessment and groundwater dynamics in the Beles basin. On the other hand, to enable proper water management, the findings from this work will need to be supplemented by more in-depth local research. If addressed, the following crucial issues will help to ease the challenging situation that arises in groundwater investigations in the future.

- In order to anticipate the impacts of different stress scenarios on the groundwater resource, it is recommended to conduct further groundwater modeling studies. These studies will provide valuable insights into the potential consequences of various stress situations on the groundwater system, enabling better preparedness and informed decision-making.
- The construction of observation pipe (groundwater monitoring) wells is necessary to simulate groundwater flow in more detail and to control the area's groundwater fluctuation.
- A comprehensive analysis of the geological and structural aspects is necessary to thoroughly understand the governing factors that dictate groundwater flow direction, recharge patterns, and discharge mechanisms.
- Along with other thematic maps, the groundwater recharge map can be used as a source of information that can be periodically updated by adding new data. Therefore, to offer correct information about the hydrogeological as well as other government entities, there should be well-organized database systems in various governmental organizations.
- Taking advantage of several recharge estimation techniques is essential to ensuring the correctness of the outcome; nevertheless, the majority of these techniques do not take into consideration the spatial variation and

distribution of recharge. The WetSpass model, however, is superior since it provides recharge values with both spatial and temporal fluctuations.

- The alteration of natural vegetation due to agricultural practices and deforestation leads to a significant increase in evapotranspiration compared to groundwater recharge and surface runoff within the watershed. Consequently, it is imperative to conduct a comprehensive study on land use and land cover to facilitate rehabilitation efforts.

References

Achu A.L., Raghunath R., Thomas J. Mapping of groundwater recharge potential zones and identification of suitable site-specific recharge mechanisms in a tropical river basin. Earth Syst. Environ. 2020; 4(1):131–145. [Google Scholar]

Allison, M.., Hughes, G.., 1978. The use of environmental chloride and tritium to estimate total recharge to an unconfined aquifer. Aust. J. Soil Res. 16, 181–195. https://doi.org/10.1071/SR9780181.

Allison, G.B., et al. 1988. A Review of Some of the Physical, Chemical and Isotopic Techniques Available for Estimating Groundwater Recharge, in Springer. pp. 49–72.

Arnold, J.G, Muttiah, R.S., Srinivasan, R., and Allen P.M. (2000). Regional estimation of base flow and groundwater recharge in the upper Mississippi river basin. Journal of Hydrology, 227 (1-4) pp; 21-40

Ashebir H (2017). Characterization of Beles River Basin of Blue Nile Sub-basin in North-Western Ethiopia using Arc-Hydro tools in Arc-GIS. Int. J. of Water Resources and Environmental Engineering. 9(5): 113120

Aster Denechew and Seleshi Bekele (2009).Characteristic and Atlas of the Blue Nile basin and its sub-basin, International Water Management Institute.

Batelaan, O., Z., M., Wang, and De Smedt, F. (1996). An Adaptive GIS Toolbox for Hydrological Modeling, in Application of Geographic Information Systems in Hydrology and Water Resources Management, eds. K.Kovar and H. P. Nachtnebel, IAHS Publ. no. 235.

Batelaan, O., & De Smedt, F. (2001). WetSpass: A flexible, GIS-based, distributed recharge methodology for regional groundwater modeling. In H. Gehrels, J. Peters, E. Hoehn, K., Jensen, C., Leibundgut, J., Griffioen, B., Webb, & Zaadnoordijk, W. (Eds.), Impact of human activity on groundwater dynamics (pp. 11 –17). International Association of Hydrological Sciences, IAHS Publ. no. 269.

Batelaan, O. and Woldeamlak, S.T. (2007). Arc view interface for Wetspass, user manual, version 13-06-2007, Department of Hydrology and Hydraulic Engineering, Vrije Universiteit Brussel, Belgium.

Bazuhair, A.S., Wood, W.W. ,1996. Chloride mass-balance method for estimating ground water recharge in arid areas: an example from western Saudi Arabia. Journal of Hydrology, 186, 153–159

BCEOM. (1998). Abbay River basin integrated master plan, main report ministry of water resource, Addis Ababa.

Conway, D. (2000). The Climate and hydrology of the Upper Blue Nile River, The Geographical J., 166, PP: 49–62

Cooper, C.A., Hershey, R.L., Healey, J.M., and Lyles, B.F., 2013. Estimation of Groundwater Recharge at Pahute Mesa using the Chloride Mass-Balance Method. U.S. Department of Energy, Publication No. 45251

Daniel Gemachu. (1977). Aspects of Climate and Water Budget in Ethiopia. Addis Ababa University Press.

Daniel Nuramo, (2016). Temporal changes in Groundwater Recharge in the Upper Awash Basin with particular emphasis on Becho and Koka areas, Central Ethiopia. Unpublished MSc Thesis, Addis Ababa University, Addis, Ababa, Ethiopia.

De Smedt, F., Batelaan, O. (2003). Investigation of the human impact on regional groundwater systems. In: Tiezzi, E., Brebbia, C., A., Uso, J.L. (Eds.), Ecosystems and Sustainable Development, Advances in Ecological Sciences, WIT Press. 19:1145– 1153.

Ebrahim G . Y (2008), Hydrological Response of a Catchment to Climate

Change, Case Study on Upper Beles Sub-Basin, Upper Blue Nile,

Ethiopia

Engida, (2007). Groundwater resources in Lake Tana basin and adjacent areas rapid

assessment and terms of reference for further study.

ENTRO (2013). Surface –groundwater resource evolution and water balance for conjunctive use in the Tana Beles sub-basin, The Eastern Nile Technical Regional office (ENTRO), Addis Ababa, Ethiopia

EIGS (Ethiopian Institute of Geological Survey) (2010). A report on Geology of An explanatory Note on Hydrogeological and Hydrochemical map of Bhir dar Map A. Published Report, Addis Ababa, Ethiopia

EIGS (Ethiopian Institute of Geological Survey) (2011). An explanatory Note on Hydrogeological, Hydrochemical map of Abu Ramla Map (NC 36-7, NC 36-8) sub-sheet. Published Report, Addis Ababa, Ethiopia

Fetter G.W. (2001). Applied Hydrogeology. University of Wisconsin Oshkosh, USA, pp598.

Freeze. R, Allan, and Cherry, J., A. (1979). Groundwater Prentice-Hall, New Jersy. 616 pp.

Getachew Hadush, 2008). Groundwater Contribution to the Flow of the Upper Blue Nile. ITC MSc Thesis, the Netherlands.

Getahun Seyid (2002): Geology of the Abu Ramla area.

Gustard, A., Bullock, A. Dixon, J.M., 1992. Low Flow Estimation in the United Kingdom. Institute of Hydrology, Wallingford, p.88 (IH Report N0.108)

Hem, J. D., 1985.Research and Interpretation of the Chemical Characteristics of Natural Water (3rd edition), U.S Geological Survey Water-Supply Paper 2254: 1-263.

Huang, T., Pang, Z., 2010. Estimating groundwater recharge following land-use change using chloride mass balance of soil profiles: a case study at Guyuan and Xifeng in the Loess Plateau of China. Hydrogeology Journal, (19), 177–186.

Kebede, S., Travi, Y., Alemayehu, T., and Ayenew, T., (2005). Groundwater

recharge circulation and geochemical evolution in the source region of the Blue Nile river, Ethiopia Applied geochemistry, 20(9), pp: 1658-1676

Kebede et. al (2006). water balance of Lake Tana and its sensitivity to fluctuation in rainfall, blue nile basin, Ethiopia Journal of Hydrology 316(1-4) pp:233-247

Kirubakaran M., Johnny J.C., Ashokraj C., Arivazhagan S. A geostatistical approach for delineating the potential groundwater recharge zones in the hard rock terrain of Tirunelveli taluk, Tamil Nadu, India. Arab. J. Geosci. 2016;9(5) [Google Scholar]

Kovalevsky SV, Kruseman PG, Rushton KR (2004) An international guide for hydrogeological investigations, UNESCO, IHP-VI, series on groundwater NO.3

Livingstone, D.A., 1980. Environmental Changes in the Nile Headwaters. In: Williams, M.A.J., Faure, H. (Eds.). The Sahara and the Nile. A.A. Balkema, Rotterdam, Pp. 339–359.

Mccartney, M.P., Alemayehu; T.S., Easton, Z.M, Awulachew S.B., (2012) Simulating current and future water resources development in blue Nile river basin. Routledge Taylor and Francis Group, pp269-291(ch-14)

Naranjo, G., Fuentes, T.C., Cabrera, M.C., and Custodio, E., 2015. Estimating Natural Recharge using Chloride Mass Balance in a Volcanic Aquifer: Northeastern Gran Canaria (Canary Islands, Spain). Water, (7), 2555-2574

NMA (Ethiopian National Meteorological Agency) (2001). Initial National Communication of Ethiopia to the United Nations Framework Convention on Climate Change (UNFCCC), NMA, Addis Ababa, Ethiopia.

SMEC. 2007. Hydrological Study of the Tana-Beles Sub-Basins. Draft Inception Report. Snowy Mountains Engineering Corporation, Australia

Seifu, K., Tadesse, Y., Tamiru, A., & Tenalem, A. (2005). Groundwater recharge, circulation, and geochemical evolution in the source region of the Blue Nile River, Ethiopia. Applied Geochemistry, 20(12), 1658–1676.

Seifu Kebede, (2013). Groundwater in Ethiopia, Springer-Verlag Berlin Heidelberg, 293pp.

SOGREA (2012) Detailed Groundwater Investigation & Monitoring In Tana And Beles Sub-Basins Final Stage 1 Report Ministry Of Water And Energy.

Somaratne and Smettem (2014).Theory of the generalized chloride mass balance method for recharge estimation in groundwater basins characterized by point and diffuse recharge. Hydrology and Earth System Sciences, 11: 307–332.

Tenalem Ayenew and Tamiru Alemayehu (2001). Principle of Hydrogeology, Addis Ababa University, Department of Geology and Geophysics, Addis Ababa.

Wale (2008). The hydrological balance of Lake Tana Upper Blue Nile Basin, International Institute for geo-information Science and earth observation Enschede, Netherlands.

Walker, D., Parkin, G., Schmitter, P., Gowing, J., Tilahun, S.A., Haile, A.T., Yimam, A.Y., 2019. Insights From a Multi-Method Recharge Estimation Comparison Study. Groundwater 57, 245–258. https://doi.org/10.1111/gwat.12801

Annex -1 water point inventory

S/NO	Easting	Northing	Elevation (m)	Depth (m)	Type	S/NO	Easting	Northing	Elevation (m)	Depth (m)	Type
1	236115	1264380	1207	62	SW	189	239560	1237721	1848	13	HDW
2	239842	1264049	1295	9.3	HDW	190	244684	1235463	1835	12.5	HDW
3	241503	1263320	1260	9	HDW	191	242775	1246112	1852	11	HDW
4	242752	1264240	1264	8	HDW	192	260105	1253415	2080	7	HDW
5	244458	1294630	1244	8	HDW	193	259385	1253593	2093	8.5	HDW
6	241879	1295034	1351	7.5	HDW	194	263516	1255314	2068	21	HDW
7	232108	1291712	1123	8	HDW	195	261004	1253718	2083	21	HDW
8	235392	1293439	1160	6.2	HDW	196	261498	1254526	2122	13	HDW
9	225127	132378	964.3	3.9	HDW	197	275397	1249734	2004	21	HDW
10	216568	1323492	1336	68	SW	198	270716	1249724	2045	12	HDW
11	232045	1248196	1285	12	HDW	199	264926	1246256	2087	9	HDW
12	230321	1249545	1119	6	HDW	200	260139	1254104	2037	15	HDW
13	232037	1248187	1293	14	HDW	201	256330	1251327	2167	14	HDW
14	194213	1322544	795	7	HDW	202	255825	1251534	2137	15.5	HDW
15	194716	1322645	784	6	HDW	203	246538	1245546	1893	10.5	HDW
16	194717	132730	276	5.5	HDW	204	262383	1238904	2206	11	HDW
17	194316	1323486	772	5.5	HDW	205	263227	1238527	2223	10.5	HDW
18	192704	1322165	732	5.5	HDW	206	263723	1238538	2203	13	HDW
19	244105	1254478	1336	74	SW	207	264221	1238317	2208	8	HDW
20	244056	1253047	1372	80	SW	208	263626	1234629	2212	5	HDW
21	246528	1252940	1425	10	HDW	209	262528	1238805	2202	7	HDW
22	219506	1295197	918	86	SW	210	264637	1238546	2188	9	HDW
23	219097	1287146	1003	12.5	HDW	211	264685	1238488	2193	8.5	HDW
24	219072	1310034	852	10	HDW	212	272424	1244828	2040	12	HDW
25	214597	1308474	879	5	HDW	213	247112	1227614	1914	12	HDW
26	238755	1255996	1141	62	SW	214	246877	1226660	1943	13	HDW
27	238824	1258076	1236	9	HDW	215	260981	1235651	2161	11	HDW
28	209175	1303730	869	10	HDW	216	238565	1241945	1869	12	HDW
29	271000	1301727	869.7	10	HDW	217	270172	1235661	2142	4	HDW
30	208492	1302931	800	5	HDW	218	270284	1237676	2166	5	HDW
31	219097	1290888	959	4	HDW	219	271092	1236647	2163	7	HDW
32	215333	1287590	1003	8	HDW	220	270778	1237089	2161	6	HDW
33	215331	1234591	1000	13	HDW	221	278382	1237460	2152	5	HDW
34	215634	1234750	1008	8	HDW	222	258453	1257619	2163	6	HDW
35	226725	1240954	1322	14	HDW	223	259090	1257622	2133	10	HDW

36	226480	1238848	1299	12	HDW	224	257451	1261371	2178	5	HDW
37	209095	1322346	405.3	7.5	HDW	225	257929	1260196	2185	9	HDW
38	208195	1320237	410.5	3.5	HDW	226	276015	1239883	2075	8	HDW
39	213374	1316994	412.1	4	HDW	227	267654	1240090	2067	7	HDW
40	208428	1308011	822	12	HDW	228	249469	1243053	1942	14	HDW
41	205672	1307618	867	4.5	HDW	229	267594	1236665	2251	8	HDW
42	199479	1314384	1047	10	HDW	230	267809	1237163	2226	9	HDW
43	205372	1304266	837	6	HDW	231	268062	1236871	2235	8.5	HDW
44	206867	1358268	857	7	HDW	232	254349	1225446	2099	12	HDW
45	273770	1187915	2133	12	HDW	233	254289	1225877	2118	13	HDW
46	275077	1189097	2155	13.5	HDW	234	249888	1224658	2033	14.5	HDW
47	274532	1192182	2202	13	HDW	235	269848	1221179	2567	15	HDW
48	272188	1186873	2105	12	HDW	236	272261	1224302	2465	9.5	HDW
49	211759	1183264	2039	15	HDW	237	269948	1225329	2492	16	HDW
50	268412	1196674	2238	13	HDW	238	270534	1223362	2552	15.5	HDW
51	274950	1190375	2180	13	HDW	239	255732	1229242	2377	12	HDW
52	263406	1202718	2262		HDW	240	260926	1230271	2400	65	SW
53	258941	1208056	2479	14	HDW	241	286490	1220068	2409	18	HDW
54	264192	1205829	2388	13	HDW	242	285297	1219878	2440	8	HDW
55	250363	1205216	2286	15.5	HDW	243	264512	1217469	2561	10	HDW
56	256600	1208977	2320	16	HDW	244	261740	1231680	2346	17	HDW
57	252174	1208875	2216		HDW	245	262164	1231805	2364	13	HDW
58	268847	1193219	2180	12	HDW	246	262518	1230082	2391	4	HDW
59	259965	1205976	2333	18	HDW	247	2735091	1210555	2564	15	HDW
60	260142	1205725	2332	13.75	HDW	248	271553	1220606	2547	19	HDW
61	266991	1207356	2459	10	HDW	249	263516	1255314	2068	8	HDW
62	257513	1204038	2306	12	HDW	250	274826	1221256	2572	10	HDW
63	250365	1205213	2286	11.25	HDW	251	251189	1227251	2125	14.5	HDW
64	263606	1196596	2170	12.5	HDW	252	279797	1219838	2601	15	HDW
65	265206	1197020	2196	13.5	HDW	253	278549	1222631	2508	16	HDW
66	265392	1197264	2194	13	HDW	254	280228	1220565	2568	12	HDW
67	265308	1197028	2190	17.65	HDW	255	278896	1222543	2504	13	HDW
68	261852	1204592	2283	11.35	HDW	256	279766	1220192	2596	16	HDW
69	269065	1200521	2318	9.5	HDW	257	279536	1219764	2619	12	HDW
70	269065	1200521	2080	9	HDW	258	280078	1222657	2510	16	HDW
71	271999	1185258	2108	13	HDW	259	279603	1220683	2585	11	HDW
72	272188	1186877	2102	8.75	HDW	260	280259	1220753	2569	13	HDW
73	269065	1200521	2075	12	HDW	261	254631	1223241	2240	11	HDW

74	271991	1185245	2114	13	HDW	262	279441	1224322	2437	12	HDW
75	263404	1202704	2280	13	HDW	263	266814	1223536	2444	11	HDW
76	265075	1198590	2233	13.56	HDW	264	266658	1223757	2456	18	HDW
77	268579	1196614	2235	15	HDW	265	270172	1235661	2142	4	HDW
78	265673	1197330	2198	13	HDW	266	270284	1237676	2166	5	HDW
79	266538	1196672	2261	13.45	HDW	267	271092	1236647	2163	7	HDW
80	266914	1196672	2198	11.25	HDW	268	270778	1237089	2161	6	HDW
81	268457	1196577	2238	8.75	HDW	269	278382	1237460	2152	5	HDW
82	268413	1196508	2231	14	HDW	270	276490	1230253	2252	10.5	HDW
83	268439	1196574	2230	13	HDW	271	275566	1230757	2265	6.5	HDW
84	268593	1196721	2242	12.75	HDW	272	275967	1230896	2258	13.5	HDW
85	268441	1196757	2240	16	HDW	273	277938	1233210	2161	46	SW
86	268517	1196747	2243	9	HDW	274	280406	1234115	2146	10	HDW
87	268626	1196767	2239	13	HDW	275	250723	1224996	2050	15	HDW
88	268377	1196611	2233	14.35	HDW	276	250468	1224216	2039	12.5	HDW
89	268410	1196524	2229	17	HDW	277	263405	1210354	2445	13	HDW
90	275053	1192643	2196	8.75	HDW	278	264307	1210443	2465	9	HDW
91	275011	1192619	2189	14	HDW	279	254661	1224115	2304	8.5	HDW
92	265168	1198176	2234	17	HDW	280	260403	1224959	2387	8	HDW
93	261885	1200647	2226	15	HDW	281	261663	1222551	2389	13	HDW
94	252789	1201917	2794	14	HDW	282	262052	1224280	2388	10.5	HDW
95	265029	1194779	2163	13	HDW	283	257163	1226123	2248	14	HDW
96	264775	1195055	2161	14.5	HDW	284	275630	1222789	2764	9	HDW
97	262239	1187290	2020	12	HDW	285	236380	1194530	2146	8.5	HDW
98	262793	1184446	1947	16	HDW	286	235298	1198460	2106	21	HDW
99	259722	1185155	1941	15	HDW	287	240267	1189758	1822	19	HDW
100	262266	1184248	1931	17	HDW	288	247964	1198968	2266	8.65	HDW
101	263525	1184558	1958	13	HDW	289	244769	1196956	2005	13	HDW
102	255890	1186546	2029		HDW	290	245502	1196878	1988	8.5	HDW
103	250116	1197644	2168	24	SW	291	245240	1196657	1987	13.5	HDW
104	248410	1193626	2133	17	HDW	292	244499	1196406	1994	15	HDW
105	246740	1190422	1994	15	HDW	293	244130	1196200	1996	23	HDW
106	246517	1190689	2004	15	HDW	294	245952	1195100	1989	15.5	HDW
107	248134	1190360	2098	19	HDW	295	242310	1197705	2127	15.7	HDW
108	244751	1181076	1835	13	HDW	296	245424	1198651	2084	18.5	HDW
109	244425	1181311	1830	13	HDW	297	247798	1211924	1588	14.3	HDW
110	245765	1182364	1856	15	HDW	298	241138	1209427	1929	12.8	HDW
111	244952	1182317	1815	8	HDW	299	241710	1210173	1954	16.3	HDW

112	245064	1182825	1817	12	HDW	300	215822	1208084	1627	9.8	HDW
113	244293	1182572	1820	11	HDW	301	218902	1205617	1524	22	HDW
114	245760	1185200	1900	25	SW	302	225194	1219464	1657	23	HDW
115	251618	1167791	1481	48	SW	303	220885	129812	1667	16	HDW
116	256573	1186950	2040	48	HDW	304	229183	1218530	1677	12.5	HDW
117	260943	1183931	1409	10	HDW	305	205298	1193262	1602	4.5	HDW
118	251623	1188823	2135	14	HDW	306	205264	1193270	1605	5.8	HDW
119	251426	1188397	2129	19.5	HDW	307	223792	1196617	1716	11	HDW
120	251640	1188357	2135	21	HDW	308	219097	1198377	1673	8	HDW
121	254055	1180734	1934	11	HDW	309	218212	1198525	1682	14	HDW
122	249960	1197949	2560	10	HDW	310	223364	1197541	1677	7	HDW
123	250946	1195578	2505	17	HDW	311	219555	1198416	1687	13	HDW
124	250701	1195851	2445	10	HDW	312	218522	1203675	1506	18.7	HDW
125	251043	1193725	2390	13	HDW	313	240609	120441	1787	10.5	HDW
126	253941	1193591	2117	15	HDW	314	230043	1208189	1699	19.5	HDW
127	255719	1191806	2190	8	HDW	315	225389	1207051	1571	13	HDW
128	258064	1187136	1953	15	HDW	316	240331	1219540	1822	7	HDW
129	257703	1187047	1944	17	HDW	317	240662	1219738	1828	8	HDW
130	253393	1185729	1960		HDW	318	235818	1220681	1768	14	HDW
131	248594	1186215	2166	13	HDW	319	236888	1221503	1779	7.3	HDW
132	241689	1179190	1748	4	HDW	320	235278	1223361	1773	17.8	HDW
133	268411	1183590	2075	6	HDW	321	234021	122162	1769	18.5	HDW
134	248652	1189447	2084	13	HDW	322	238061	1223253	1781	7.5	HDW
135	250186	1192338	2202	18	HDW	323	244533	1224894	1897	19.4	HDW
136	246716	1190726	1995	15	HDW	324	226350	1223272	1817	9.6	HDW
137	262293	1187231	2020	10	HDW	325	233706	1212227	1714	9.7	HDW
138	261027	1186092	1972	16	HDW	326	233728	1211935	1757	14.5	HDW
139	269632	1213241	2872	9	HDW	327	223053	1183846	1784	16.5	HDW
140	269821	1211830	2573	7	HDW	328	224310	1188443	1840	12.5	HDW
141	260133	1213306	2301	12	HDW	329	220307	1188350	1602	13	HDW
142	279334	1207430	2495	60	SW	330	218266	1185278	1663	10	HDW
143	274813	1207712	2516	60	SW	331	218166	1184944	1657	10.5	HDW
144	244102	1116899	2508	55	SW	332	217063	1187045	1580		HDW
145	277214	1209832	2516	60	SW	333	218399	1181244	1615	15	HDW
146	264621	1212983	2588	11.5	HDW	334	219213	1180251	1652	14	HDW
147	263823	1212072	2567	10	HDW	335	218977	1179184	1624	11	HDW
148	264181	1212420	2563	13.5	HDW	336	218840	1779098	1622	9	HDW
149	245295	1217137	1905	50	HDW	337	222769	1181113	1680	15	HDW

150	245056	1217621	1992	8.5	HDW	338	221237	1181838	1756	17.5	HDW
151	280170	1215390	2566	15	HDW	339	215916	1179613	1614	10.5	HDW
152	279906	1215425	2585	19.5	HDW	340	218796	1180007	1638	11	HDW
153	275023	1206850	2560	9	HDW	341	214910	1187076	1506	16	HDW
154	276023	1207870	2565	11.5	HDW	342	218431	1178332	1608	22	HDW
155	275358	1214418	2614	12	HDW	343	214792	1179123	1590	7	HDW
156	267471	1210319	2512	50	SW	344	214917	1180077	1579	54	SW
157	251611	1212455	2303	5.5	HDW	345	212308	1175575	1640	55	SW
158	250956	1212546	2306	7	HDW	346	218431	1178332	1598	11	HDW
159	257757	1255059	2107	19	HDW	347	219026	1177873	1592	14	HDW
160	258205	1256142	2097	10	HDW	348	228658	1181875	1698	16	HDW
161	259395	1253508	2088	9	HDW	349	229074	1175948	1662		HDW
162	261301	1249402	2100	26	SW	350	220469	1185974	1863	20	HDW
163	258325	1250711	2103	17	HDW	351	227170	1187558	1755	12	HDW
164	259551	1250083	2078	8.5	HDW	352	229263	1185253	1786	13	HDW
165	256677	1254221	2168	13	HDW	353	229394	1184649	1767	19	HDW
166	256791	1255340	2150	14	HDW	354	230629	1192359	2001	12.5	HDW
167	257361	1257175	2164	22	HDW	355	226996	1192451	2005	18	HDW
168	258189	1251007	2127	10	HDW	356	227824	1194590	2032	7	HDW
169	257836	1253177	2091	11	HDW	357	266786	1192905	2004	18	HDW
170	258072	1256606	212	12	HDW	358	227352	1191940	1988	9.5	HDW
171	260169	1250331	2062	7	HDW	359	230307	1197254	2120	22	HDW
172	260371	1250084	2070	6	HDW	360	229972	1199000	2061	10	HDW
173	257442	1249792	2169	6	HDW	361	236311	1185753	1768	26	SW
174	258480	1247695	2175	8	HDW	362	236322	1186059	1753	17	HDW
175	257271	1239566	2017	5.5	HDW	363	239475	1185703	1781	16.5	HDW
176	252610	1239448	1978	11.5	HDW	364	239182	1185547	1785	14	HDW
177	253216	1242205	2018	12	HDW	365	240424	1185648	1771	17	HDW
178	278974	1234175	2145	11.5	HDW	366	214917	1189146	1850	48	SW
179	275763	1234320	2188	9	HDW	367	245321	1190759	1992	6	HDW
180	276472	1232535	2122	8	HDW	368	245954	1191373	1996	16	HDW
181	275580	1233625	2200	17	HDW	369	245041	1190802	2015	15	HDW
182	279741	1240234	2080	11.5	HDW	370	234482	1186607	1852	22	HDW
183	281209	1238692	2130	12	HDW	371	233182	1186190	1782	20	HDW
184	258255	1232319	2346	12	HDW	372	242563	1178115	1838		HDW
185	260488	1245452	2102	11	HDW	373	241053	1177194	1775		HDW
186	243258	1234745	1819	8.5	HDW	374	245087	1173681	1527	11	HDW
187	242456	1234832	1879	552	HDW	375	242116	1177121	1833	55	SW

188	256161	1248586	2251	10.5	HDW	376	213283	1180077	1579	50	SW

Annex -2 Annual and Mean monthly flow of Main Beles river flow (inch)

year	jan	feb	mar	apr	may	jun	jul	aug	sep	oct	nov	dec	Annual
1995	0.04	0.02	0.02	0.01	0.14	1.52	4.02	6.52	2.76	0.75	0.15	0.07	16.02
1996	0.03	0.02	0.02	0.01	0.13	0.81	2.71	10.32	4.52	1.4	0.26	0.13	20.36
1997	0.23	0.15	0.13	0.1	0.27	1	4.01	5.72	3.46	4.04	1.4	0.43	20.94
1998	0.23	0.13	0.09	0.05	0.12	1.18	6.31	9.4	5.85	4.05	0.89	0.43	28.73
1999	0.26	0.14	0.12	0.1	0.44	1.45	4.78	7.91	4.07	3.39	0.8	0.43	23.89
2000	0.27	0.16	0.13	0.14	0.37	1.19	4.14	9.2	4.04	4.65	1.14	0.5	25.93
2001	0.32	0.21	0.18	0.09	0.23	1.81	5.52	12.07	4.56	4.01	1.12	0.5	30.62
2002	0.32	0.19	0.15	0.1	0.08	0.82	3.27	5.36	3.84	1.47	0.47	0.25	16.32
2003	0.17	0.12	0.1	0.05	0.03	1.39	6.34	9.92	6.51	2.71	0.62	0.28	28.24
2004	0.19	0.15	0.11	0.11	0.15	1.52	8.03	7.6	5.01	2.76	0.56	0.31	26.5
2005	0.2	0.12	0.12	0.07	0.16	1.16	4.96	6.46	4.57	2.59	0.65	0.29	21.35
2006	0.17	0.16	0.09	0.09	0.31	2.04	3.86	5.12	4.5	2.15	1.05	0.65	20.19
2007	0.25	0.1	0.09	0.07	0.17	1.45	4.05	5.95	3.98	2.4	0.6	0.25	19.36
2008	0.13	0.09	0.13	0.11	0.22	1.1	4.16	7.07	4.78	4.69	0.88	0.29	23.65
2009	0.17	0.1	0.13	0.11	0.09	1.18	4.16	7.39	4.56	2.59	0.65	0.29	21.42
2010	0.17	0.1	0.09	0.07	0.21	1.93	4.96	5.5	4.28	1.63	0.37	0.25	19.56
2011	0.15	0.09	0.06	0.05	1.32	2.1	4.16	7.39	4.56	2.59	0.65	0.28	23.4

Annex-3 Annual and Mean monthly flow of Gilgel Beles river flow (inch)

year	Jan-	Feb-	mar	apr	may	jun	jul	aug	sep	oct	nov	dec	Annual
1995	0.22	0.12	0.08	0.05	0.22	2.92	5.61	9.64	6.46	2.73	0.78	0.49	29.32
1996	0.25	0.09	0.08	0.11	0.59	2.21	6.97	8.28	6.28	2.94	0.97	0.52	29.29
1997	0.29	0.19	0.28	0.25	0.73	2.96	7.04	7.71	4.53	4.99	2.16	0.69	31.82
1998	0.44	0.16	0.29	0.27	0.37	2.45	5.64	9.49	7.01	5.73	1.94	0.63	34.42
1999	0.5	0.25	0.18	0.14	0.54	2.33	5.1	8.24	6.44	6.95	1.69	0.73	33.09
2000	0.45	0.23	0.17	0.18	0.73	1.87	4.32	13.05	7.88	7.68	2.62	0.99	40.17
2001	0.58	0.29	0.22	0.15	0.24	1.85	5.88	7.57	7.5	3.54	1.64	0.87	30.33
2002	0.51	0.26	0.26	0.39	0.28	1.24	3.1	7.3	6.94	3.91	1.46	0.57	26.22
2003	0.36	0.27	0.29	0.1	0.14	1.29	11.27	8.36	8.23	4	0.86	0.41	35.58
2004	0.24	0.26	0.2	0.21	0.16	2.19	5.81	8.37	5.95	3.38	0.85	0.47	28.09
2005	0.24	0.12	0.11	0.16	0.43	1.94	8.42	10.07	15.75	6.84	2.65	0.67	47.4
2006	1.59	0.31	0.11	0.09	0.73	3.12	5.51	7.2	5.1	4.04	1.79	1.01	30.6
2007	0.61	0.35	0.26	0.18	0.53	3.4	4.3	5.2	4.09	2.39	1.32	0.8	23.43
2008	0.52	0.33	0.26	0.37	0.8	2.23	4.71	7.06	6.05	2.11	1.36	0.62	26.42
2009	0.46	0.29	0.23	0.25	0.26	1.24	2.97	5.12	4.46	1.94	0.83	0.42	18.47
2010	0.27	0.18	0.12	0.09	0.73	3.32	7.54	7.4	7.01	2.16	1.29	0.54	30.65
2011	0.34	0.12	0.17	0.21	0.46	1.63	2.26	5.27	5.39	1.61	0.66	0.36	18.48
2012	0.21	0.11	0.09	0.05	0.49	2.46	5.18	10.78	7.15	2	1.23	1.2	30.95
2013	0.37	0.23	0.18	0.16	0.38	1.46	6.95	7.96	6.61	3.92	1.21	0.65	30.08
2014	0.41	0.25	0.28	0.35	1.56	3.75	4.6	7.97	9.35	3.75	1.42	0.6	34.29

Annex- 4 . Annual and Mean monthly rainfall (mm) distribution in and around Beles basin.

station	Jan	Feb	Mar	Apr	May	Jun	Jul	Aug	Sep	Oct	Nov	Dec	Annual
Baruda	0.6	5.09	13.2	19.62	139.26	196.76	268.31	272.7	216.2	90.01	16.79	4.89	1243.42
Bullen	0.7	2.23	13.88	29.4	148.77	254.94	295.17	320.07	281.4	134.03	13.47	2.64	1496.7
Chagni	2.77	2.95	15.09	30.95	162.11	282.79	340.84	351.21	294.7	207.79	33.65	7.17	1732.05
Dangilla	2.21	3.54	20.36	43.89	162.24	252.83	365.53	372.67	249.9	116.54	35.96	7.14	1632.84
Injibara	16.7	10.7	34.18	70.57	221.41	350.47	501.37	518.85	393.1	171.07	57.03	21.9	2367.31
Mandura	1.47	2.23	10.63	48.57	131.48	364.93	501.5	454.83	318.8	128.44	24.2	3.66	1990.69
Mankush	0	0.06	6.5	19.68	107.25	147.51	228.59	233.28	204	79.73	7.31	1.31	1035.19
meshent	6.35	5.14	18.7	33.7	107.14	232.86	382.73	279.98	167.1	95.77	12.12	9.12	1350.76
Pawe	1.85	1.07	6.04	23.75	125.98	259.66	362.64	386.2	255.8	123.88	17.2	0.73	1564.73
Wombera	0	0.79	20.14	20.49	213.61	250.98	329.87	322.52	300.2	122.61	45.64	1.65	1628.52
Yesmella	1.52	0.69	9.98	28.69	124.15	172.31	316.29	274.46	182.6	65.87	17.36	0.41	1194.33
Debrezeit	3	21.17	75	237	325.7	387	435.5	363.77	234.2	53.5	7.47	9.25	2152.58
Bahir Dar	4.3	15.2	24.3	89.4	210.5	496.4	390.1	216.8	88	17.7	4.61	5.67	1562.98
Average	3.19	5.45	20.62	53.52	167.66	280.72	362.96	335.95	245.1	108.23	22.52	5.81	1611.7

Annex -5 .summarizes the 20 years monthly average temperature of selected stations.

station	Jan	Feb	Mar	Apr	May	Jun	Jul	Aug	Sep	Oct	Nov	Dec
Bullen	20.53	22.94	24.02	24.5	22.94	20.9	19.87	19.74	20.38	20.63	20.28	20.23
Chagni	19.52	21.21	22.86	23.53	22.69	20.53	19.75	19.61	19.82	20.17	19.64	19.13
Dangilla	15.58	17.1	18.49	19.38	19.14	17.95	17.03	17	17.13	17.13	16.04	15.39
Mandura	25.18	26.16	27.17	27.42	87.75	23.72	22.02	21.46	21.57	22.76	23.87	24.19
Mankush	27.69	30.15	31.74	32.01	29.81	26.54	24.62	23.83	24.21	24.69	25.62	25.79
Pawe	23.51	25.79	27.97	28.61	27.04	24.53	23.16	22.77	23.29	23.71	23.38	22.97
Wombera	15.55	16.69	17.73	17.2	16.64	15.46	14.33	14	14.96	14.9	14.92	14.98
Debre zeit	18.83	18.98	17.59	17.35	15.97	15.85	15.41	15.17	15.89	16.71	15.65	17.32
Bahir Dar	17.6	19.47	21.25	22.31	22.31	20.97	19.47	19.26	19.54	20.11	18.84	17.61

Annex -6.Average monthly wind speed (in km/day) in and around Beles basin

station	Jan	Feb	Mar	Apr	May	Jun	Jul	Aug	Sep	Oct	Nov	Dec
Bullen	0.73	0.87	0.91	0.94	0.78	0.6	0.48	0.49	0.46	0.44	0.63	0.64
Chagni	0.77	0.83	0.95	1.01	0.9	0.79	0.65	0.55	0.55	0.44	0.48	0.65
Dangilla	0.88	0.97	1.1	1.17	1.17	1.1	1.03	1.03	0.88	0.74	0.67	0.75
Mankush	0.7	0.9	0.98	0.98	0.87	0.77	0.59	0.5	0.48	0.48	0.56	0.6
Pawe	0.6	0.73	0.93	0.95	1.01	0.97	0.78	0.69	0.6	0.46	0.41	0.48
Wombera	0.73	0.97	0.83	0.75	0.7	0.8	0.83	0.8	0.73	0.63	0.67	0.7

Annex -7. Calculated PET of 9 station by thorentwaite of in and around Beles basin

station	Jan	Feb	Mar	Apr	May	Jun	Jul	Aug	Sep	Oct	Nov	Dec
Bullen	71.18	93.85	106.94	115.5	100.56	81.09	71.24	69.46	73.54	73.24	69.28	68.56
Chagni	65.42	79.88	97.08	106.02	99.92	80.07	73.31	70.96	71.22	72.08	66.49	62
Dangilla	51.48	61.22	71.64	80.13	79.92	72.1	65.13	64.24	63.92	62.04	54.17	49.86
Mandura	112.6	127.81	146.41	155.08	130.95	102.52	80.92	74.09	73.81	84.4	95.63	98.58
Mankush	151.7	215.58	270.31	288.03	220.72	139.86	102.5	89.11	93.11	97.77	111.1	112.9
Pawe	89.81	121.76	160.79	177.96	151.63	112.32	92.69	86.99	91.66	94.16	88.24	82.56
Wombera	57.01	64.31	72.1	70.83	68.58	61.74	54.34	51.91	56.45	54.45	53.46	53.24
Debre zeit	73.45	75.2	67.51	67.94	60.24	60.04	56.72	54.72	58.02	61.3	53.78	63.14
Bahir Dar	54.77	68.6	84.32	96.33	98.2	86.89	73.5	71.14	71.95	74.24	63.31	54.27

Annex -8 Summary of the basic seasonal wetspass output parameters

TimeStep	AET	Runoff	Interception	Recharge	Qsurf[m³/mnt]	Qb[m³/mnt]
1	9.58	0.005	0.411	0.230	43835.655	7692869.786
2	15.46	0.003	0.524	0.763	138176.442	1878558.570
3	65.83	0.063	2.569	3.368	1830304.565	7156038.799
4	123.40	0.531	6.742	7.979	13579629.795	18983165.824
5	189.90	21.109	19.417	12.872	271101900.731	36203887.550
6	157.68	114.682	14.025	16.337	1149190105.99	53325129.132
7	98.71	170.961	14.508	44.103	2014274352.06	116961591.057
8	85.21	161.063	14.368	68.543	2288160763.74	208102612.817
9	81.07	88.644	14.864	60.485	1922633367.36	259294371.391
10	79.40	28.764	10.771	4.688	1276799292.68	201649824.645
11	23.19	0.187	3.884	3.380	642621945.495	156778353.899
12	11.52	0.008	0.805	0.696	321607755.867	118843613.287

Annex -9 chemical analysis of chloride concentration in groundwater and rain water

site ID	Site name/locality/woreda/zone	Easting	Northing	chloride concentration (mg/l)
HDW-43	Gilgel Beles(mender-8)	217284	1259707	10.6
HDW-38	Hamusit	257676	1252412	4.3
HDW-22	Hung talk, Dibati	203553	1190185	0.35
HDW-39	liben	279560	1297193	1.4
BH-31	Kumbur	230997	1294456	4
HDW-40	Guwalo	249113	1256810	5.7

HDW-52	Wombera town water supply	791450	1175572	5
BH-7	Mojib	821255	1192030	8
BH-5	Dachigre	8031102	1235104	11
BH-1	Gublak	826693	123669	4
BH-2	Mankush 1	749252	1246619	5
BH-43	Bedora, Geshmeshenda Benshangule gumuze	173509	1184315	1.28
BH-44	Camba, Zighi, Dibati	188801	1181728	3.44
Rain-1	Manbuk	218283	1271648	0.30
Rain-2	Gilgel Beles	210545	1234522	0.50
Rain-3	Chagni	221826	1214827	2
Rain-4	Dangilla	235565	1258470	0.15